DECENTRALIZED MULTI-ROBOT COORDINATION IN CROWDED WORKSPACES

PAR

Laleh MAKAREM

EPFL

ÉCOLE POLYTECHNIQUE
FÉDÉRALE DE LAUSANNE

Suisse
2015

Abstract

The coordination of multi-robot systems is becoming one of the most important areas of research in robotics, mostly because it is required by numerous complex applications. These applications range from intelligent transportation systems, search and rescue robots, and medical robots, to cosmology and astrophysics. The coordination of multi-robot systems is based upon cooperation. The actions performed by each robot take into account the actions executed by the others in such a way that the whole system can operate coherently and efficiently. Regardless of the application, coordination is the key to the successful design and implementation of multi-robot systems.

The number of robots involved in the aforementioned applications is increasing along with advances in miniaturization and automation. Consequently, a large number of robots need to share a workspace. This crowded workspace introduces new challenges into the coordination problem by increasing the risk of collision. To take into account communication constraints and sensor ranges, robots rely on local information. Therefore, efficient but simple coordination algorithms are required.

This thesis investigates decentralized approaches based on navigation functions for the coordination of multi-robot systems in crowded workspaces. Decentralization allows robots to rely on local information, guarantees scalability and enables real-time deployment. Navigation functions are a special category of potential functions. Their negated gradient vector-field is attractive towards the goal and repulsive with respect to fixed or moving obstacles to avoid collision.

In the first part of the thesis, we present the multi-robot coordination problem using navigation functions in a game-theory based framework. We propose a motion model along with a control law that leads the robots to a Nash equilibrium. The existence of the Nash equilibrium enables navigation functions to be exploited for studying, building, and running coordination frameworks for multi-robot systems.

In the second part, we address the coordination of autonomous vehicles at intersections. A novel decentralized navigation function is proposed. It guarantees collision-free crossing of autonomous vehicles modeled as first order dynamic systems. The inertia of the vehicles is also introduced in the navigation functions to ensure deadlock-free coordination. The proposed approach does not require adaptation of the road infrastructure and relies upon onboard vehicles sensor data. Compared with traffic lights and roundabouts, the proposed

method significantly reduces the travel time and the number of stops, thus decreasing energy consumption and pollution emission. This provides a strong motivation to pursue efforts towards the deployment of autonomous vehicles on roads.

In the third part of the thesis, we investigate a coordination framework for a large number of miniaturized fiber positioner robots. The fiber positioner robots are designed and built as parts of the next generation of telescopes enabling large spectroscopic surveys. The proposed decentralized framework ensures the collision-free coordination of the fiber positioners sharing a crowed workspace at the focal plate of the telescope. The dynamical (max speed) and the mechanical (limited actuation range) constraints of the positioners are taken into account in the proposed coordination approach, which significantly reduces the time to reach a new robot configuration, i.e. the positions of the optical fibers, between two successive observations of the sky.

The results of this thesis offer new opportunities for reactive, local and simple coordination of multi-robot systems. In particular, the proposed frameworks can be adapted and scaled up to tackle emerging coordination problems such as unmanned aerial observation and transportation.

Keywords: Multi-robot systems, Multi-robot coordination, Navigation functions, Game theory, Intelligent transportation systems, Autonomous vehicles, Astronomical instrumentation, Fiber-fed spectrographs, Fiber positioner

Résumé

La coordination des systèmes robotiques multi-agents devient un sujet de recherche de premier plan dans le domaine de la robotique grâce, principalement, à un large spectre d'applications possibles. Ces applications incluent notamment les véhicules intelligents, les robots de recherche et de sauvetage, le domaine médicale ou même la cosmologie et l'astrophysique. La coordination d'un système robotique multi-agents est réalisée de manière coopérative. Les actions effectuées par chaque robot dépendent de celles des autres afin d'avoir un système qui, dans son ensemble, soit capable d'opérer de façon cohérente et efficace. La coordination est la clé pour réaliser un système robotique multi-agents efficace et ceci, indépendamment du contexte considéré.

Grâce au progrès réalisé dans le domaine de l'automatique et de la miniaturisation des actionneurs, un nombre croissant d'agents se retrouve présent dans les domaines susmentionnés et doivent donc partager l'espace de travail dans lequel ils évoluent. L'augmentation du risque de collision, consécutif à l'encombrement de cet espace, pose un nouveau défi au niveau de la coordination. De plus, afin de réduire la communication entre les robots et de considérer la portée limitée de leurs capteurs, les robots doivent essentiellement dépendre d'informations présentes localement. De ce fait, il est crucial de disposer d'algorithmes de coordination peu complexes.

Cette thèse étudie les méthodes décentralisées à base de fonctions de navigation dédiées à la coordination de systèmes robotiques multi-agents dans un environnement encombré. Cette décentralisation permet aux robots de se baser sur les informations disponibles localement, et garantit l'extensibilité de la méthode ainsi que son implémentation en temps réel. Les fonctions de navigation appartiennent à une catégorie spéciale de fonctions de potentiel. Le gradient de leur champs vectoriel négatif est attractif en direction de l'objectif et répulsif par rapport aux risques de collision.

Premièrement, le problème de la coordination d'un système robotique multi-agents est présenté en utilisant des fonctions de navigation basées sur la théorie des jeux. Un modèle de mouvement combiné à une loi de pilotage, conduisant les robots à l'équilibre de Nash, est proposé. L'existence de l'équilibre de Nash permet l'emploi des fonctions de navigation dans le cadre de la coordination des systèmes robotiques multi-agents.

Ensuite, la coordination des véhicules autonomes est abordée dans le contexte des intersections routières. Cette thèse propose une fonction de navigation décentralisée qui garantit le croisement en toute sécurité pour des véhicules modélisés comme des systèmes dynamiques

du premier ordre. L'inclusion de l'inertie des véhicules dans les fonctions de navigation assure une coordination en toute sécurité. Les fonctions de navigation décentralisées ne nécessitent pas de changement dans les infrastructures routières et reposent entièrement sur des données issues des capteurs disponibles à l'intérieur des véhicules. En comparaison avec les feux de circulation ou les ronds-points, la méthode proposée montre une amélioration significative en termes de réduction du temps de parcours et de nombre d'arrêts. La diminution de la consommation d'énergie et des émissions polluantes consécutives au nombre réduit d'arrêts est une contribution significative au déploiement futur de véhicules autonomes sur les routes.

Finalement, la coordination d'un grand nombre de robots miniatures partageant un espace confiné est abordée. Ces robots sont utilisés pour le positionnement de fibres optiques exploitées pour effectuer des observations cosmologiques à grande échelle. La coordination décentralisée qui est proposée assure le fonctionnement des robots-positionneurs en assurant l'absence de collision dans l'espace qu'ils partagent. Les robots-positionneurs peuvent se déplacer simultanément tout en respectant leurs contraintes dynamique (la vitesse des moteurs) et mécanique (gamme de l'actionneur). La méthode proposée permet de réduire considérablement le temps de mise en place des robots (et donc de configuration du télescope), ce qui permet d'accroitre la durée d'observation du ciel pour les astrophysiciens.

Les résultats de cette thèse ouvrent de nouvelles opportunités pour la coordination réactive, localisée et à faible complexité de systèmes robotiques multi-agents. En particulier, les solutions proposées peuvent être adaptées pour résoudre de nouveaux problèmes liés à la coordination dans d'autres contextes comme la supervision ou le transport aérien autonome.

Mots-clés : Systèmes robotiques multi-agents, Coordination, Fonctions de navigation, Théorie des jeux, Systèmes de transport intelligent, Voiture autonome, Instrumentation astronomique, robots-positionneurs

Acknowledgement

I would like to thank a number of people who have helped me to make the accomplishment of this thesis a reality. First and foremost, I would like to thank my supervisor, Denis Gillet, for his support and encouragements. I am deeply indebted to him for teaching me how to clearly present my ideas and work. It certainly took him a great deal of patience and I am grateful that he trusted me to work on my own way.

I would like to thank the committee members, Hannes Bleuler, Arnaud de La Fortelle, Oscar Crisalle and Jean-Paul Kneib for taking the time to review this thesis and offering their invaluable comments.

I started my PhD in Automatic Control Laboratory and I am very thankful to Roland Longchamp, Dominique Bonvin and Alireza Karimi for accepting me in the group and providing such a friendly research environment. I met very nice people and learned lots of things from them the time I was in the lab. All the lab traditions made my first year in Switzerland a real fun one.

The last year of my PhD, I had the chance to work on an interdisciplinary project. I would like to thank all the partners. Specifically, I would like to express my gratitudes to Jean-Paul Kneib for being the source of motivation and positive energy and for never getting tired or disappointed. I warmly thank Mohamed Bouri for always being ready and eager to discuss about anything and for all his suggestions on my work. My particular thanks go to Laurent Jenni and Philipp Hörler. I had fun time working with them and I learned a lot from them.

It would have been impossible to come to the office and stay motivated if I did not have Li Na, Evgeny and Wissam as peers. Thank you all for our tea breaks, movie nights and discussions. I am thankful to Wissam, Moe, Sten and Adrian for reading and editing some parts of my thesis and to Fabien and Laurent for helping me with the french abstract.

I have been lucky to have supervised smart and hard-working students: Benjamin, Gergely, Daniel, Igor, Martin, Yves, Cedric and Corinne. I am thankful for their enthusiasm and for our collaborations.

I would like to express my deepest gratitude to my family for their boundless support; Ali and Mansoure for valuing education so much and always being there for us; Leili, Fariba and Reza for their encouragements; Amin, my brother, for being a real friend and for his ability to tell jokes in my most stressful moments; and especially my parents, Mehri and Bagher, for their unconditional love and patient guidance.

Contents

Contents

Contents

List of Figures

List of Tables

Introduction Part I

1 Motivation

Overview

WHY does dynamic coordination of robots matter? This is the question that we will answer in this chapter. We first define "coordination" in this thesis. Then, we go through the importance of multi-robot systems and their effective coordination. The motivation for our choice of coordination frameworks and algorithms will be discussed. The rational behind the choice of coordination approaches for the multi-robot systems with unknown number of robots and in a crowded workspaces will be explained.

1.1 Multi-robot coordination

According to the Merriam Webster dictionary, coordination means the process of organizing people or groups so that they work together properly and well. When dealing with a group of robots, the coordination has the same meaning. According to Jacques Farber, coordination of multi-robot systems is a cooperation in which the actions performed by each robot take into account the actions executed by the others in such a way that the whole system can operate in a coherent way with high performance [1].

There are practically two categories of applications that engage more than one robot. First, the robots that were traditionally manually guided and have been automated. Many intelligent transportation agents such as driverless cars, autonomous underwater vehicles, and unmanned aerial vehicles belong to this category. The problem of coordination arises in this category by the objective to automate the single agents. Although in many cases it is feasible to control a single robot, emulating the coordination that was previously done by human is still an open problem. Considering this category of applications, the goal is to coordinate the

robots in order to get better performance and reliability than the manual controllers.

The second category of applications are the ones that are specifically designed to benefit from the redundancy and scalability of a multi-robot system in comparison with a single robot. Design, construction and coordination of a group of robots called rovers that explored the surface of Mars is a successful example of this type of applications [2].

The following two sections explain the real world coordination frameworks studied in this thesis, where multi-robot coordination is a crucial step to realize an autonomous system.

1.2   Autonomous vehicles at intersection

Nowadays, traffic lights and stop or priority signs assist human drivers to safely cross intersections. However, in the future, with computers behind the wheel, innovative driver assistance systems or autopilots have to be designed, bearing in mind that the first license for an autonomous vehicle to legally commute on public roads was issued in May 2012 in the Nevada state. Nonetheless, the widespread commercial exploitation of these vehicles is only conceivable once coordination problems, such as crossing intersections, can be safely and efficiently handled. Coordination of the driverless vehicles at intersections is a multi-robot coordination problem in which the number of vehicles is not known before hand. In addition, to benefit from the full potential of vehicle-to-vehicle communication and to pass the intersection as fluently as possible, the vehicles need to move very closely to each other. This means that the problem of coordination of autonomous vehicles at the intersections is a multi-robot coordination challenge where the number of robots are unknown and the workspace of the robots (intersection) is crowded (Figure 1.1).

1.3   Fiber positioner robots

Since 1930 it has been known that our universe is in expansion. But surprisingly, at the turn of last century astronomers showed that the universe expansion is accelerating [3; 4]. To explain this acceleration, another dark ingredient was added to the universe composition, the dark energy [5]. The nature of dark energy has become a key question in cosmology and fundamental physics, and many dedicated projects using different techniques attempt to solve this puzzle, and more generally, to provide a model for the cosmological world (e.g., curvature, spectral index, neutrinos mass, non-gaussianities) [6; 7; 8].

In particular, massive redshift survey of galaxies and quasars are needed to map the large-scale structures of the universe [9]. The redshift-distance relation could be understood through the measurement of Baryonic Acoustic Oscillations (BAO) and putting constraints on the gravity model through the study of the redshift space distortions (RSD) [10]. As measurement systems, many projects are planning to use a large number of small planar robots. The robots have two degrees of freedom and move and place a fiber located at their end-effector. Figure 1.2
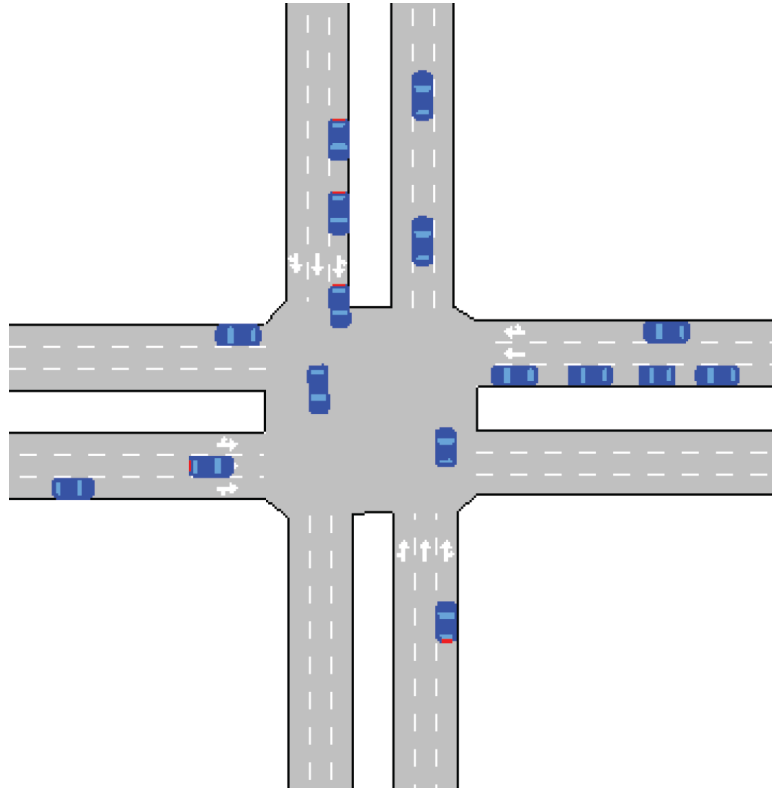
Figure 1.1: Vehicles crossing an intersection will share a workspace that increase the risk of collision.

shows one of these robots built in collaboration between EPFL and Universidad Autónoma de Madrid (UAM). To get a large map of the universe, a large number of these robots will be positioned in a focal plane of a telescope in a hexagonal geometric order (Figure 1.3). Each robot moves from its initial configuration to a final one where it places a fiber on a target. Multiple robots share the workspace and thousands of them need to be moved simultaneously to guarantee maximum time for observation.

Figure 1.2: A fiber positioner robot developed in collaboration between EPFL and UAM [11; 12].
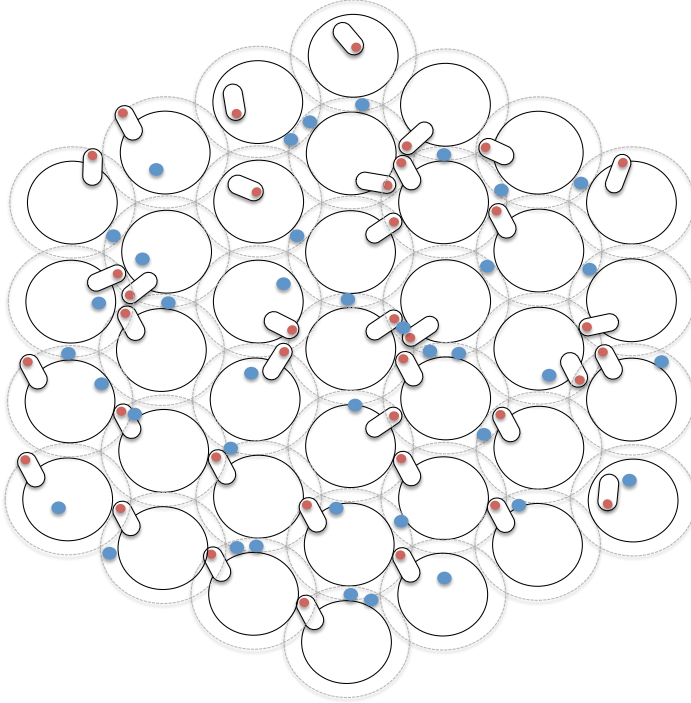
Figure 1.3: Network of 37 fiber positioners with 2DOF robot arms. Large circles, dotted gray circles, red dots and blue dots denote the first arm, the reachable area of the second arm, the optic fiber and the target point of each positioner, respectively. Ongoing projects will use up to 5000 robots in their observations.

1.4 Decentralized navigation functions

The main research question in both the abovementioned frameworks is how to coordinate robots to reach a goal point while avoiding collisions with their neighbors. The proposed approach in both cases should be scalable and extendable to a larger-scale problem, either for larger intersections or larger telescopes. A centralized solution for such a problem would be practically infeasible and costly, due to the presence of numerous robots. Therefore, among all the methods found in the literature for coordinating agents, decentralized and reactive control approaches will be investigated in this thesis.

Inspired by the emergent behaviors among biological agents, methods based on local reactive control have received great interest [13]. Therefore, artificial potential fields are often exploited for the coordination of autonomous agents. The main drawback of most of the potential field approaches is that convergence to the target is not guaranteed due to the presence of spurious local minima. Navigation functions were introduced [14] to solve this problem and present a complete exact solution for the coordination problem.

Navigation functions have been used in various robotic and control applications [15]. In these applications the actuation torque or other inputs (e.g., acceleration and velocity) are derived

from some potential functions that encode relevant information about the environment and the objective. In the framework of this thesis, the use of navigation functions in a decentralized scheme is investigated, as it can be implemented in real-time and it also offers flexibility with regard to adding new heterogeneous robots and changing the problem constraints.

Although navigation functions guarantee collision avoidance and deadlock free motion at the same time, their long convergence time does not allow to realize the full benefits of a reactive motion planning method. In both of our coordination frameworks, convergence time is very important. On the other hand, the higher the probability of collisions among robots, the more deadlock situations are likely to happen. Our objective in this thesis is first to show that it is still possible to reach a collision-free and deadlock-free coordination using potential functions while some of the conditions on being a navigation function according to [14] are relaxed. We call these potential functions "decentralized navigation functions" as they coordinate the robots in a decentralized way and ensure collision-free and deadlock-free motion.

For the two proposed coordination frameworks, we will then introduce navigation functions that could take into account the dynamic constraints of the robots. We will give proofs for deadlock free motions and show the performance of the robots through simulation.

2 Alternative Coordination Approaches

Overview

MULTI robot coordination techniques are very much dependent on the requirements of recent applications. Accordingly, this chapter introduces briefly the alternative approaches in coordination of multi-robots systems. We review the highlights of centralized and decentralized control options and examine their gains and pains for different applications. In addition, we study two different robot control strategies, deliberative and reactive. The review of the state of the art on decentralized navigation function and the two applications that we study in this thesis are included in their related sections.

2.1 Multi robot coordination history

Research in the field of multi robot systems started in the early 80s. Very similar to the single-robot case at the time, the focus of most of the published articles was on obstacle avoidance. Figure 2.1 shows the number of articles per year on multi robot coordination according to Scopus [16]. It clearly shows that research has grown over the previous years, mostly in the fields of computer science and engineering (Figure 2.2). Applications considering multi robot systems are very diverse, ranging from manufacturing and construction, medical assistance, and search and rescue to humanoid soccer games. In these applications, using multi robots and coordination can lead to faster task completion, increased robustness, higher quality solutions, and the completion of tasks impossible for single robots. However, introducing more than one robot at a time can present many challenges to effective coordination. These challenges include limits on time, energy, computation resources, sensing and computational capabilities as well as mobility. Therefore, coordination requires overcoming many complex
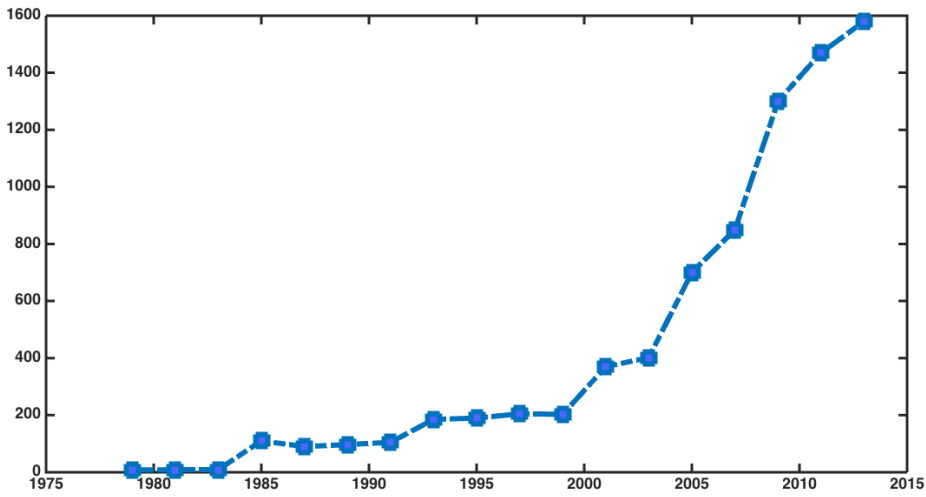
Figure 2.1: Number of articles on multi robot coordination published each year from 1980 to 2013. The numbers are approximate and are retrieved from Scopus [16].

challenges, which have been the focus of research in previous years.

The literature on multi robots systems and their coordination methods and challenges is huge and beyond the scope of this thesis. According to our choice of direction in this field, we review the deliberative and reactive control methods as well as centralized and decentralized architecture of coordination. The interested reader is encouraged to read the survey articles by Farinelli [17], Parker [18], Cao [19] and their coworkers.

2.2   Deliberative versus reactive

For planning a motion, a robot gathers information about its state and its surrounding environment. This motion plan is then translated to actuator signals that changes the state of the robot and consequently its environment. The motion plan can be executed only for the next time step and can only use the information gathered in the current state, or it can be a sequence of motion which uses the information stored in a historical record. In the literature, these two extreme motion planning methods are referred as reactive and deliberative methods [20].

In the deliberative control method, the robot gathers the necessary information on its states, the environment (for example a map of the place) in addition to the information on the current states of other robots and their predicted states. Then the robot computes a series of actions that would optimize a given cost function (risk of collision, energy consumption, time to destination, etc.). Therefore, a deliberative control method:

- needs complete models of the robot, the environment and the other robots (in case of
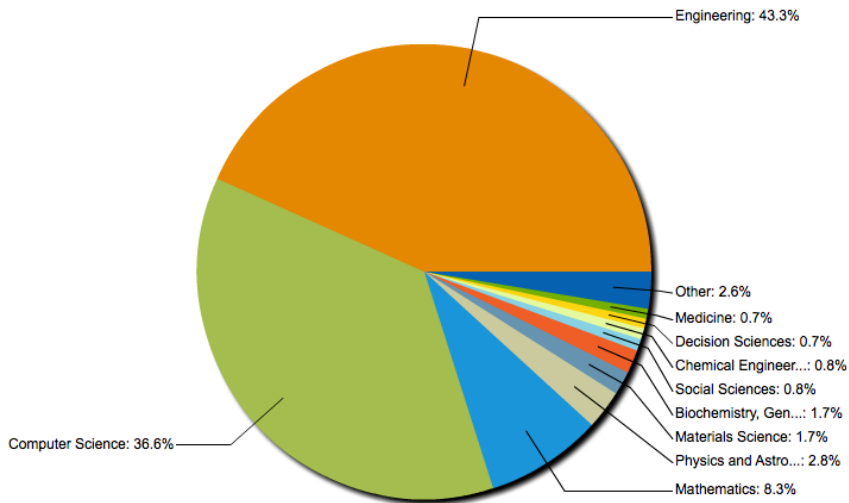
Figure 2.2: Focus of different fields of research on multi robot coordination.

multi-robot applications).

- does not have real-time response because of the time necessary for processing all gathered data and optimization.

- can perform high-level, intelligent and complex behaviours.

The reactive methods compute the action of the robot using only the information gathered by sensors at a given time. Hence, a reactive control method:

- is able to run in real-time and on the platforms with constraints on the resources (such as communication constraints).

- does not need a complete model of the robot and its surrounding.

- is capable of performing lower level tasks (the tasks that could be accomplished using the sensory data, because the robots do not have a complete representations of the environment).

2.3   Centralized versus decentralized

Coordination in a system with many robots can be considered as a process during which a robot selects a course of action from several alternative scenarios. In a multi robot system decision making can be centralized or decentralized, in accordance with the communication architecture of the robots.

In a centralized architecture, there is a central control agent that has global information about the environment as well as information about all robots. In most applications, the

central agent can communicate with all the robots and can be used as a liaison to share the information between robots. The central control agent could be a computer, or one of the robot of the system acting as a leader. A centralized architecture:

- has a global view of the environment, hence it can produce globally optimal decisions.

- is an appropriate architecture for most systems with small numbers of robots, but does not have enough scalability for large teams with more robots.

- has a great dependancy on synchronisation, and therefore is not robust with respect to dynamic environments or failures in communication.

Many studies with focus on motion planning have introduced solutions in a centralized way [21; 22; 23; 24]. The main goal of coordination and motion planning can range from formation [25] to consensus [26] and rendezvous [27].

In a decentralized architecture, there is no central control agent, so all robots are equal and autonomous with respect to the control and decision-making process. Generally, in contrast to a centralized architecture, a decentralized architecture:

- can better respond to unknown or changing environments.

- usually has better reliability, flexibility, adaptability and robustness.

- can only reach a suboptimal solution.

Applications mentioned in centralized architecture are also addressed in decentralized fashion, such as formation and consensus [28]. As an example, Feddema and his coworkers [29] focused on controllability and connection stability for decentralized control of robotic vehicles. They showed a case study of a multi-robot formation control. Many researches focus on negotiation and auction-based systems for decentralized coordination [30; 31]. Other interesting applications where robots are coordinated in a decentralized fashion can be found in [32], [33], and [34].

The state of the art related to motion planning using potential functions, navigation functions and decentralized navigation functions will be discussed in more depth at the beginning of Section II, Chapter 4. We will also give a description on the history and highlights of the two coordination frameworks considered in this thesis.

Summary

In this chapter, we highlighted alternative research approaches related to coordination of multi robot systems. The number of coordination methods and their applications are growing each year. We classified the coordination methods in two dimensions; deliberative versus reactive, and centralized versus decentralized control. Then, we summarized the conclusions of related key articles. The pros and cons of the methods are given in bullet points. The choice of the control method and of the architecture are directly relevant to the type of application, the number of robots, their communication capabilities, and even the speed at which the surrounding environment is changing. In applications with a crowd of robots (like the two coordination frameworks presented in this thesis), real-time computation and robustness to communication failures are the most important aspects that need to be considered in the selection of the coordination approaches.

3 Scope of the Thesis

Overview

THIS thesis focuses on coordination of multi robot systems in crowded workspaces, and more particularly on the coordination of large number of robots sharing the same workspace. This chapter describes how this thesis is outlined, along with our methodologies and contributions.

3.1 Outline

This thesis is organized in six parts, as described below.

Part I - Introduction (Chapters 1, 2, and 3)

Part I gives an introduction to multi-robot systems and coordination problems. The importance of this field of research and the motivations behind are explained in this part. It includes a brief state of the art on the coordination solutions, and presents the selected methods. In addition, this part lists our main objectives and contributions.

Part II - Decentralized navigation functions (Chapters 4 and 5)

This part gives a comprehensive introduction to motion planning using artificial potential fields and navigation functions along with their strengths and weaknesses on coordinating robots of Chapter 4. Chapter 5 shows that, by relaxing a general condition previously put on navigation functions to ensure their convergence, we can design more reactive navigation functions.

Part III - Coordination of autonomous vehicles at intersections (Chapters 6, 7, 8, and 9)

This part focuses on the first coordination framework that we study in this thesis, the coordination of autonomous vehicles at intersections. We study the state of the art on autonomous vehicles, their current state, potential and possible future technologies. We formulate the crossing of autonomous vehicles as a multi robot coordination problem and propose a decentralized navigation function that guarantees collision and deadlock avoidance. Three different methods are investigated in this part to show the benefits of using decentralized navigation functions for collision-free intersection crossing.

Part IV - Coordination of fiber positioner robots (Chapters 10 and 11)

In this part we investigate the coordination of fiber positioner robots in the field of astrophysics and cosmology. We formulate the coordination challenges of these robots in a crowded environment (i.e., the telescope focal plate). We then propose a decentralized navigation function to coordinate the robots while taking into account the mechanical constraints.

Part V - Conclusion (Chapters 12)

Finally, in this part we summarize this thesis and restate the benefits of the proposed coordination methods and their effectiveness in solving the coordination problems in the two frameworks. We also give an intuitive look at the possible extensions of our work.

3.2   Contributions

Each of the described parts of this thesis contains contributions. To guid the reader, we summarize the contributions at the end of each chapter. We also briefly gather them together here.

Part II - Decentralized navigation functions

- In Chapter 5, we show that coordination of robots using decentralized potential functions could be formulated as a normal form game. In the game, the potential functions could act as an inverse form of a utility function. We show that moving in the gradient descent direction is a weakly dominated strategy (a Nash equilibruim), which means that by using that utility function the robots can converge to their goal. We then use this proof to relax a constraint on potential functions to find more reactive and rapid robot trajectories. Depending on the application, if we find conditions of deadlock-free coordination, the potential functions are called navigation functions.

Part III - Coordination of autonomous vehicles at intersections

- In Chapter 7, we propose a decentralized navigation function for vehicles crossing an intersection. By modeling each autonomous vehicle as a first order dynamic system, the decentralized navigation function along with the gradient descend control law guarantee

collision free passing for vehicles. We provide proof for deadlock-free motion of vehicles crossing an intersection. Beside the possibility to address the acceleration and velocity constraints, we show that using the inertia of the vehicles can facilitate handling the deadlock situations in addition to giving indirect priority to heavier vehicles.

- In Chapter 8, we propose a modified version of the decentralized navigation function method so that it takes into account the desired speed and arrival time to the intersection. We call it a spatio-temporal navigation function. We provide proofs for collision and deadlock avoidance. The proposed spatio-temporal navigation function leads to smoother velocity profiles as the number of vehicles passing the intersection will not significantly change over time.

- In Chapter 9 we formulate the coordination problem of autonomous vehicles at intersections in a linear-quadratic model predictive control framework (MPC). To the best of our knowledge, this is the first time that the coordination of autonomous vehicles at intersections is presented in form of a decentralized MPC. Using a second-order dynamic model for vehicles, we introduce a quadratic cost function and translate the collision avoidance problem as a set of linear constraints. The approach takes velocity and acceleration constraints into account, as well as realistic vehicle communication models. We showed the practicality of the proposed method for a platoon of vehicles crossing an intersection.

Part IV - Coordination of fiber positioner robots

- In Chapter 11, we propose a decentralized navigation function that enables to devise trajectories for 5000 robots whose goals are placing fibers attached to their end-effectors in a position that corresponds to the location of a galaxy in the telescope focal plane. The method takes into account the velocity constraints of the two motors of each robot as well as their mechanical constraints based on their specific design. Fiber positioners that are packed very closely in a focal plate can move in parallel and in near-minimum time. We have designed a visual simulation environment that animates the 5000 positioners for the testing and validation of motion-planning and collision-avoidance algorithms.

Decentralized Navigation Part II Functions

4 Introduction to Navigation Functions

Overview

DECENTRALIZED navigation functions (DNF), are a family of potential functions that were shown to guarantee collision and deadlock avoidance for multi-robot coordination. In this chapter we start with reviewing motion-planning methods based on potential functions for a single robot. We then study the extension of potential functions for coordination of multi-robot systems. Navigation functions belong to a family of potential functions that can guarantee both collision and deadlock avoidance by introducing a Lyapunov function. If each robot in a multi-robot system uses an identical navigation function for motion planning, the function is called a decentralized navigation function. Finally, we provide an overview of the theoretical and practical advantages and disadvantages of using decentralized navigation functions.

4.1 Potential Functions

Motion planning using potential functions was first introduced in 1986 by Oussama Khatib, who used the method to control a PUMA 560 manipulator in real-time [35]. This article has been cited more than two thousand times when potential function are used for motion planning in robotic manipulators [36], as well as single [37] or multiple mobile robots [38; 39]. In this Chapter we briefly review the motion planning based on potential functions reviewed in [40]. For more details and examples, see [40].

A potential function, also known as a potential filed, is a real function $\phi : \mathbb{R}^m \to \mathbb{R}$, which is differentiable on $\mathbb{R}^m$. If we look at the potential function as energy, its gradient is a force field. The gradient is a vector $\bigtriangledown\phi(q) = D\phi(q)^T = [\frac{\partial\phi}{\partial q_1}, \ldots, \frac{\partial\phi}{\partial q_m}]^T$ which points in the direction that locally maximally increases ϕ. We use the gradient to define a vector field, which assigns a
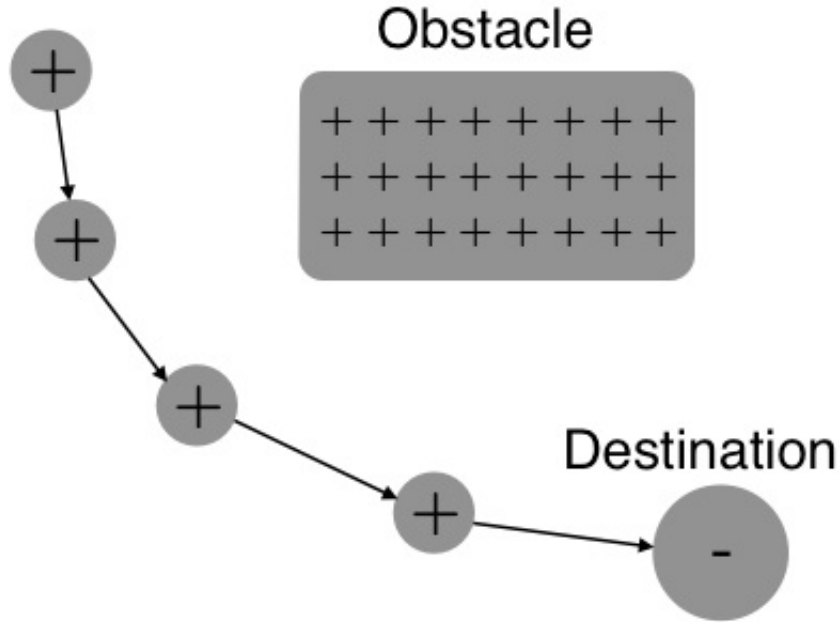
Figure 4.1: The negative charge (destination) attracts the particle (robot) and the positive charges (obstacle) repels it, resulting in a path shown by the arrows.

vector to every point in the working space.

The potential function approach takes the robot as a particle and moves it according to the gradient vector field. Viewing the potential fields as electrical potentials field, gradients are forces on a positive-charged particle (robot) which is attracted to the negative-charged goal (destination). Obstacles also have positive charges, which forms a repulsive force directing the robot away from them. The combination of repulsive and attractive forces could direct robot from the start location to the goal location while avoiding obstacles (Fig. 4.1).

For simplifying the concept, assume that we mainly deal with first-order systems (second-order and non-holonomic systems will also be studied in this Chapter). In this case the gradients are velocity vectors. looking at potential functions as gravitational potentials, robots movement is like following a path downhill by following the negated gradient of the potential function. Following such a path is the well known gradient descent method

$$\dot{c}(t) = -\nabla \phi(c(t)) \tag{4.1}$$

where c and $\dot{c}$ denote position and velocity. The robot stops moving when it reaches a point where the gradient is no longer noticeable. i.e. it has reached a $q^\star$ where $\nabla \phi(q^\star) = 0$. This point $q^\star$ is called a critical point of ϕ. The point $q^\star$ is either a maximum, a minimum or a
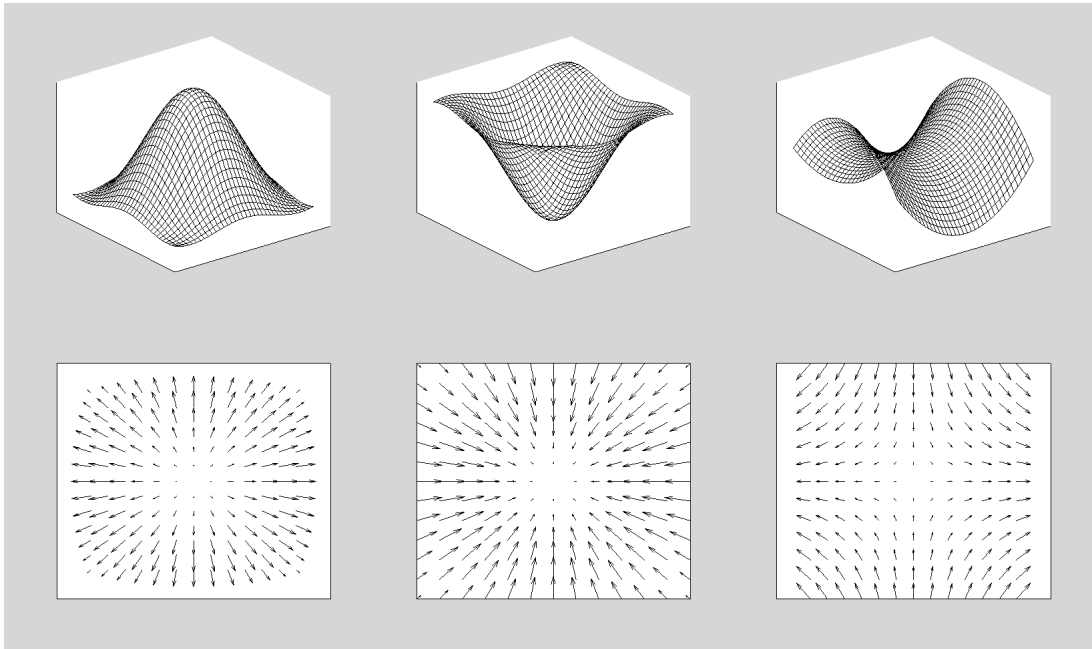
Figure 4.2: Different types of critical point. Top row of graphs show the functions, and the bottom row shows the gradients of the functions.

saddle point (Fig. 4.2). The second derivative of ϕ determines the type of critical point. For real functions, the second derivative is the Hessian matrix

$$\begin{pmatrix} \frac{\partial^2 \phi}{\partial q_1{}^2} & \cdots & \frac{\partial^2 \phi}{\partial q_1 \partial q_n} \\ \vdots & \ddots & \vdots \\ \frac{\partial^2 \phi}{\partial q_1 \partial q_n} & \cdots & \frac{\partial^2 \phi}{\partial q_n{}^2} \end{pmatrix} \tag{4.2}$$

If the Hessian is nonsingular at $q^\star$, the critical point at $q^\star$ is called non-degenerate, meaning that the critical point is isolated. A positive-definite Hessian shows that the critical point is a local minimum. If the Hessian is negative-definite, then the critical point is a local maximum, otherwise it is a saddle point.

When using the gradient descent method for moving the robot, It is not necessary to compute the Hessian. The robot stops moving at a local minimum, not at a local maximum or a saddle point. Since the gradient descent decreases the function ϕ, the robot cannot arrive at a local maximum. However, not all the minima are the destination of the robot.

It is worth mentioning that the potential function method has no limitation on the dimension of the robot workspace. So, unless stated otherwise, algorithms introduced in this chapter could be used both for mobile robots and robot manipulators.

4.1.1 Attractive and Repulsive Potential Fields

The intuition behind combining the two attractive and repulsive potential fields is coming from the electrical potential fields. The goal attracts the robot and the obstacles push it away. When combining the two behaviors, the robot can reach its goal while avoiding the obstacles. The attractive and repulsive potentials could be added

$$\phi(q) = \phi_{att}(q) + \phi_{rep}(q) \tag{4.3}$$

where ϕ_{att} and ϕ_{rep} are respectively the attractive and repulsive potential fields.

The attractive potential

To be an attractive potential field, ϕ_{att} should satisfy several conditions. ϕ_{att} should be monotonically increasing with the distance (d) from the destination of the robot. The most straight forward choice is a conic function, measuring the distance to the goal, i.e , $\phi(q) = \zeta d(q, q_{goal})$ where the ζ is the scaling parameter and q_{goal} is the destination of the robot. The gradient is $\bigtriangledown \phi(q) = \frac{\zeta}{d(q,q_{goal})}(q - q_{goal})$. The gradient points away from the goal with magnitude ζ at all points of the configuration space except the goal, where it is undefined. Starting from any point other than the goal, by following the negated gradient, a path is traced toward the goal.

When numerically implementing this the potential function, gradient descent may experience rapid oscillations, because of the discontinuity at the origin. That is the reason why a continuous function is more desirable. A quadratic function could be a simple example of such a function.

$$\phi_{att} = \frac{1}{2}\zeta d^2(q, q_{goal}) \tag{4.4}$$

with gradient

$$\bigtriangledown \phi_{att} = \bigtriangledown(\frac{1}{2}\zeta d^2(q, q_{goal})) = \frac{1}{2}\zeta \bigtriangledown d^2(q, q_{goal}) = \zeta(q - q_{goal}) \tag{4.5}$$

which is a vector at q, points away from q_{goal}, and has a magnitude proportional to the distance from q to q_{goal}. The longer the distance, the larger the magnitude of the vector. This means, when the robot is far away from the goal, it approaches its goal very quickly. The robot moves very slowly toward the goal in its vicinity. This property helps the mobile robots,

because it imposes no oscillation in the vicinity of the goal point.

While the quadratic function behaves properly near the goal point, It results in a very large velocity when the robot is far from its goal. Therefor, the idea of combing the two quadratic and conic functions seems promising. The robot will move toward its goal with a constant velocity if its is further that $d^{\star}_{goal}$ from its goal. The robot switches to the quadratic function when near the goal (distance less than $d^{\star}_{goal}$). The gradient in the boundary (at the point when the distance is exactly equal to $d^{\star}_{goal}$) needs to be defined. Such a field can be defined by

$$\phi_{att}(q) = \begin{cases} \frac{1}{2}\zeta d^2(q, q_{goal}) & d(q, q_{goal}) \leq d^{\star}_{goal} \\ d^{\star}_{goal}\zeta d(q, q_{goal}) - \frac{1}{2}\zeta(d^{\star}_{goal})^2 & d(q, q_{goal}) \geq d^{\star}_{goal} \end{cases} \tag{4.6}$$

and in this case we have

$$\nabla\phi_{att}(q) = \begin{cases} \frac{1}{2}\zeta(q - q_{goal}) & d(q, q_{goal}) \leq d^{\star}_{goal} \\ \frac{d^{\star}_{goal}\zeta(q-q_{goal})}{d(q,q_{goal})} & d(q, q_{goal}) > d^{\star}_{goal} \end{cases} \tag{4.7}$$

To ovoid any jump in the velocity, it is desired that the gradient of the quadratic function is equal to the gradient of the conic function $\nabla\phi_{att}(q) = \zeta(q - q_{goal})$ at the boundary.

The repulsive potential

A repulsive potential repels the robot from any obstacle in its workspace. The force and its magnitude is a function of the distance of the robot with the obstacle ($D(q)$). The repulsive force should grow in magnitude if the robot is moving toward an obstacle. Like attractive potential field, many functions could be chosen as candidates dependent on the application. Here, we give a classical example of such a function:

$$\phi_{rep}(q) = \begin{cases} \frac{1}{2}\eta(\frac{1}{D(q)} - \frac{1}{Q^{\star}})^2 & D(q) \leq Q^{\star} \\ 0 & D(q) > Q^{\star} \end{cases} \tag{4.8}$$

where the $Q^{\star} \in \mathbb{R}$ defines the distance the repulsive force is active. If the obstacle is further than $Q^{\star} \in \mathbb{R}$, it could be ignored. η can is the gain of the repulsive force These scalar values are

Table 4.1: Gradient descent algorithm for motion planning with artificial potential functions

Gradient descent algorithm
Input: Function $\phi(q)$
output: A sequence of points toward the minimum point $\{q(0), q(1), \ldots, q(i)\}$
$q(0) = q_{initialpoint}$
$i = 0$
repeat until $\bigtriangledown \phi q(i) = 0$
$q(i+1) = q(i) + \alpha(i) \bigtriangledown \phi q(i)$
$i = i + 1$
end repeat

usually determined by trial and error.

Gradient descent

In optimization problems, the gradient descent approach is a well-known method. The idea behind gradient descent is straight forward. In its initial configuration, the robot takes a step in the direction opposite to the gradient. This gives a new configuration, in which the potential field has a lower value. The robot repeats the same procedure until it reaches a point that the gradient is zero (Algorithm in Table 4.1).

In the gradient descent algorithm, the $q(i)$ is the value of q at the ith iteration. The final path consist of the sequence of these iterations $q(0), q(1), \cdots, q(i)$. $\alpha(i)$ is a scalar that determines the step size in the ith iteration. $\alpha(i)$ should be selected in a way that the robot avoids sudden jumps into an obstacle. $\alpha(i)$ plays an important role in the amount of time it takes to reach the goal point. In practice it is not always possible to reach a point, where in the gradient is zero $\bigtriangledown \phi(q(i)) = 0$. Therefore, to implement the algorithm in practice, the zero gradient condition is replaced with a weaker condition $|| \bigtriangledown \phi(q(i))|| < \epsilon$.

4.1.2   Local Minima Problem

The gradient descend method guarantees the move toward a minimum point. However, the reached point could be different from the robot's goal point. Like many optimization problems that use the gradient descend method, the local minimum could fail the robot in getting to its goal point.

Fig. 4.3 shows one of this local minimum situations. The robot is attracted to a goal which is on the other side of an open box-shaped obstacle. The goal attracts the robot, which guides it inside the obstacle. At some distance, the obstacle repels the robot out. The robot could reach a point, where the effect of the obstacle's repulsive force is equal to the attraction force of the goal. Mathematically, the robot reaches a $q^\star$ where $\bigtriangledown \phi(q^\star) = 0$ and $q^\star$ is not the goal point
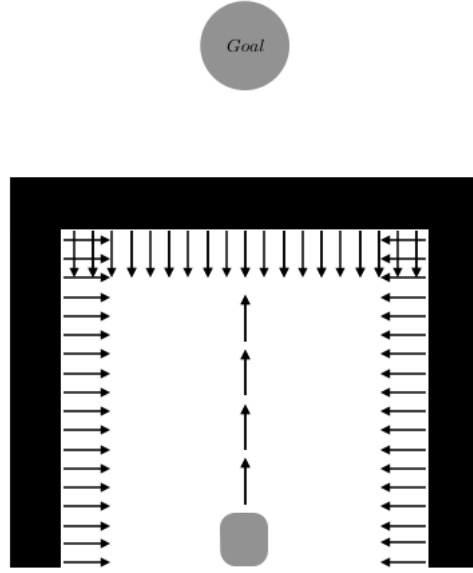
Figure 4.3: Using the potential field method, the robot moves toward the obstacle and stops in a point where the attractive force from the goal is equal to the repulsive force from the obstacle.

of the robot. The local minimum problem is not limited to concave obstacles (We show a concave obstacle here to ease the explanation of the local minimum problem). So the potential function technique is not yet complete for coordination of robots.

There are potential functions other than the attractive/repulsive potential. Many of these potential functions could be efficiently computed in real-time. Unfortunately, they all have one problem which is the existence of local minima not corresponding to the destination of the robot. In general three different approaches tackle the problem of local minima. The first two approaches use additive random or rotational vector fields to disturb the robot from these local minima [41] (Fig. 4.4).

In potential function with a randomized path planner (RPP), the robot follows the negative gradient of a potential function. When the robot gets stuck at a local minimum, it starts a series of random walk. The random walk method often let the robot get out of the local minimum. When the robot is out, it will follow the gradient descend direction of the potential function. The third approach relies on using a potential function that only has one minimum point. In literature, such a function is called a navigation function.

4.2 Navigation Function

So far, we studied potential field methods and their draw backs. In this subsection we introduce a family of potential functions that have only one minimum point. This family of potential functions is called navigation functions [42]. A potential function is called a navigation
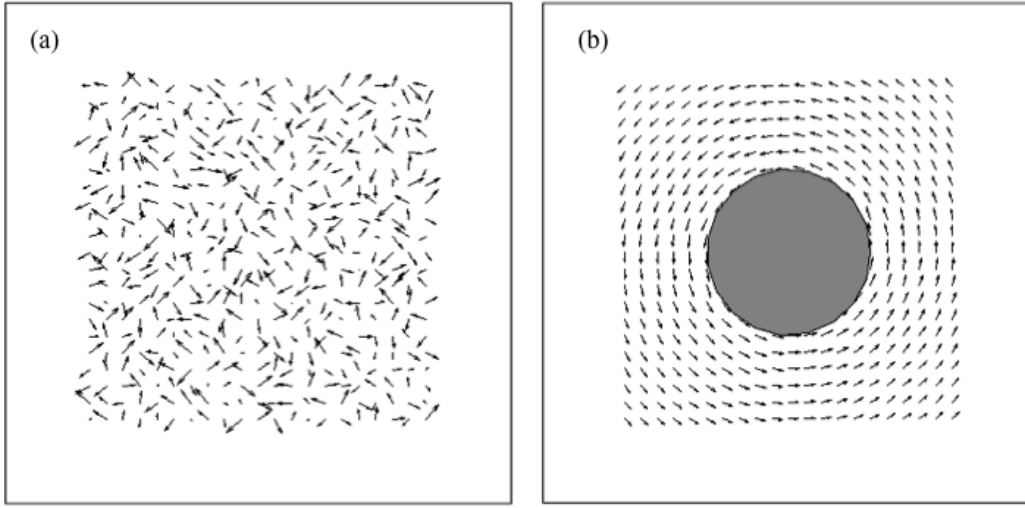
Figure 4.4: Random (a) and Rotational (b) vector fields can be aded to the gradient of the potential field to get the robot out of a local minimum point.

function if it:

• is smooth
• is uniformly maximal on boundaries of the free space
• has a unique minimum at q_{goal} in the connected component of the free space that contains q_{goal} and
• is Morse.

A Morse function [43] is one whose critical points are all non-degenerate. This means that critical points are isolated and if a Morse function is used for gradient descent, any random perturbation will destabilize saddles and maxima.

Theorem 1. *(Existence of a navigation function)*
If a robot's destination and the obstacles are in the workspace $\mathcal{F}$ of the robot and the obstacles do not intersect, then there exists a positive integer $N \in \mathbb{N}$ such that for every $k \geq N$

$$\psi = \left(\frac{\lambda_d^k}{\lambda_d^k + \beta}\right)^{\frac{1}{k}} \tag{4.9}$$

is a navigation function on $\mathcal{F}$ where λ_d is an attractive field toward the destination and β is a repulsive force from obstacles.

The detailed proof of this theorem is provided in [42].

4.3   Decentralized Navigation Function

In this section, we study the extension of the navigation function method to a multi-robot case. In practice, robots are supposed to deal not only with dynamically moving obstacle but also other robots. In 2003, Dimarogonas and his colleagues showed that a modified version of the navigation function in Theorem 1 could be extended in a decentralized fashion for coordination of multiple robots. The function is thus called decentralized navigation function [44].

Consider a system of N robots operating in a single workspace $\mathscr{F} \subset \mathbb{R}^2$. Each robot occupies a disk $R = \{q \in \mathbb{R}^2 : \| q - q_i \| \le r_i$ where $q_i \in \mathbb{R}^2$ is the center of the disk and r_i is the radius of the robot. The configuration of the robot and its desired destination are respectively $q = [q_1, \cdots, q_N]^T$ and $q_d = [q_{d1}, \cdots, q_{dN}]^T$.

Making the following assumptions:
• Each robot knows the positions of the other robots at each time instant
• Robots do not share their desired destination
• Robots could be fitted in a sphere
• Robots' workspace is bounded and spherical

a decentralized navigation function ψ_i is defined as:

$$\psi_i = \frac{\lambda_{di} + f_i}{((\lambda_{di} + f_i)^k + G_i)^{\frac{1}{k}}} \tag{4.10}$$

The term $\lambda_{di} = \| q_i - q_{goal,i} \|$ is the squared distance of the robot i from its destination $q_{goal,i}$. f_i is added to guarantee that ψ_i attains positive values near the destination point. G_i is the distance of the robot i from the other robots. The exponent k is a positive scalar.

4.3.1   Holonomic robots with single integrator dynamics

In this section we review the decentralized navigation function method used for the case of multi-robot systems, in which all robots can be modeled as the holonomic single integrator system

$$\dot{q}_i = u_i \tag{4.11}$$

Theorem 2.   *(Decentralized navigation function for robots with a single integrator dynamics)*
If a robot's dynamics is described by the single integrator (4.11), the system is asymptotically

stabilized with a decentralized navigation function

$$\psi_i = \left(\frac{\lambda_{di}^k + f_i}{(\lambda_{di} + f_i)^k + \beta_i)^{\frac{1}{k}}} \right) \tag{4.12}$$

under the control law

$$u_i = K_i \frac{\partial \psi_i}{\partial q_i}, \tag{4.13}$$

where K_i is a positive gain.

4.3.2 Holonomic robots with double integrator dynamics

In many multi-robot systems, a better dynamic model for the robots is the double integrator

$$\ddot{q}_i = \dot{v}_i = u_i \tag{4.14}$$

Theorem 3. *(Decentralized navigation function for robots with a double integrator dynamics)*
If a robot's dynamics is described by a double integrator (4.14), the system is asymptotically stabilized with a decentralized navigation function

$$\psi_i = \left(\frac{\lambda_{di}^k + f_i}{(\lambda_{di} + f_i)^k + \beta_i)^{\frac{1}{k}}} \right) \tag{4.15}$$

under the control law

$$u_i = K_i \frac{\partial \psi_i}{\partial q_i} + \theta_i (v_i, \frac{\partial \psi_i}{\partial t}) - g_i v_i, \tag{4.16}$$

where K_i, g_i are positive gains and

$$\theta(v_i, \frac{\partial \psi_i}{\partial t}) = - \frac{c v_i}{tanh(\| v_i \|^2)} \mid \frac{\partial \psi_i}{\partial t} \mid \tag{4.17}$$

and

$$\frac{\partial \psi_i}{\partial t} = \sum_{j \neq i} \frac{\partial \psi_i}{\partial q_j} \dot{q}_j \tag{4.18}$$

Proof. In [45], Dimarogonas and Kyriakopoulos showed that $V = \sum_i K_i \psi_i + \frac{1}{2} \sum_i \| v_i \|^2$ is a Lyapunov function that can guarantee asymptotical stability at the destination point for each robot.

4.3.3 Nonholonomic robots

Loizou and his colleague extended the decentralized navigation function method to nonholonomic robots [46]. They showed that the same navigation function that is used for double integrator robot dynamics (4.15), with a proper selection of G_i can be used for decentralized motion panning of multiple nonholonomic robots.

4.4 A comparison between potential fields and navigation functions

Potential field methods are supported by models that describe the flocking of animals [47], schooling of fish [48], and pedestrian coordination in a crowded area [49] (social potential fields). If such a method is working in nature, why is the multi-robot coordination problem not considered as solved?

A mobile robot is supposed to move from its initial position to a destination in an environment and avoid the collision with obstacles. Figure 4.5 shows the different behavior of the mobile robot moving from the same start position, using a potential function and a navigation function. The potential function is the one introduced in previous section:

$$\phi_1(q) = \phi_{att}(q) + \phi_{rep}(q) \tag{4.19}$$

$$\phi_{att}(q) = \begin{cases} \frac{1}{2}\zeta d^2(q, q_{goal}) & d(q, q_{goal}) \leq d_{goal}^\star \\ d_{goal}^\star \zeta d(q, q_{goal}) - \frac{1}{2}\zeta(d_{goal}^\star)^2 & d(q, q_{goal}) \geq d_{goal}^\star \end{cases} \tag{4.20}$$

$$\phi_{rep}(q) = \begin{cases} \frac{1}{2}\eta(\frac{1}{D(q)} - \frac{1}{Q^\star})^2 & D(q) \leq Q^\star \\ 0 & D(q) > Q^\star \end{cases} \tag{4.21}$$

A navigation function could be also introduced for a single mobile robot as such:
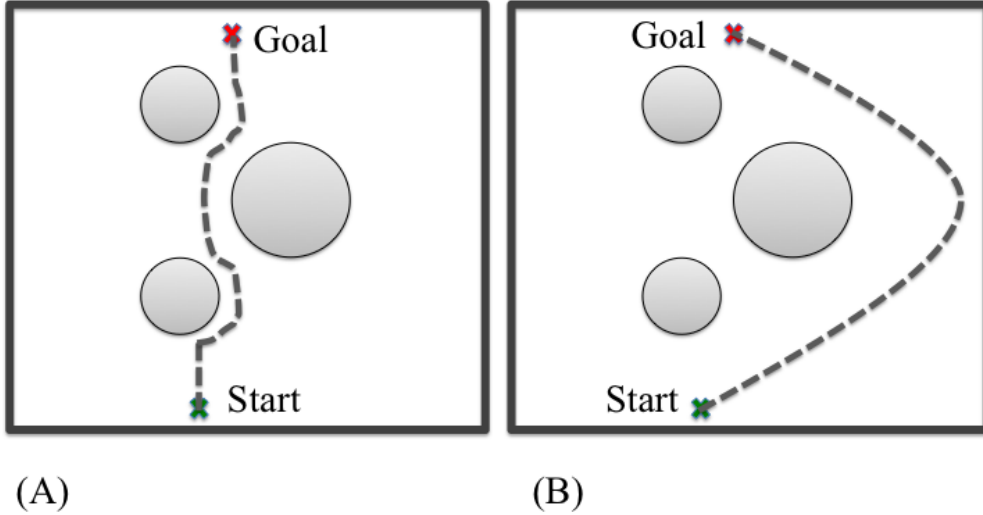
Figure 4.5: (A) shows the motion of a robot going from the start point to the goal point and avoiding the obstacles using a potential field. (B) shows the motion of the robot, with the same obstacle arrangement and from the same start point to the same goal point. The behavior of the robot using the potential field is more reactive and local in comparison with the navigation function.

$$\phi_2(q) = \frac{d^2(q, q_{goal})}{(d(q, q_{goal})^{2k} + \beta(q))^{1/k}} \tag{4.22}$$

$$\beta(q) = \prod \beta_i(q) \beta_i(q) = d^2(q, q_i) - r_i^2 \tag{4.23}$$

q_i and r_i are the position and the radius of the obstacle number i respectively.

Comparing the behavior of the robot in the two figures, we can conclude that the navigation function does not exhibit the most reactive behavior for motion planning. In addition to the different tracks, the two methods has a different convergence time, with the navigation function having a double the convergence time of the potential field. The shorter convergence

time and less deliberation of the response, motivated us to study the potential fields in the framework of coordination of robots in crowded workspaces.

In [50], the authors compare the the efficiency and applicability of the navigation function introduced in 4.10 with those of the potential fields for a RoboCup competition framework. They conclude that although the navigation functions guarantee the existence of no local minimum point, to ensure a more reactive behavior for players (specially in front of the players from the other team), potential fields exhibit a better performance. Therefore, they introduce a new numerical potential field, that guarantees the safety of the robots as well as their quick reactions.

Summary

Potential fields are reactive control methods for motion planning and collision avoidance for both mobile robots and robotic manipulators. A family of potential fields that have no deadlocks are called navigation functions. Many potential fields give a more reactive response for motion planning and have shorter convergence time relative to previously introduced navigation functions. Taking this into account, in the next chapter we study the potential fields as a normal form game and extract new conditions for a potential field to be a navigation function.

5 Nash Equilibrium of Potential Fields

Overview

T HIS chapter presents a game theory approach toward the potential field technique for the coordination of multi robot systems. Potential functions act as utility functions for robots to ensure collision avoidance. As the main contribution of this chapter, the coordination of robots is shown to be achievable by finding the Nash-equilibrium. In such way, deadlock situations should be handled separately.

5.1 An overview of game theory

Game theory is decision making among independent, rational agents. The agent that plays the game is called a player. In game theory, the aim is to study the behavior of the players and predict the outcome of the whole system consisting of many agents when all playing rational.

Game theory has been pursued for over seventy years after publication of "Theory of games and economic behaviour" by the mathematician John Von Neumann and the economist Oskar Morgenstern in 1944. Thereafter, different branches of game theory have been introduced. The main difference between the various branches is the amount of cooperation between the players. A branch of games where players collaborate, is called a cooperative game [51]. The subset, in which the players collaborate but each one has a utility function to maximize, is a type of multi-objective optimization problem [52]. Without collaboration, the players can choose actions that are in total conflict with other players' interests. This branch is called noncooperative games [53]. The most extreme case of conflict of interests is called zero-sum game, in which a player's gain of utility is exactly equal to the losses of utility for the other players.

A strategy is the behavior of a player in the form of a set of actions. The players determine their actions based on information on their states. A strategy specified deterministically is called pure strategy, or if specified with a probability distribution over a set of actions is called a mixed strategy.

5.1.1   Game theory frameworks for multi-robot coordination

After a very vast exploration in many fields such as economics, politics, and military strategy planning, game theory made its way towards robotics applications. In 1993 LaValle proposed the use of game theory as a general formalism for representing, comparing, and providing insight into solutions to a wide class of robotics problems. His article concluded that game theory can be applied to problems of multiple robot coordination as well as high-level strategy planning. Thereafter, game theory has been applied to many multi-robot coordination problems. The main motivations in presenting the multi-robot coordination problem as a game is centred on the following points:

- Game theory provides insight into the nature of many coordination problems, and could suggest solution methods for robotic task [53].

- Game theory provides a solid formulation of trades off [54].

- Competition and conflicts could be formulated by different types of games [55].

- Many types of games rely on the statistical modeling at different levels [56].

A classical example that shows the ability of game theory in finding a feasible solution for a complicated coordination problem is shown in Figure 5.1. The goal of the example is to coordinate two mobile robots in a corridor maze. The robots have different goals and initial locations. Running their individual optimal path, the robots need to occupy the same corridor at the same time. However, adapting the problem in a game theory framework, the robots can obtain a solution that is mutually beneficial, although suboptimal for each. The cost function that could bring a solution for coordination of the two mobile robots in the corridor maze from any initial locations to arbitrary goals is identical for both robots. The cost function has two additive terms. The first term is a cost dependent of the stage. Therefore, if the robot decides to stay or move at each stage, there is cost. The cost of moving is more than that of staying. The second term is the cost associated by the location of the robot. It becomes higher if the robot is further from its goal. The costs are precomputed for all the locations in the map and the situation, in which the two robots occupy the same place is associated with an infinite cost for both robots.
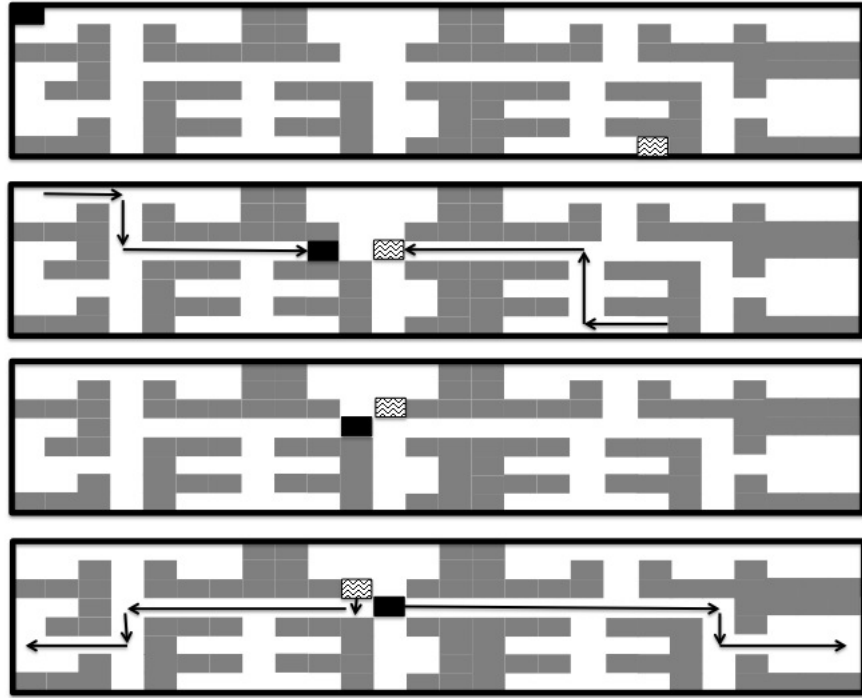
Figure 5.1: Illustration of a game-theory based solution for a complicated coordination problem.

5.2 Normal form games

Normal form is one of the basic forms of representing a game with mathematical tools. We cover this form because it is the one that helps us formulate potential functions as utility functions. Interested readers could refer to one of many tutorials and books for more details on different forms of games and their representations, such as [57].

Definition 1 *A finite, N-player normal form game is a tuple* $(\mathcal{N}, \mathcal{A}, u)$, *where*

- $\mathcal{N}$ is a set of the players

- $\mathcal{A} = \mathcal{A}_1 \times \mathcal{A}_2 \ldots \mathcal{A}_N$, where $\mathcal{A}_i$ is the set of action that player i can choose from

- $u = (u_1, u_2, \ldots, u_N)$, u_i is a utility function of the player i for one of the actions

It is impossible to study game theory and miss the most famous game, the prisoners' dilemma. We also show this game as an example for normal form game representation. Figure 5.2 shows a matrix representation of this game where there are two players. Each player has two actions either to cooperate (C) or to defect (D). The game gets its name from a scenario where two members of a gang get arrested by the police. If the two remain silent, each will get a one year in prison each. If one of them betrays the other one, he gets free but puts the other 4 years in prison. If the two arrested talk, they will each get 2 years in prison.

	Cooperate	Defect
Cooperate	2 , 2	4 , 0
Defect	0 , 4	1 , 1

Figure 5.2: Normal form presentation of a famous game called prisoners' dilemma.

When a game is described, we then look for ways to analyse how the players act. A dominant strategy is one that is known to be selected by a player in game theory.

Definition 2 (Dominant strategy) *A strongly dominant strategy s_i^d is a strategy that brings a higher payoff to a player than any other strategy, independent of the strategies of the other players. Mathematically, it could be formulated as: $u_i(s_i^d, s_{-i}) > u_i(s_i, s_{-i})$ for all s_i that $s_i \leq s_i^d$. For a weakly dominant strategy, the conditions is $u_i(s_i^d, s_{-i}) \geq u_i(s_i, s_{-i})$, where s_{-i} represents* a set of the strategies of all players except player i.

If the players are rational and have no idea about the actions of other players, a dominant strategy is a fairly good prediction of a player's behavior.

5.2.1   Nash equilibrium of a normal form game

A question that arises in game theory is that if all players play rationally and follow their best strategy taking into account the other players strategies, where will the game go? A group of players is said to be in a Nash equilibrium if each player is making the best decision taking into account the decisions of all other players.

Definition 3 (Nash equilibrium) *A strategy profile is a Nash equilibrium if for all players i*
$u_i(s_i^*, s_{-i}^*) \geq u_i(s_i, s_{-i}^*) \forall s_i$
where s_{-i}^* is a set of strategies chosen by other players.

A Nash Equilibrium gives a strategy profile in which it is not beneficial for any of the players to change their strategy. The art of game theory is to formulate the games, in a way to calculate the equilibrium, where most of the time it is not obvious why players would decide to actually play one.

A game may have zero, one, or more than one Nash equilibria. The case of multiple equilibria is particularly problematic since it is often not clear which ones the players would end up

operating on, while only one is the desired of the game designer and typically a globally optimum point.

5.3   Potential fields in form of normal games

In this section, as the first contribution of this thesis, we show that the potential fields method in which the robots are modeled via first-order dynamics and follow the gradient descent, is a normal form game with a Nash equilibrium. In [58] Roozbehani and Gillet introduced a Hamilton-Jacobi formulation for cooperative control of multi-agent systems. We use their steps of formulation of a Nash equilibrium in the framework of a Hamilton-Jacobi equation. We show that viewing the potential functions as utility functions of a normal form game, the gradient descent drives the robots to the Nash equilibruim.

Definition 4 *A set (J_i) of control inputs for the robot i in this game is a Nash-equilibrium for a game if*

$$J_i(u_1^*,...,u_i^*,...u_N^*) \le J_i(u_1^*,...,u_i,...u_N^*), \forall i$$

Theorem 4.   *Existence of Nash equilibrium in coordination by potential functions*
The set of inputs $(u_1,\ldots,u_N)$, where $u_i = -k_i \frac{\partial \psi_i}{\partial v_i}$, represent a Nash equilibrium for a normal form game using the following cost function:

$$J_i = \int\limits_0^T (uu^T + k_i \nabla \psi_i^T \nabla \psi_i) dt \quad i = 1,...,N \tag{5.1}$$

Proof. We want to show that the gradient descend method, as the control law of the potential field, is a weakly dominant strategy for every robot in the game. So, the set of these dominant strategies will present a Nash-equilibrium for the game. Any local optimal control is weakly dominant [59], so we need to show that the gradient descend satisfies the local optimality axiom. We define the Hamiltonian function as follows,

$$H = uu^T + k_i \nabla \psi_i^T \nabla \psi_i + \lambda^T u \tag{5.2}$$

Optimality requires that

$$\lambda^* = -2u^* \tag{5.3}$$

which is

$$\lambda^* = 2k_i \nabla \psi_i \tag{5.4}$$

It only remains to show that

$$\dot{\lambda} + \frac{\partial H}{\partial v} = 0 \tag{5.5}$$

We start from $\lambda^* = 2 k_i \nabla \psi_i$ and calculate the derivative of both sides over time. To obtain

$$\dot{\lambda}^* = 2 k_i \nabla \dot{\psi}_i = 2 k_i \nabla^2 \psi_i \dot{v}_i = 2 k_i^2 \nabla^2 \psi_i \nabla \psi_i \tag{5.6}$$

Using $\dot{\lambda}^*$ from equation 5.4:

$$\dot{\lambda}^* + \frac{\partial H}{\partial v} = -2 k_i^3 \nabla^2 \psi_i \nabla \psi_i + 2 k_i \nabla^2 \psi_i^T \nabla \psi_i \tag{5.7}$$

Choosing $k_i = 1$ for every i leads to

$$\dot{\lambda}^* + \frac{\partial H}{\partial v} = 0 \tag{5.8}$$

which satisfies 5.5 $\qquad\qquad\square$

Just like conditions for being a navigation function, the Nash equilibrium shows the convergence of robots to a solution and therefore could guarantee collision avoidance. However, Nash equilibrium is a weaker condition compared with the Lyapunov function that insures the convergence of the navigation function. This means, using the potential functions, the robots might end up in an equilibrium rather than the desired convergence point. These points are the ones known as deadlock situations, very common for potential functions. Therefore, to guarantee both collision avoidance and deadlock-free motion while using potential fields, we should ensure the equilibrium is the desired point of the system, according to the application and the designed potential field. Thereafter, that potential field is called a navigation function.

🖋 Summary

In this chapter we presented potential fields as a normal-form game framework for the first time. Considering a first-order dynamics for the robots, and a gradient descend method for the control, we show that the potential field brings the robots to the Nash equilibrium. Decentralized navigation function constraints could be translated to a weaker set. The Nash equilibrium ensures that the system avoids collisions and converges to the destination. In the next two parts of this thesis, we elaborate on the decentralized navigation function approach for the coordination of multi-robot systems by benefiting from the existence of a Nash equilibrium that guarantees the convergence of the solution. In the next part, we study the framework for decentralized coordination of autonomous vehicles at intersections. In part IV, we extend the approach to a coordination framework of a very recent application of multi-robot systems, the fiber-feb spectrographs.

Coordination of Autonomous Vehicles at Intersections

6 Coordination of Autonomous Vehicles

Overview

GROUND transportation is evolving into networks of connected mobile robots. From a user perspective, autonomous vehicles could mean safety, convenience and continued mobility for the ageing population. From the viewpoint of society, autonomous driving could help reduce accidents, traffic jams and pollution to a larger extend. Vehicle manufacturers, military units of research and development, and academia have led advances through various projects aiming at the realization of driverless vehicles on urban streets. In this chapter we summarize the leading and main attempts on this area. Then, we review the recent investigations on the coordination of autonomous vehicles at intersections, which is the focus of this part of the thesis.

6.1 State of the art on fully autonomous vehicles

Fully autonomous vehicles were considered for long as a fictitious component of our imaginary future. However, it has been largely shown that the technologies for deployment of fully autonomous driver systems in real traffic situation potentially exist regarding sensors as well as algorithms. While a full review of all attempts is not possible due to growing interest in this field, a few important efforts will be highlighted.

One of the first attempts for deploying fully autonomous vehicles started with two projects. The first project, partners for advanced transportation technology (PATH) [60], focused on autonomous vehicles on highways. In PATH, the goal was to design an automated highway system and find controllers suitable for such a complex system. Over the years, researchers working on PATH designed and implemented advances in actuator and sensor technologies. They also contributed on analysis, simulation, and testing of large-scale, hierarchical hybrid control systems. The second early project in the area of fully autonomous vehicles was hands-free across America [61]. This project from Carnegie Mellon University integrated and tested

advance technologies into a vehicle called NAVLAB (same name as the Laboratory working on it). Unlike PATH, which focused mostly on hybrid control systems for the vehicles, NAVLAB was pioneering methods of vision, path tracking and obstacle avoidance [62; 63].

More recently, fully autonomous vehicles were focused on three grand challenges sponsored by US defense advance project agency (DARPA) in 2004, 2005, and 2007. In the first DARPA grand challenge fifteen out of one hundred and seven registered teams were able to take part in the final race. The race required vehicles to complete a 142 mile track in less than 10 hours. At the time, none of the teams could complete more than 5% of the track.

A year and a half later, on the second grand challenge twenty three teams out of the one hundred ninety five that registered entered the competition. Five teams completed the race, a track very similar to the one in the first grand challenge. The winner, "Stanley" from Stanford, completed the track in less than seven hours.

The third grand challenge, also known as urban challenge, introduced two more challenges to the competition. Vehicles were driving in an urban environment and they needed to comply with driving rules of California. Only eleven vehicles out of eighty nine were qualified for the race, six of which completed the track. Carnegie Mellon's vehicle, "Boss", was the winner [64].

By no means were the DARPA grand challenges the only active movements toward promoting autonomous vehicles. Before the first grand challenge, De la Fortelle and Parent started the Cybercars project in Europe [65]. The aim of the Cybercars was not only to act autonomously, but also to safely drive in areas with pedestrian traffic. Through many years of research at the European level, key technologies for guidance, collision avoidance, energy management, fleet management, and friendly user interface were developed and tested. The Cybercars project was continued by CybrCars-2 and CityMobil projects in 2006.

The prototyped vehicles of the Cybercars project had the capability to travel on existing road infrastructures, without the need for dedicated guide ways. However, they were designed for low-demand road traffic. In Cybercar-2 the main focus was to empower the vehicles to communicate with other vehicles as well as with the infrastructure [66]. The idea was to enable Cybercars to cooperate on the road through their communication tools [67], and then evaluate how standard vehicles that could be equipped with communication-based driver assistant systems could share the same infrastructure with Cybercars. This contributes to answer a key question of how to open the way to the large scale introduction of fully autonomous driving while humans are still behind the wheels of the vehicles.

Starting in 2011, Google vehicles [68] drew lots of attention from the public and academia. The first publicly displayed Google vehicle was a Toyota Prius passenger car equipped with a multilayer 360° laser scanner that was more expensive than the car itself. The control system could change the heading and the speed. As of January 2014, Google self-driving cars have driven more than 200,000 miles autonomously.

6.2   Coordination of autonomous vehicles

Coordination of autonomous vehicles lies within the broader area of multi-robot coordination [69], where the goal is to coordinate multiple autonomous robots in a unstructured and unknown environment either in a modular or a hierarchical approach. However, autonomous vehicles differ on many aspect from the robots that were the target of the multi-robot coordination field of research. After all the advances in control and sensor technologies that led to the realization of different types of autonomous vehicles, many researchers tried to smooth the way for coordination of these vehicles by studying vehicle-to-vehicle and vehicle-to-infrastructure communication abilities. They address in particular the coordination between vehicles running at close ranges, like when platooning or crossing an intersection, based on wireless local area network technologies [70]. To summarize the essence of research in communication of vehicles, experts have proven that the direct and wireless vehicle-to-vehicle and vehicle-to-infrastructure communication is feasible. Many of the important and essential modules in terms of communication protocols could be found. Those modules are provided by the IEEE 1609 WAVE framework that guarantees power control to avoid channel congestion and information dissemination [71].

Still, there are many challenges ahead. First of all, could vehicles that can drive autonomously and communicate efficiently impact the traffic flow in its bottlenecks? The two bottlenecks, highways and intersections, are the points of congestion and have high risk of accidents. Attempts toward using autonomous cars and trucks seem very promising. Not very surprisingly, the common conclusion of the three main platooning projects, SARTRE, iQFleet and Energy ITS is that platooning trucks are not only feasible but also a way to decrease the energy consumption and accident risks [72].

SARTRE, a european project started at 2009 [73], envisioned to develop an integrated solution to drive vehicles in platoons on public roads for the first time. SARTRE defines a platoon as a group of vehicles that are connected through vehicle-to-vehicle communication. The lead vehicle is driven manually, and joined vehicles follow the leader automatically on the same lane. Vehicles can join or leave the platoon dynamically. The information sent via vehicle-to-vehicle communication is the most vital part of the system, and allows sharing of local vehicle signals such as their sensor information and speed. This information is used to coordinate the vehicles in the platoon as individual cars. A platoon of five vehicles at low speed was conducted on public roads in Spain in 2012 [74].

iQFleet [75], the intelligent real-time fleet control and management, is a collaboration between the Royal Institute of technology (KTH), the Swedish national road and transportation research institute, the Swedish transport administration and is partly funded by the Swedish government. The main goal of the project is to reduce the fuel consumption of heavy loaded vehicles by driving them in platoons. The vehicles will follow a leader automatically, but unlike SARTRE, drivers are responsible to keep the vehicles in the lanes. In the first step of the research vehicles were tested between two Swedish cities, coordinating using their local

sensor information like radar. In the second phase, vehicle-to-vehicle communication will be added to decrease the gap between the vehicles. The goal is to provide the leader vehicle with some information on traffic flow prediction that can help energy saving for the whole platoon.

Energy ITS [76] is a Japanese national project that aims a coordinating autonomous trucks to save energy and compensate for the lack of experienced drivers in the country. Currently, a platoon of three trucks dives at the speed of $80km/h$ with $10m$ of gap between the trucks. Along with automation of the trucks, the realization of the project involved putting lane markers on the road for more precise line detection and lane keeping. They have shown that platooning can reduce energy consumption by about 15% by only decreasing the aerodynamic drag.

Many of the research projects that aim at coordinating vehicles in platoons started with a main goal of energy saving. Along the way, they investigated and advanced in many other directions, such as vehicle-to-vehicle and vehicle-to-infrastructure communication, vision, lane detection, dynamic modeling, cyber security issues, and socioeconomic effects of the autonomous vehicles. The intersection crossing of autonomous vehicles might seem a more challenging problem in terms of safety and diversity of the crossing scenarios, but one can take advantages of the shown potentials in platooning vehicles to tackle the intersection problem.

6.2.1 Coordination of autonomous vehicles at intersections

There are generally two different approaches to coordinate autonomous vehicles at intersections. One approach is to design a centralized controller for the intersection where autonomous vehicles are passing. Peter Stone and coworkers [77] investigated the coordination of autonomous vehicles at an intersection in a centralized framework. Their idea was to replace the traffic lights at the intersection with an agent called "the intersection traffic manager". In their first attempt in 2004, they replaced the traffic lights with an intersection manager that gives priority to the vehicles to pass the intersection based on a reservation system. Each vehicle approaching the intersection sends a message to the intersection manager containing the arrival time to the intersection, the velocity at which the vehicle will arrive, the direction the vehicle is coming from (it is assumed that all vehicles are driving straight), the vehicle's maximum velocity, its maximum and minimum acceleration, and its length and width. The intersection manager divides the intersection area into small cells, and at each time step calculates if that cell is occupied by a vehicle. If so, the intersection rejects a new vehicle's request to enter the intersection. The vehicles that are not given permission to enter the intersection at their requested time will decelerate and submit another request at the next time step. The simulation results showed that the system can perform two to three times better in terms of average delay of the vehicles at the intersection, compared to a simple traffic lights system.

The intersection manager was improved by letting the vehicles turn and accelerate at the intersections [78]. To give more flexibility to the system to handle the normal human-driven

vehicles, a mode is added to the intersection manager to insure the safe crossing of these cars. Compatibility with human drivers can clearly facilitate the transition between human drivers and autonomous vehicles. However, there is a compromise in terms of efficiency because the intersection is closed to all autonomous vehicles while a human-driven one is crossing [79].

Stone and his colleagues extended their studies beyond the case of an individual intersection to control a network of interconnected intersections. While observing the minute-by-minute traffic conditions of all the intersections, they run an A* algorithm to find the best path from the vehicle's current location to its destination though the network of the intersections.

Another centralized approach for coordination of autonomous vehicles at intersection was introduced in the framework of the Cybercar project [65]. Similar to the intersection manager of Stone's group, the idea is to have a supervisor at the intersection. In this case, when a vehicle approaches the intersection, it requests the geometry of the intersection from the supervisor. According to its velocity, the vehicle builds a reservation request which is sent back to the supervisor and then the supervisor decides if that request is acceptable. In the case of the intersection manager, square cells are the parts of the road space to reserve. The smaller the cells are, the more vehicles could pass the crossroads in a given time period because the vehicles reserve only the space they need. However, considering the communication load of the intersection supervisor and the number of vehicles that can enter a large intersection, Mehani and De la Fortelle introduced a different set of reservation zones that insures the scalability of their algorithm [80].

To improve the performance of the intersection supervisor in terms of robustness, De la Fortelle and coworkers introduced a priority graph framework, which is a high-level description of the coordination strategy and embeds the possible collision scenarios [81]. They built a coordination space whose dimensions are the number of vehicles at the intersection, and the obstacle regions has a cylindrical structure that represents the vehicles passing over the time. Under their framework, the intersection supervisor is proven to be collision-free and deadlock-free. As the reservation algorithm is the critical part of this approach, in [82] they optimized the intersection supervisor by running a more centralized algorithm to find the arrival times, instead of accepting arrival requests. Moreover, they solved the collision problem of their previous work that was happening outside of the intersection. An advanced cruise control (ACC) was simulated to guarantee collision avoidance out of the intersection. The fact that all the algorithms that are introduced in this scope are already tested on the cybercars gives an added value in terms of reliability and robustness.

Articles focused on centralized coordination of autonomous vehicles at intersection are not limited to the abovementioned lines of research. In [83] the authors solve the collision avoidance problem based on a decomposition of the problem into a continuous optimization part and a scheduling problem. In [84] the authors designed a system that shows a "green" or "red" signal on a screen for a semiautonomous or even an autonomous vehicle based on a sequenced protocol.

In this thesis, our first aim and key focus is on investigating coordination algorithms that could take advantage of the autonomy of the vehicles in crossing the intersections without any change in the infrastructure. This means that each vehicle needs to decide, coordinate, and control itself in a decentralized fashion. At the same time, a decentralized control method can benefit from advances on vehicle-to-vehicle communication methods. The decentralized approaches for coordination of autonomous vehicles at intersections started before the beginning of the current century [85; 86], but they did not grow as much as the idea of replacing traffic lights with some sort of intelligent supervisor at the intersection. In both of the mentioned papers, collision avoidance is ensured by using an algorithm that allows only one vehicle to stay in an intersection region. All the vehicles calculate a priority for all including themselves according to their arrival time to the intersection. When one vehicle finds itself having the highest rank in the list, it passes the intersection.

Summary

The deployment and the coordination of autonomous vehicles are becoming important areas of research in intelligent transportation systems. The advances made in different sensors as well as vehicle-to-vehicle and vehicle-to-infrastructure communications paves the way toward the realization of driverless vehicles on urban roads. The challenges toward coordination of autonomous vehicles at intersections rely on the fact that a large number of vehicles share a common workspace. In the literature, the coordination problem has been tackled in both centralized and decentralized frameworks. In this part of the thesis, we focus on decentralized coordination of autonomous vehicles at intersections. In the next chapter, we propose a novel decentralized navigation function that guarantees collision-free coordination. We derive the parameters of the navigation function in a way that vehicles avoid deadlock situations.

7 Coordination of Autonomous Vehicles at Intersections Using Decentralized Navigation Functions [*]

Overview

In this chapter, we propose a multi-robot coordination approach for crossing intersections that takes into account vehicle dynamics as well as realistic communication constraints. We introduce a decentralized navigation function and combine it with a sensing model. The proposed method is compared with adaptive traffic lights and roundabouts in terms of throughput. The simulations show that the proposed approach results in smoother trajectories when vehicles are crossing a four-way intersection. They also indicate that by using a decentralized navigation function for coordination, the autonomous vehicles consume less energy and therefore reduce pollution emission.

7.1 Introduction

Passing an intersection for autonomous vehicles is principally a multi-robot coordination problem. The number of vehicles could vary for different intersections at different times. In order to deploy autonomous vehicles in roads without changing the infrastructure at each intersection, the solution for passing intersection should be independent of the number of vehicles and exploit vehicle-to-vehicle communication.

In this thesis, we investigate the decentralized navigation function (DNF) method for coordination of vehicles at intersections. In traditional mobile robotics, the agents are free to use the full workspace. However, in traffic coordination, additional constraints are imposed on the paths of the robots. The DNF should be adapted to take into account the fixed-path coordination of the vehicles, as they can not deviate from the lanes. The propulsive force that results in

---

[*]   Chapter published partly as ([87; 88]): "Microsimulation Modeling of Coordination of Automated Guided Vehicles at Intersections," in journal of Transportation Research Record, 2324, p. 119-124, 2012.
and "Decentralized Coordination of Autonomous Vehicles at Intersections," in 18th IFAC world congress, Milano, Italy, 2011.

collision avoidance should take into account the limited sensing and communication range for vehicles. Moreover, like any dynamic system, autonomous vehicles have constraints on inputs such as acceleration and braking. In addition, there are different constraints according to traffic regulations such as speed constraints. We should take into account the fact that autonomous vehicles can not drive reversely on the road entering the intersection.

Taking all the mentioned constrains into account, in this chapter we propose a new DNF that can guarantee collision free passing for vehicles. We provide proof for deadlock-free motion, considering dynamic constraints of the vehicles. Adding a new term to the DNF relative to the inertias of the vehicles, the heavier vehicles get indirect priorities to pass the intersection by braking less than the lighter vehicles. The indirect priority results in less fuel consumption and less pollution emission.

7.2   Problem formulation

The considered network consists of a four-road intersection. Each road has one lane in each direction. The whole system involves N vehicles whose goals are passing the intersection as fluent as possible. The position of vehicle $q_i = (x_i, y_i)$ is known as in a global frame attached to the intersection. In practice, position data could be provided using localization methods for autonomous vehicles. The path of each vehicle is predefined and could be described by the path parameter s_i.

Hence, the location of the vehicle along its path could be calculated from its position in the global frame using the parametric function $q_i = f_k(s_i)$ corresponding to the path k the vehicle has chosen for its travel. The motion of each vehicle along its path is modeled using first order dynamics:

$$\dot{s} = \frac{1}{m_i} u_i \tag{7.1}$$

where u_i is the control input and m_i is the inertia of the vehicle i. The dynamics proposed for the vehicles is simple yet quite realistic. First order dynamics has been already used to describe the behaviors of the vehicles [89].

Each vehicle is controlled using its own navigation function, which is built and updated at each time step. The main challenge is to find an appropriate navigation function. This navigation function could be combined with a proper control input such that:

1. Each vehicle can reach its destination

2. Each vehicle avoids collision with other vehicles located in its sensing zone.

3. The motion of the vehicles follows the dynamics given by 7.1.

A circular sensing zone is introduced. Its radius corresponds to a predefined detecting length, unless there is an obstacle blocking the communication. This zone emulates detection capabilities of the sensors in autonomous vehicles. It is also considered that vehicles can communicate with each other when they are located in their respective sensing zone.

It should be emphasized that the main concern of this work is the behavior of the vehicles at the intersections. Hence, it has been assumed that the desired destinations of the vehicles are further away from the intersection. Hence, the convergence to a final configuration is not a critical issue as long as the vehicle has passed the intersection.

7.3 Decentralized control method

The control of each vehicle is based on a navigation function. A navigation function is a mapping from the workspace of every vehicle to a scalar value. The gradient of the navigation function would be attractive to its destination and repulsive from other vehicles. Therefore, an appropriate navigation function could be combined with a proper control law in order to obtain a trajectory for every vehicle leading to the destination and avoiding collisions. When vehicles are crossing intersections, we can assume that they drive in preassigned lanes. Apart from emergency situations, no static obstacle is present on the road. So, the navigation function of each vehicle should be responsible for two main tasks. First, the vehicle should cross the intersection and either continue that same road or turn to another one. Second, the vehicle should avoid collisions with other vehicles. Thus, the navigation function we propose here is composed of two terms. For vehicle i, the first term is the squared distance of the vehicle from its destination along its path and attains small values as the vehicle approaches the goal. For a vehicle passing an intersection, a moving goal along its path will ensure no deadlock in at crossing. The $s_{i,goal}$ is moved forward so that the attractive force stays in the interval of $[f_{min}, f_{max}]$. More details are given in analysis subsection (7.4). The second term aims at avoiding collision between vehicle i and all other vehicles located in its sensing zone. This term should be large when vehicle j is close to vehicle i in order to create a strong repulsive force and avoid collision risks. This function is equal to 1 when the vehicle j is out of the sensing zone of vehicle i. A navigation function with these characteristics can be written as:

$$\psi_i = \lambda_1 (s_{i,goal} - s_i)^2 + \lambda_2 \sum_{i \neq j} V(i,j) \frac{1}{\beta_\sigma(q_i, q_j)} \tag{7.2}$$

λ_1 and λ_2 are the weight coefficients. $V(i,j)$ is a matrix of priority coefficients that gives higher or lower priority to vehicle i over vehicle j so that the vehicle i will change its speed according to the priorities given to vehicles j. A larger priority coefficient leads to higher acceleration or deceleration of vehicle i.

In order to satisfy the specifications on repulsive force from other vehicles we set $\beta(.)$ as a third degree polynomial function. The value of this function is close to zero for very short distances between two vehicles. So, its corresponding term in the navigation function get values near infinity in order to provide a strong repulsive force. It is equal to 1 when there is no vehicle in its vicinity.

$$\beta_\sigma(q_i, q_j) = \begin{cases} 3(\frac{\|q_i - q_j\|}{\sigma})^2 - 2(\frac{\|q_i - q_j\|}{\sigma})^3 & \text{if } \|q_i - q_j\| \leq \sigma \\ 1 & \text{otherwise} \end{cases} \tag{7.3}$$

To move toward the minimum point of the navigation function, which is the goal point on the other side of the intersection, we use a standard function minimization tool, the gradient descent. The input of each vehicle at each time step is the negative of the gradient of the navigation function:

$$u_i = \nabla_{q_i} \psi_i \tag{7.4}$$

7.3.1 Sensing and estimation

Sensing conditions for the vehicles are defined in order to consider the sensor observation constraint. The sensing conditions represent a camera model, which nearly depicts recent technologies for sensors of vehicles. These technologies in fact replicate the information that could be gathered by a human driver. Therefore, the comparisons between the autonomous vehicles with current methods of passing an intersection mainly show the difference in control strategies. Consequently, differences in information and sensory data would not be an issue. Figure 7.1 shows the sensing zone of every vehicle as defined in this work. The other vehicles are taken into account in the navigation function if they are in the sensing zone. Vehicles are taken into account in the navigation function if they are potentially dangerous. For instance, vehicle 2 in figure 7.1 is not a potential danger for the vehicle 3, as they are traveling in two separate directions and lanes. Three conditions are required to emulate the detection and prediction of vehicles in real world. First, the field of vision of a vehicle is 1.4 radian on both sides. Any nearby vehicle outside of this zone is invisible. Second, there is no danger of collision if the heading vector of a nearby vehicle is inside the light green zone (directional visible zone). Third, if the nearby vehicle is in front of the vehicle (in forced visible zone) it should be seen in any rate. These three conditions could be expressed, using the distance vector and heading rotation shown in figure 7.1.

Condition 1: $0 \leq \delta \leq 1.4$ and $\pi + \delta < \phi < 2\pi$
Condition 2: $2\pi - 1.4 \leq \delta \leq 2\pi$ and $0 < \phi < \sigma - \pi$ $\tag{7.5}$
Condition 3: $1.4 \leq \delta \leq 2\pi - 1.4$ and $|d.sin\delta| \leq d_{desired}$
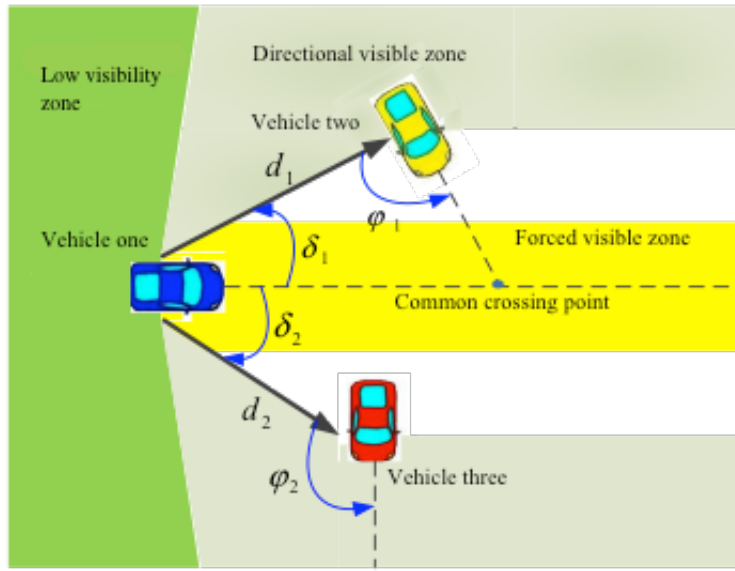
Figure 7.1: Illustration of a vehicle's sensing zone. Any other vehicle is considered in the navigation function if it satisfies three conditions. First, the vehicles should be in the sensing zone in which, two vehicles can see each other. Second, if there is the probability of collision according to distance and direction of the vehicles. Third, the other vehicle is close enough to cause a risk of collision.

In this thesis, we use near realistic sensing model but do not enter the estimation phase. Many estimation techniques exist which has been tailored to different sensing platforms for autonomous vehicles. Our focus is mostly on motion planning and control of vehicles, and thus instead of obtaining the distribution of observations, we simply use the perfect sensing values and add measurement noise in all the simulations.

7.3.2 Priority assignment

All vehicles could be treated equally. However, prioritizing the vehicles could be advantageous. Giving priorities can help avoid blockades of two crossing vehicles. Relying on the presented method, all vehicles will avoid collision by braking. Nonetheless, considering the fact that for passing the intersection the deceleration of one vehicle could be sufficient, one vehicle is encouraged to brake earlier and give priority to the other, thus avoiding any deadlock.

In order to avoid discrete jumps in the navigation function and to guarantee collision avoidance, the given priority is an indirect one imposed by the matrix V in the equation (7.2) . Here, we chose $V(i, j)$ as the ratio between the inertia of vehicle i and vehicle j. The rational behind using inertias of the vehicles as a priority metric is that heavier vehicles are normally responsible for transportation of more people and goods. Besides, heavier vehicles consume more energy than lighter ones. Other metrics related to energy consumption or energy deficiencies could be also integrated in this matrix.

7.4 Analysis of the navigation function

In this section we analyse the properties of the proposed navigation function, which could be used to control each vehicle to reach its desired destination. As previously mentioned, the main goal is to guarantee the collision avoidance while passing the intersection. The existence of a global maximum at the situations of collision, where the navigation function is infinity along with gradient decent method guarantees that vehicles would not approach collision situations. However, to fulfill the crossing mission we need to guarantee that vehicles would not fall into a deadlock situation. Deadlocks are situations in which two (or more) vehicles intercept each other's motions and are prevented from reaching their goals.

The objective in this section is to identify potential deadlock situations and to investigate practical solutions to overcome them. Critical points can be identified by analyzing the gradient of the navigation function introduced in (7.2):

$$\nabla_{q_i}\psi_i = 2\lambda_1(s_i - s_{i,goal})\frac{\partial s_i}{\partial q_i} - \lambda_2\sum_{i \neq j}\frac{V(i,j)}{\beta_\sigma(q_i,q_j)}\frac{\partial\beta_\sigma(q_i,q_j)}{\partial q_i} \tag{7.6}$$

The first term is the gradient of the attractive potential and shows the distance between current position of the vehicle and its destination. This term plays an important role because it results in a smooth trajectory on a predefined lane to reach the destination in absence of other vehicles. As the main focus is the coordination of the vehicles at intersections, the destination is changed over time in order to get an invariant attractive force. The second term corresponds to the gradient of the term associated with propulsive force from other vehicles.

Deadlock avoidance for autonomous vehicles crossing intersections
Given the DNF in equation 7.2 and using the gradient descent method to control the speed of the vehicles and considering the attractive force of the destination between a minimum value f_{min} and a maximum value f_{max}, if the elements of the priority matrix satisfy the following inequality:

$$\frac{V(i,j)}{V(j,i)} < \frac{f_{min}}{f_{max}} \tag{7.7}$$

we show that DNF is deadlock free for two vehicles and ψ drives the vehicles to their destination on the other side of the crossing.

The critical points of ψ_i are obtained when its gradient is set to zero:

$$\text{if } \nabla_{q_i}\psi_i = 0 \text{ then } 2\lambda_1(s_i - s_{i,goal})\frac{\partial s_i}{\partial q_i} = \lambda_2\sum_{i \neq j}\frac{V(i,j)}{\beta_\sigma^2(q_i,q_j)}\frac{\partial\beta_\sigma(q_i,q_j)}{\partial q_i} \tag{7.8}$$

If $(s_i - s_{i,goal}) = 0$ and $\lambda_2 \sum\limits_{i \neq j} \frac{V(i,j)}{\beta_\sigma^2(q_i,q_j)} \frac{\partial \beta_\sigma(q_i,q_j)}{\partial q_i} = 0$ (Case 1) the vehicle has reached its destination.

Hence, from $\frac{\partial \beta_\sigma(q_i,q_j)}{\partial q_i} = 0$ we can say that there is no other vehicle in the sensing zone of vehicle i. This case is not a critical one and just help in finding the instant of convergence to the desired destination.

If $(s_i - s_{i,goal}) \neq 0$ and $\lambda_2 \sum\limits_{i \neq j} \frac{V(i,j)}{\beta_\sigma^2(q_i,q_j)} \frac{\partial \beta_\sigma(q_i,q_j)}{\partial q_i} \neq 0$ (Case 2) the first condition implies that the vehicle i does not reach the desired destination and the second condition implies that there is at least one other vehicle in its sensing zone. The equality of these two conditions means that the repulsive force from the other vehicle is exactly equal to the attractive force from the destination point. Clearly, this equilibrium might not be a desired one. A deadlock happens when all the vehicles near the intersection stop at the same time and do not start moving for a considerable amount of time. To pursue the deadlock analysis, we consider the case with two vehicles near the intersection and then we extend the analysis empirically for a larger number of vehicles. When the gradient of the potential function is zero for vehicle i, the gradient of the potential function of vehicle j is:

$$\nabla_{q_j} \psi_j = 2\lambda_1(s_j - s_{j,goal})\frac{\partial s_j}{\partial q_j} - \lambda_2 \sum_{j \neq i} \frac{V(j,i)}{\beta_\sigma^2(q_j,q_i)} \frac{\partial \beta_\sigma(q_j,q_i)}{\partial q_j} \tag{7.9}$$

The repulsive function, $\beta(.)$ in equation 7.3 is a function of the distance between two vehicles. So, the repulsive force sensed by vehicle i caused by vehicle j is exactly equal to the repulsive force sensed by vehicle j caused by vehicle i:

$$\frac{1}{\beta_\sigma^2(q_j,q_i)} \frac{\partial \beta_\sigma(q_j,q_i)}{\partial q_j} = \frac{1}{\beta_\sigma^2(q_i,q_j)} \frac{\partial \beta_\sigma(q_i,q_j)}{\partial q_i} \tag{7.10}$$

By combining the two equations 7.9 and 7.10 we have:

$$\nabla_{q_j} \psi_j = 2\lambda_1(s_j - s_{j,goal})\frac{\partial s_j}{\partial q_j} - 2\lambda_1 \frac{V(j,i)}{V(i,j)}(s_i - s_{i,goal})\frac{\partial s_i}{\partial q_i} \tag{7.11}$$

By actively moving the target point of the vehicles along their path, the attractive force of both vehicles remain between f_{min} and f_{max}. Therefore, if $\frac{V(i,j)}{V(j,i)} < \frac{f_{min}}{f_{max}}$ the equation 7.10 cannot get zero value. This means, if vehicle i has stopped before the intersection, vehicle j will not stop. This assumption is correct if vehicle i stops before the intersection, which puts it out of the forced visible zone of the vehicle j (See Figure 7.1).
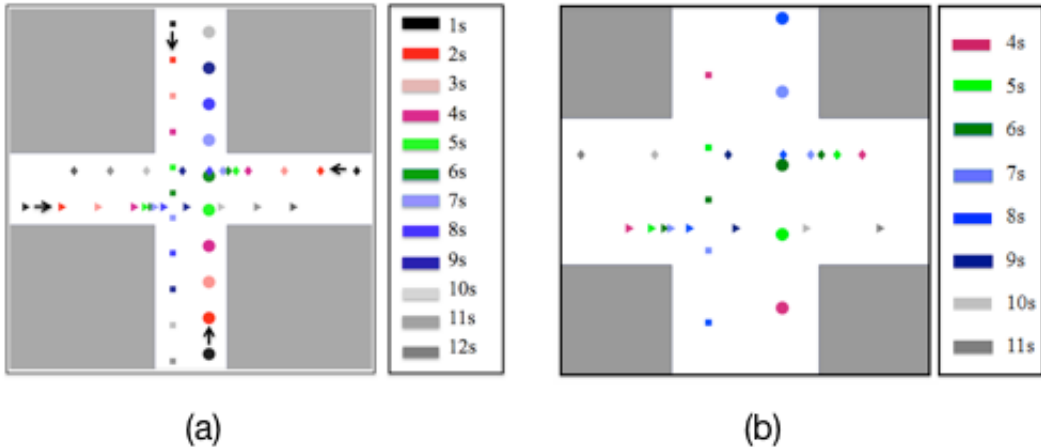
Figure 7.2: (a) Four vehicles are passing an intersection. Arrows show the direction of movement for each vehicle. The four vehicles are represented with four different shapes (circle, square, diamond, triangle). A given color corresponds to a given simulation instant listed on the left side of the figure. (b) shows the interval between the time vehicles enter the center of intersection and the time they successfully solve the intersection problem. This interval corresponds to the time interval between forth second and eighth second.

7.4.1 Four vehicles crossing an intersection

In this subsection we consider the control of four vehicles entering an intersection using their navigation functions given in equation 7.2. The vehicles are modeled with first order dynamics. The effect of taking inertia into account to get a smoother flow for vehicles is also illustrated. In the simulation, the four vehicles start at the same time from four different positions located at the same distance of the intersection. Hence, without manoeuvres, all the vehicles are expected to reach the intersection at the same time. The distance from the intersection is long enough so that each vehicle can reach its maximal velocity before getting close to the intersection.

The chosen time-step for the simulation is 20 ms. Values of the parameters in the navigation function are $\lambda_1 = 0.1$ and $\lambda_2 = 0.035$. Figure 7.2 illustrates the motion of the vehicles by displaying their position at each second. A given shape corresponds to a given vehicle and a given color corresponds to a given time. The black arrows indicate the direction of motion. After four seconds, all vehicles enter simultaneously the visibility zone of the others and their velocities start to change. The vehicle represented with circles (Figure 7.2) is five times heavier than other three vehicles. Thanks to the chosen navigation function, its velocity does not change significantly. All other three vehicles have the same weight, though it can be seen that the vehicle represented by squares keep also almost the same velocity. This is because the two other vehicles have to decelerate to free the intersection for the heavier vehicle.

Figure 7.3 shows the velocities of the four vehicles before, during and after crossing the
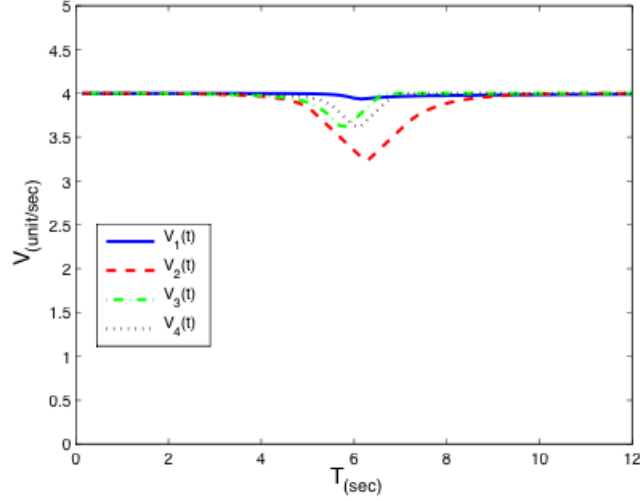
Figure 7.3: Change of the velocities for four vehicles passing an intersection. The heavier vehicle (shown in blue) has the least change in velocity than the others.

intersection. As mentioned previously, the velocity of the heavier vehicles does not change significantly.

7.5 How far is the DNF from a centralized optimal solution?

The goal of this section is to study the performance of the DNF in comparison with a central optimal solution. We pursue the optimal control strategy by introducing a cost function that takes the energy into account. The objective is to show whether a decentralized approach that relies only on local information and on limited computation power can exhibit performances close to the optimal controller. A standard LQR problem could not be run for a large number of vehicles because the collision avoidance constraints are non-linear and non-convex. However, keeping only the four vehicles and repeating the flow of four vehicles toward the intersection could imitate the best case central optimal controller. To compare the energy consumption according to the introduced index, we solve the centralized optimal problem for a certain throughput that allows repeating the flow of the vehicles over and over. However, this limits the comparison of the two methods to that certain throughput. In order to compare the throughput of intersection for the two different methods we use an adaptation of a near optimal method, introduced in [90]. The method provides a general scheme for collision-free trajectories using a cooperative control law based on optimal control. Avoidance control laws was presented as a barrier function added to the value function. We extend the cooperative avoidance control law in [90] to second order dynamics by defining a new barrier function. We also introduce a Collision Risk Indicator (CRI) to improve total performance of the multi-vehicle system . Theoretical proofs show the cooperative avoidance control in general nonlinear model. The centralized optimization is not the target of this thesis and could

Table 7.1: Simulation parameters used for comparing the efficiency of the autonomous vehicles passing an intersection either by using a DNF or a centralized optimal controller at the intersection

Simulation parameter	Value
λ_1	0.1
λ_2	0.035
Simulation duration	600 s
Length of the raod	150 m
Types of vehicles	2
Maximum velocity	30 km/h

be focused as a different approach, therefore the details have been presented in appendix A.

7.5.1 Simulation results

We introduce two different criteria for comparing the efficiency of the DNF method with a centralized optimal solution . The first criterion is the weighted average of energy used by the vehicles passing through the intersection. Energy consumption corresponds to control signal, i.e. acceleration and deceleration of the vehicles at the intersection. It is worth mentioning that it has been considered that vehicles with higher inertia are consuming more energy in acceleration and deceleration. The energy consumption index is defined as follows:

$$\bar{E} = \frac{1}{T_f N} \sum_i J_i = \frac{1}{T_f N} \sum_i \int_0^{T_f} u_i^T R_i u_i \tag{7.12}$$

In equation 7.12, T_f is the duration of the experiment and N is the total number of vehicles introduced in the system. The control signal is considered zero when the vehicle exits the system. The second criterion is the maximum pace at which vehicles could enter the intersection without generating queues longer than four non-moving vehicles.

The vehicles are created simultaneously and symmetrically in the four directions. Each vehicle is created at the same distance of the intersection and with their maximum velocity. In such a way, their initial acceleration has no impact. The vehicle creation rate is 2 vehicles per second for the first criterion. This means that, every two seconds four vehicles enter the whole system from the four different directions. The same vehicle generation pattern is applied for both control strategies.

The creation of vehicles to compute the second criterion is slightly different. In this case, vehicles are continuously created, providing that there are not more than four vehicles in a queue to enter the intersection. In other words, every time one vehicle could pass the intersection successfully, one new vehicle is created in the same direction of the previous one. This vehicle is created in a distance from the intersection similar to the previous vehicle. By

Table 7.2: Technical specifications of the two types of vehicles simulated for comparing the efficiency of the autonomous vehicles passing an intersection either by using a DNF or a centralized optimal controller at the intersection

Vehicle type	Mass $[kg]$	Max braking $[m/s^2]$	Max acceleration $[m/s^2]$
Type 1	1300	80.0	30.47
Type 2	20000	20.9	10.54

Table 7.3: Comparison of three control methods for vehicles passing through an intersection by indices as mean of energy consumption (MEC) of every vehicle and maximum rate of vehicles entering the intersection (MRV).

Control method	MEC (equation 7.12)	MRV
Traffic lights	45.6	1.4
Decentralized controller using DNF	14.14	2.4
Central optimal controller	9.86	2.6

this method of creating the vehicle, we compute the total number of vehicles that could enter the whole system in 600 seconds and calculate the rate of vehicles entering the intersection per second. Table 7.1 shows all the specification of the simulation and the DNF. Table 7.2 shows the technical specifications of the two type of vehicles considered in these sets of simulations.

Table 7.3 shows the comparison of the two different control methods according to the the two introduced criteria. It can be observed that the proposed navigation function induces energy consumption between the two other methods. The easily implementable proposed method is almost three times more efficient than the traffic lights in terms of MEC, while being only 30% less effective than the centralized method.

7.6 Micro-simulation of autonomous vehicles crossing an intersection using the DNF

In this section we introduce a new micro-simulation package that allow us to simulate large number of vehicles during a relatively long period and compare different coordination methods, including the ones running at the time such as traffic lights and roundabouts. The term "micro-simulation" refers to a family of simulation tools that study the traffic flow taking into account the characteristics and features of individual vehicles. This term has been introduced in comparison with "macro-simulation" where the goal is to study traffic flow as a whole without considering single vehicle dynamics. Micro-simulators are useful for studies in many field of intelligent transportation systems (ITS) as they are compatible with new traffic modules such as vehicle detectors, adaptive traffic signals and ramp metering. In general, micro simulators use different types of vehicle models and most of them provide car following and lane keeping strategies. Despite these advantages and capabilities of this family of simulators, none of them provide a direct access to control individual vehicles. Therefore, we connect a well-known micro-simulator, AIMSUN, to MATLAB in order to control each vehicle in a
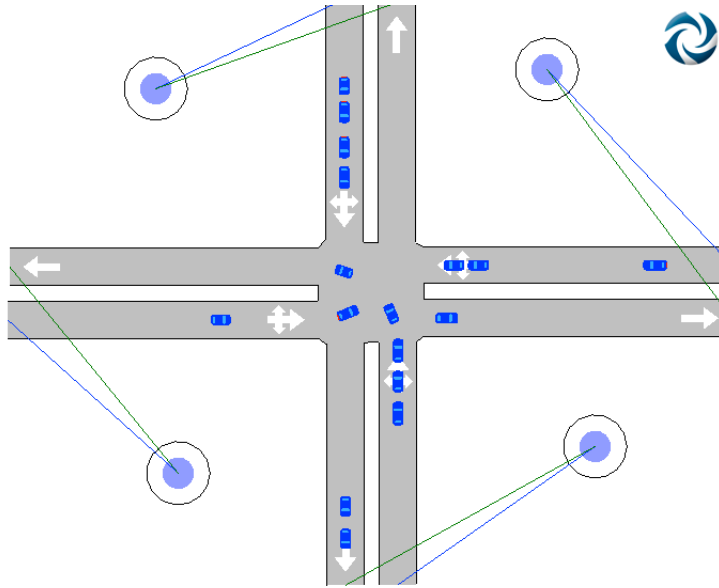
Figure 7.4: A simulated network in AIMSUN which consists of one junction and eight sections. The length of each section(street) is 60 meters and every section have a one lane. The simulation videos could be found:
https://www.youtube.com/watch?v=q68StIdpRGQ and
https://www.youtube.com/watch?v=9g4pt7Pzv10

decentralized manner. The architecture of combining the two software packages using an API is discussed in the next subsection.

To assess the performance of the DNF for controlling the vehicles crossing an intersection we simulated the two standard intersection control methods, traffic lights and roundabouts in addition to the DNF. Details of different scenarios and control of adaptive traffic lights will be discussed in the subsection dedicated to the results. The simulated intersection consist of one junction and eight sections, which correspond to 4 two-way streets (Figure 7.4). AIMSUN has a strong core for animating vehicles and controlling them according to car following models and defined controls as well.

7.6.1   Simulation environment

In order to make decentralized controllers for autonomous vehicles, the controllers and the model of communication have been coded in MATLAB. We connected MATLAB and AIMSUN to each other through an API. If a vehicle enters the network, this vehicle is tracked through the AIMSUN in order to make it easy to get the information and change the velocity of the vehicle. In every time step, the information of all vehicles are passed to MATLAB to model the communication and decentralized controller of the vehicles. The decentralized controller is programmed as described in section 7.3 and an appropriate control input for every vehicle is computed. This input is proportional to proper acceleration of the vehicle. The input is passed to AIMSUN in order to change the velocity and position of each vehicle on that time

step. Statistical information of vehicles such as their travel time, number and time of stops are gathered in order to compare different methods. Figure 7.5 shows the flowchart of simulation and information exchange according to important steps of AIMSUN.
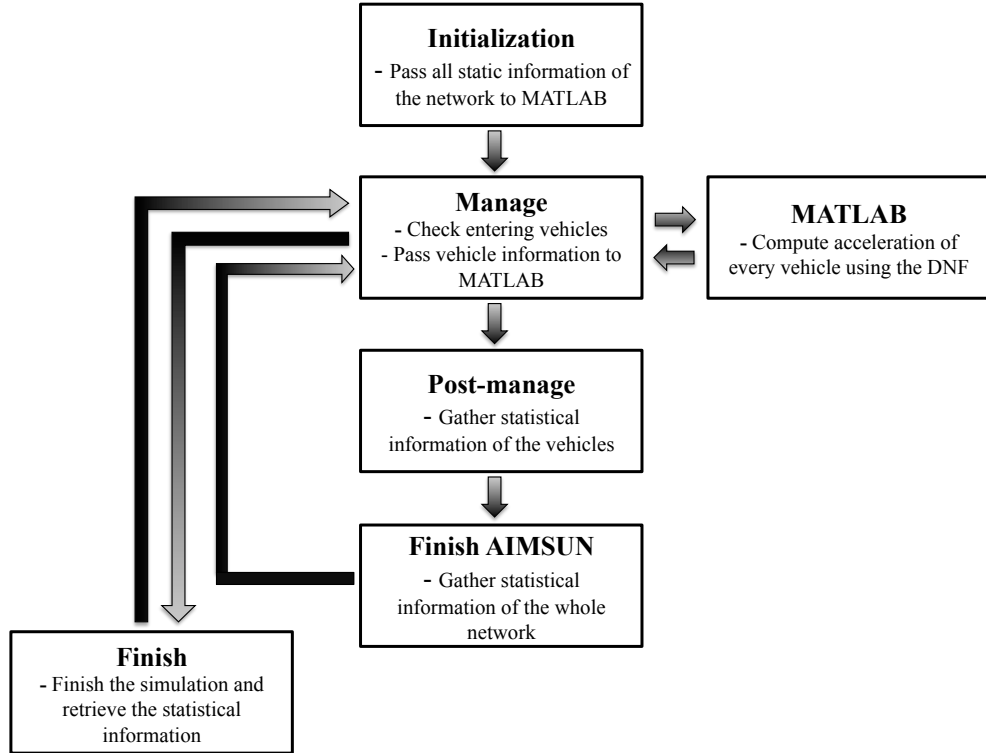
Figure 7.5: Steps of the simulation according to main steps of AIMSUN. Connection between MATLAB and AIMSUN is made in initialization step and in every time step when AIMSUN calls Manage module.

7.6.2 Results

The micro-simulation environment let us compare different control methods for crossing an intersection using detailed performance indices. This helps verifying the performance of the proposed method and also comparing it with other classical methods of crossing. Classical methods are those that are currently selected to manage intersections for vehicles controlled by human drivers, such as traffic lights, give way rules and roundabouts. The intersection consists of one junction, eight sections which correspond to 4 two-way streets (Figure 7.4). The length of each street is 200 meters, ending to an isolated intersection at the junction point. The maximum speed is 50 km/h, like the standard speed limit in urban areas. This speed limit is considered in the DNF method as well as the methods for comparison.

Traffic lights are a classical way of managing intersections and the most efficient way of controlling normal vehicles in terms of liability and controllability. Here, we simulated fully actuated

traffic lights, using the detectors integrated in all sections. To obtain useful information, the detectors are located at a long distance from the stop line (100 meters). No pedestrian pass time is considered to enable comparison with the autonomous approach. Detectors are working in a locking mode in which they count the number of vehicles passing in red and yellow intervals. The traffic light controller is designed as a single ring with minimum green light of 20s and maximum green light of 50s.

Vehicles entering the intersection have all the same inertia and velocity, acceleration and braking limits. Different levels of traffic have been directed in order to compare the three intersection control methods. In a low-level traffic situation, vehicles will not make spill backs, which mean there would not be any vehicle waiting to enter the intersection outside of the network.

The chosen simulation step is 100 ms. The parameters chosen for the navigation function are the ones shown in Table 7.1 and Table 7.2.

Sets of simulations have been carried out with vehicles having three choices at intersection. Vehicles could go straight, turn left or turn right, with the same probability. Simulations have been carried out for 5 sets, each set for one hour. The three intersection control methods are compared using performance indices, which are defined in following. These indices are chosen to show the total performance of the proposed method for the whole intersection, not just for one vehicle.

Vehicle average speed

This index of performance is the average speed for all vehicles that have left the network. This is calculated using the mean journey speed for each vehicle and then averaged over the total number of vehicles that have exited the network.

Number of stops

The number of stops is the mean number of stops of all the vehicles that have left the network from its exit section.

Vehicle throughput

Vehicle throughput or flow is the number of vehicles per hour that have passed through the network during the simulation time. It is worth mentioning that the vehicles are counted when leaving the network via an exit section. This means that if a blockade occurs the flow of the vehicles would decrease significantly. The average number of cars that should enter the network could be defined using the O/D matrix of the network.

Fuel consumption

According to the fuel consumption model presented in AIMSUN, every vehicle is either idling, cruising at a constant speed, accelerating or decelerating. The state of each vehicle is de-

Table 7.4: The fuel consumption for different phases of a vehicle's journey.

Vehicle phase	Fuel consumption rate
Idling	F_i
Decelerating	F_d
Speeding up with acceleration $a(m/s^2)$ and speed $v(m/s)$	$c_1 + c_2 a v$
Cruising at speed $v(m/s)$	$k_1(1+(\frac{v}{2v_m})^3)+k_2 v$

Table 7.5: Pollution emission rates for different phases of a vehicle's journey.

Vehicle phase	CO emission rate (g/s)	NOx emission rate (g/s)
Idling	0.060	0.0008
Decelerating	0.377	0.0100
Accelerating	0.072	0.0005
Cruising at speed		
10 km/h	0.060	0.0006
20 km/h	0.091	0.0006
30 km/h	0.130	0.0017
40 km/h	0.129	0.0022
50 km/h	0.090	0.0042
60 km/h	0.110	0.0050
70 km/h	0.117	0.0058

termined and the model then uses the appropriate relation to compute the fuel consumed for that state. For idling and decelerating vehicles, the rate is assumed to be constant. Fuel consumption rate during these four phases is shown in Table 7.4.

According to the UK department of transportation [91], the constants c_1, c_2, F_i and F_d are considered as 0.42, 0.26, 0.333 and 0.537 respectively. v_m is also the speed at which the fuel consumption rate is at its minimum value for a vehicle cruising at constant speed. This speed is 50km/h for cars simulated in this work.

Pollution emission

Pollution emission is also defined in the simulation in four states like that of fuel consumption. This is done by referring to a look-up table for each pollutant, which gives emissions (g/s) for every relevant combination of vehicle behavior [91]. The look up table used in this work is shown in Table 7.5.

Figure 7.6 and 7.7 show the performance indices for the DNF is comparisons with the two other control methods. The comparison between DNF method and traffic lights shows a 300% of improvement of the network throughput using decentralized control. Although traffic lights could show better performance with more lanes at the intersection, the structure of the intersection has to be kept the same for the sake of fairness in comparing the methods.

Regarding the number of stops, the DNF method induces fewer stops, even in a very highly
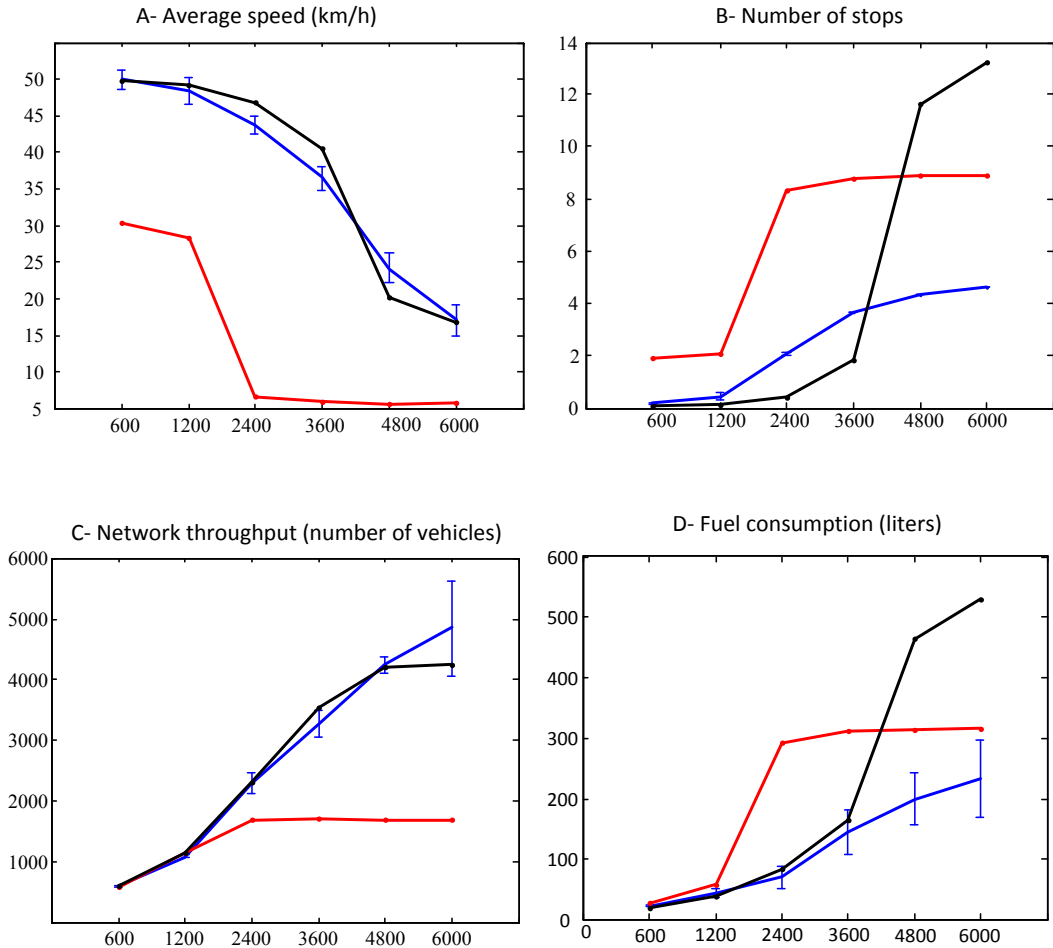
Figure 7.6: Simulation results for the three methods of control of intersection. DNF is shown in blue, actuated traffic lights in red and roundabout in black. For DNF, the error bars are showing the standard deviation. The horizontal axis shows the total vehicle input to the network.

congested situation, which directly influence the amount of fuel consumption and pollution emission. Even in low and medium traffic levels, the numbers of stops are less than the two other methods. This shows the basic idea behind the decentralized method, which propose smoother trajectories. Smooth passing of intersection may result in a lower average speed (as seen in Figure 7.6) but by reducing number of stops, decelerations and accelerations it reduces the fuel consumption and CO_2 emission.

The main goal in intersection management using DNFs is to get smoother trajectories for vehicles. As it could be seen in the comparison of the three methods, there is no significant difference between the proposed method and roundabout in terms of vehicle throughput and average speed. On the other hand, number of stops in the proposed method is significantly less than for the two other methods. This shows that the vehicles have smoother trajectories, which leads to less fuel consumption (verified in simulation and shown in figure 7.6). Limiting
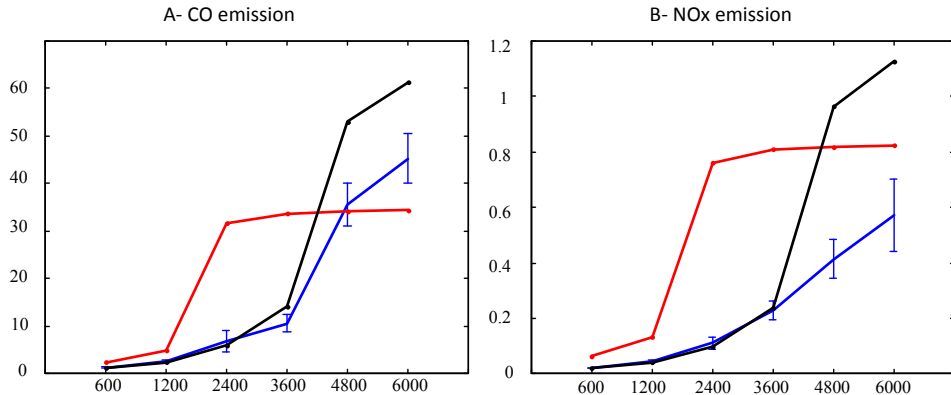
Figure 7.7: The pollution emission (CO and NOx) for the three methods of control of intersection. DNF is shown in blue with error bars showing the standard deviation from mean. Pollution emission with of adaptive traffic lights and roundabout is shown in red and black respectively. The horizontal axis shows the total vehicle input to the network.

decelerations and accelerations decreases fuel consumption. As vehicles are mainly cruising in decentralized navigation method, they consume significantly less energy. In this set of simulations, the performances with traffic lights are poor compared to the two other methods. However, the simulated method is an actuated scenario. In fact, traffic lights are not the best choice for this intersection as every section has only one lane. Adding lanes might increase the traffic lights performance.

Results are shown in figure 7.7. As we can see the CO emission with the DNF method is less than that of in roundabout. However it does not show better results in comparison with traffic lights. These results are not unexpected despite the fact that, in traffic light method, the flow of vehicles is considerably less than the other methods in high level of traffic. This means most of the vehicles are idling in the network in this case and emission of NOx is notably less than cruising. On the other hand, it is not the case with CO emission. Vehicles idling in front of traffic light are producing the same amount of CO as the vehicles cruising with speed of $10km/h$. Considering the low flow of vehicles in traffic lights method, DNF can reduce the energy consumption and pollution emission for every journey.

7.7 Conclusion

In this chapter we introduced a DNF which could enable autonomous vehicles cross intersections without collisions. This paves the way towards an on-board energy optimization by investigating the decentralized control of autonomous vehicles at intersections. The proposed method has been compared with current methods of managing intersections, which are adaptive traffic lights and roundabouts. The proposed method shows a significant improvement in comparison with classic traffic lights from a travel time and stop times point of view. The flow of the vehicles crossing is also improved simultaneously. With respect to many of the indexes,

the DNF method is vey near to a roundabout but has a better performance with respect to number of stops. Therefore,the major improvement is related to the number of stops, which directly means less energy consumption and less pollution emission. The proposed method also brings more comfort to passengers as the journey is held in a smoother way.

Identical navigation functions for vehicles could guarantee fairness and optimization for crossing vehicles. However, when there is a vehicle in a sensing zone of each of these vehicles, deceleration is inevitable. We have shown in this chapter that the designed navigation function does not have deadlock point, but for a smooth trajectory one can think of less deceleration. In the next chapter we will see how we can generate smoother motions with less decelerations and stops by letting some vehicles accelerate at the intersection.

Summary

Our main contribution in this chapter is the proposition of a novel DNF for vehicles crossing an intersection. To our best of knowledge, this is the first time that DNF is used as a coordination framework of vehicles passing an intersection. The DNF guarantees collision free passing for vehicles. In addition, we provide a sketch of proof for deadlock-free motion of vehicles crossing an intersection by guaranteeing no deadlock for two vehicles crossing. Beside the possibility to address the collision and deadlock problems, we showed that using inertia of the vehicles can facilitate the motion of the vehicles in addition to giving indirect priorities to heavier vehicles. We provided an API that can connect a micro-simulator environment like AIMSUN to a controller software like MATLAB and control each vehicle individually. Vehicles passing the intersection using DNF, consume three times less energy than vehicles passing the intersections managed by traffic lights.

8 Coordination of Autonomous Vehicles at Intersections Using Spatio-temporal DNF [*]

Overview

I N this chapter we introduce a new decentralized navigation function for coordination of autonomous vehicles at intersections. The main contribution is a navigation function designed for vehicles with predefined paths that uses expected time to intersection for collision avoidance. Because the navigation function uses both the position of the vehicles and their estimated arrival time at the intersection, we call the approach spatio-temporal Decentralized Navigation Function (DNF). In such a way, deadlock situations are avoided. As in the previous Chapter, different inertias of the vehicles are taken into account to enable on-board energy optimization for crossing. Heavier vehicles that need more energy and time for acceleration or braking are given an indirect priority at intersections. The proposed decentralized coordination scheme shows a significant improvement in energy consumption and in motion smoothness compared with traditional crossing with human drivers.

8.1   Problem formulation

As in the previous chapter, we considered a system composed of N autonomous vehicles. The goal of each vehicle is to cross an intersection with a minimal nominal speed deviation and without having any collision with other vehicles.

The position of vehicle i is known as $q_i = (x_i, y_i)$ in a global frame attached to the intersection. The path of the vehicle is predefined and is described by the parameter s_i . Therefore, the position of the vehicle in the global frame is directly derived from its location along the path using the parametric function $q_i = f_k(s_i)$, where k is the index of the chosen path. This

---

parametric function is an injective function, which means that computing the location of a vehicle along its path is straightforward knowing its global location. However, unlike the previous chapter, the motion of each vehicle along its path is modeled using second order dynamics:

$$\ddot{s}_i = a_i \tag{8.1}$$

where a_i is the acceleration of the vehicle along the path. The proposed dynamic model is realistic taking into account the assumption that the vehicles follow predefined paths to reach their destinations. Additionally, using this dynamic model, it is possible to introduce real-word acceleration and braking constraints, defined as a_{max} and b_{max} , respectively.

The speed limit is given by a function $v_{max} = v_{lim}(s_i)$ of the path parameter such that the centripetal acceleration in the bends remains below a predetermined value. Hence, the speed of vehicle along its path s_i is bounded in the interval $[0, v_{max}]$.

The problem is now to find a decentralized controller that guarantees vehicle safety and high capacity at intersection under the mentioned real-world constraints related to acceleration, speed and braking. We introduce a navigation function for each vehicle to enable decentralized control.

8.2 Spatio-temporal control approach

In the literature, a navigation function is introduced as a smooth mapping from a working manifold of the vehicles to a scalar, which should be analytic in the workspace of every vehicle [45]. The gradient of navigation function is attractive to the destination point of the vehicle and repulsive from other vehicles. So, an appropriate navigation function could be combined with a proper control law in order to obtain a trajectory for every vehicle leading to the destination and avoiding collisions. We propose a new navigation, which avoids simultaneous braking of all vehicles at intersection. In addition, using this DNF significantly improves the applicability and scalability.

8.2.1 Spatio-temporal DNF

The following navigation function is proposed:

$$\psi_i = \lambda_1 (v_i - v_{d,i})^2 + \lambda_2 \sum_{i \neq j} \beta(\tau_i, \tau_j, v_i) \tag{8.2}$$

where v_i is the speed of vehicle i along its path and $v_{d,i}$ is its desired speed. Note that

the desired speed is not necessarily the maximum speed. The maximum speed is given by the traffic regulations while the desired speed could be calculated to minimize vehicle's energy consumption along the path considering vehicle related factors. τ_i and τ_j are the expected time of arrival at the intersection for vehicle i and j respectively. The first term in the navigation function forces the vehicle to drive at the desired speed while the second term guarantees the crossing of the intersection without collision with other vehicles. λ_1 and λ_2 are the weights for the two terms in the navigation function. The function β is defined as follow:

$$\beta(\tau_i, \tau_j, v_i) = \begin{cases} \frac{1}{\sigma} \log(\frac{\sigma}{\tau_i - \tau_j}) v_i & 0 < \tau_i - \tau_j < \sigma \\ \frac{-1}{\sigma} \log(\frac{-\sigma}{\tau_i - \tau_j}) v_i & -\sigma < \tau_i - \tau_j < 0 \\ 0 & |\tau_i - \tau_j| > \sigma \end{cases} \tag{8.3}$$

where σ is the desired time difference between two vehicles reaching the intersection.

Vehicle will move toward the minimum point of the navigation function. If one vehicle is the nearest to the intersection the time differences of its arrival with others are negative. So, according to the β-function given in equation (8.3) it will accelerate and cross the intersection. On the other hand, the farthest vehicle from intersection will decelerate because the time difference is always positive. The β-function has non-zero value till the expected time of arrival for vehicles has the difference larger than σ. Tuning σ depends on the dimension of the intersection and the maximum speed allowed on the road.

8.2.2 Decentralized control of each autonomous vehicle

As control input, we use the gradient of the navigation function presented in equation (8.2) and the dynamics of the vehicles defined in equation (8.1)

$$u_i = -\nabla_{v_i} \psi_i \Psi \tag{8.4}$$

As the vehicles are moving on their predefined path and the gradient is calculated along the same path, the control actions are also acting in the expected direction.

8.2.3 Analysis of collision avoidance

In this subsection we discuss the potential of the proposed navigation function to guarantee collision avoidance at intersections. For this purpose we first consider a situation where two vehicles are crossing an intersection. We then extend the sketch for a system with a larger number of vehicles in simulation. Let us consider two vehicles entering an intersection (Fig. 8.1). Without changing its speed, the first vehicle would reach the middle of the intersection after time T_1, while the expected arrival time for the second vehicle is T_2. Without any loss of
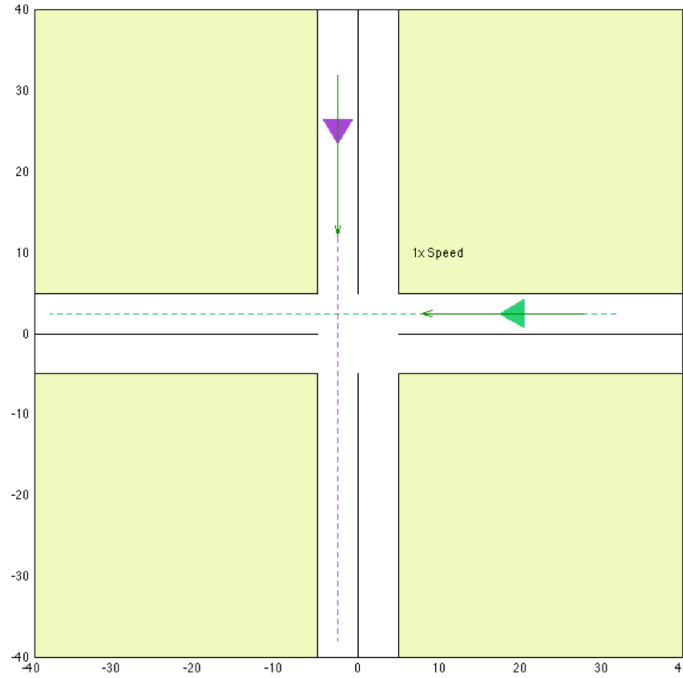
Figure 8.1: Two vehicles arriving at the intersection arround the same time.

generality, we consider a case where $T_1 > T_2$. This means, the second vehicles is predicted to arrive first at the intersection. Therefore, according to β-function in equation (8.3) the first vehicle will decelerate to guarantee a collision free pass for both vehicles. Collision avoidance is guaranteed if the first vehicle reaches the intersection at least σ seconds after the second vehicle. This time difference allows the second vehicle to leave the intersection before the first vehicle enters.

Collision avoidance conditions for two vehicles crossing an intersection

If the two weighting parameters λ_1 and λ_2 satisfy the following inequality:

$$\lambda_2 > \frac{\sigma}{log(\frac{\sigma}{T_1 - T_2})}(\frac{1}{T_2 + \sigma})v_{1,max} + \frac{1}{2}\lambda_1 v_{d1} \tag{8.5}$$

we can guarantee that the two vehicles passing the intersection will not collide.

To avoid collision in the worst-case scenario the first vehicle has to stop before reaching the intersection. So we can assume that the first vehicle has $t = T_2 + \sigma$ seconds to stop. This time interval gives a safe margin for the second vehicle to pass.

The change in the vehicle's speed during this time interval can be written as:

$$dV_1 = -\int_0^{T_2+\sigma} \frac{1}{2}\lambda_1(v_1(t) - v_{d1}) + \lambda_2 \frac{1}{\sigma} log(\frac{\sigma}{\tau_1(t) - \tau_2(t)}) dt \tag{8.6}$$

Both terms is the integral equation (8.6) will change over time. However we can compute an upper bound for the speed difference.

$$-\int_0^{T_2+\sigma} \frac{1}{2}\lambda_1(v_1(t) - v_{d1}) dt < -\int_0^{T_2+\sigma} \frac{1}{2}\lambda_1(0 - v_{d1}) dt \tag{8.7}$$

so

$$-\int_0^{T_2+\sigma} \frac{1}{2}\lambda_1(v_1(t) - v_{d1}) dt < \frac{1}{2}\lambda_1(T_2 + \sigma) v_{d1} \tag{8.8}$$

for the second term in equation (8.6) that is responsible for collision avoidance we can also write:

$$-\int_0^{T_2+\sigma} \lambda_2 \frac{1}{\sigma} log(\frac{\sigma}{\tau_1(t) - \tau_2(t)}) dt < -\lambda_2 \frac{1}{\sigma} log(\frac{\sigma}{T_2 - T_1})(T_2 + \sigma) \tag{8.9}$$

As mentioned, for a safe crossing of the intersection in the most conservative case, the first vehicle should fully stop before the time needed for the second vehicle to clear the intersection. If the vehicle starts with a maximum allowed speed, and its final speed is zero, we can write the speed difference by:

$$dV_1 = 0 - v_{1,max} \tag{8.10}$$

To guarantee the full stop, we can rewrite equation (8.6) as:

$$v_{1,max} < \lambda_2 \frac{1}{\sigma} log(\frac{\sigma}{T_1 - T_2})(T_2 + \sigma) - \frac{1}{2}\lambda_1(T_2 + \sigma) v_{d1} \tag{8.11}$$

So the conditions to guarantee collision avoidance could be rewritten as:

$$\lambda_2 > \frac{\sigma}{log(\frac{\sigma}{T_1 - T_2})}(\frac{1}{T_2 + \sigma}) v_{1,max} + \frac{1}{2}\lambda_1 v_{d1} \tag{8.12}$$

According to equation (8.12), we can tune the two parameters of λ_1 and λ_2 in order to get a
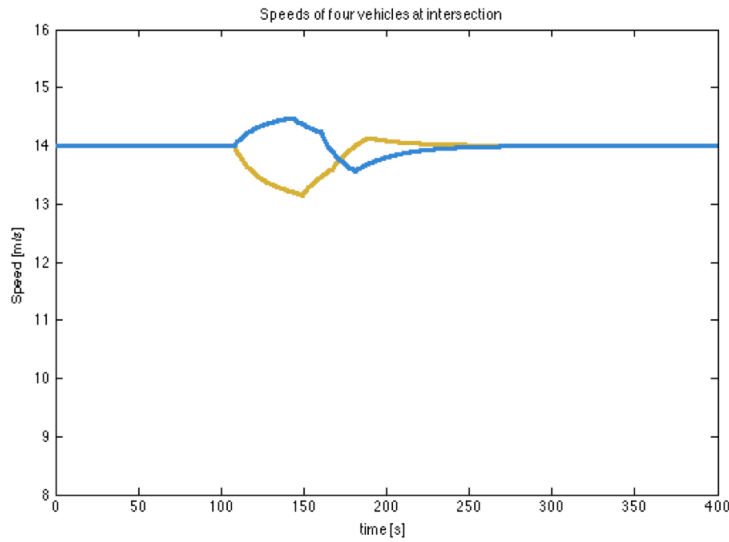
Figure 8.2: Change in the speeds of two vehicles at intersection, in order to safely pass the intersection. One of vehicle can accelerate to clear the intersection for the other one.

safe passing. It is worth mentioning that computing the parameters and using equation (8.12) does not mean that one of the vehicles stops before the intersection. Because the difference between expected arrival times is increasing along the path of vehicles, which will lead to less changes in speed of vehicles. Fig. 8.2 shows the speed of two vehicles crossing the intersection. A small change in the speed of two vehicles leads to the safe crossing of intersection.

For intersections with more than one vehicle we could give the same reasoning for every pair of vehicles, and guarantee that the ones decelerating will stop before intersection. Note that this way of tuning the parameters is the most conservative one that guarantees collision avoidance at intersection. Thanks to the proposed β-function, vehicles calculate smoother trajectories that lead to more fluent traffic (See Fig. 8.2).

8.2.4   Priority assignment

So far, all vehicles have been treated equally. However, based on certain criteria, the crossing of vehicles can be prioritized. The most obvious criterion is to give priority to heavier vehicles with higher inertia, thus saving energy. This can be implemented by weighting the β-function with a factor $V(i, j)$, which correspond to a matrix of inertia as proposed in the previous chapter.

$$\psi_i = \lambda_1 (v_i - v_{di})^2 + \lambda_2 \Sigma V(i, j) \beta(\tau_1, \tau_2, v_i) \tag{8.13}$$

$$V(i, j) = \frac{m_i}{m_j} \tag{8.14}$$

where m_i and m_j are the inertias of vehicles i and j respectively. Weighting the β-function with matrix of inertia is an indirect way of giving priority. Unlike direct priority assignment, it does not necessarily force lighter vehicles to decelerate, but it will put more control on them than on the heavier vehicles. The advantage of giving indirect priority is that it does not violate safety guarantees.

8.2.5   Information sharing

For constructing the navigation function, each vehicle needs information about itself and also other vehicles. Every vehicle needs its position, velocity and path. This information could be easily accessed with the today onboard sensors. Moreover, vehicles should communicate to get information about expected time of arrival of other vehicles as well as the inertia of other vehicles.

By keeping the number of messages and the amount of information transmitted to a minimum, it is possible to put more communication reliability measures in place. Furthermore, each vehicle, as an autonomous agent, may have privacy concerns, which should be respected. On the other hand, vehicles can only communicate when they are in distance smaller than their communication range. A notable advantage of the proposed method is to keep the communication complexity as low as possible as well as to take into account the communication range of vehicles. These points show that the proposed method is reliable considering the communication between vehicles.

8.3   Simulation and results

In this section, the performance of the proposed method is evaluated by simulation. The proposed navigation function is evaluated and compared with three other methods (i.e. intersection with traffic lights, centralized control and navigation function in [5]. The effectiveness of the proposed navigation function in coordinating the crossing of four vehicles is investigated. The convergence is obtained when vehicles leave the intersection without collision.

8.3.1   Four vehicle scenario

First, the control of four vehicles entering an intersection using their navigation functions given in equation (8.13) is considered (Fig. 8.3). The effect of taking inertia into account to get a smoother flow for vehicles is also illustrated.

In the simulation, the nominal trajectories of the vehicles are chosen in a way that without having control collisions will occur. All vehicles entered the area of the intersection at the same
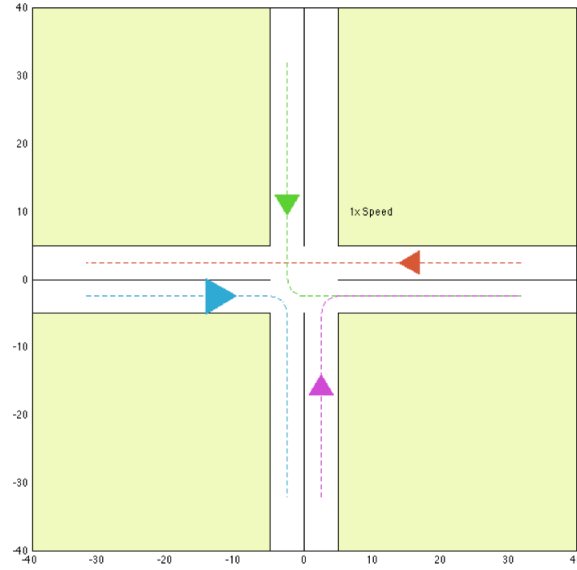
Figure 8.3: Intersection with four vehicles, the sizes of the triangles presenting the vehicles are proportional to their inertia. So, in this scenario blue vehicle is heavier than the other three. The simulation videos could be found:
https://www.youtube.com/watch?v=kUUK_oTwt3Y

time. So, the expected time of arrival to the intersection is more or less the same. Vehicles can communicate in a range corresponding to one third of the length of the road at each side of intersection. The chosen integration step for the simulation is 50 ms. The values of the parameters in the navigation function are $\lambda_1 = 0.5$, $\lambda_2 = 0.8$ and $\sigma = 4$. The desired velocity for all four vehicles is $50 km/h$ which is equal to $14 m/s$ and the maximum allowed velocity is $60 km/h$ equal to $16 m/s$.

Fig. 8.4 shows the velocities of the four vehicles before, during and after the crossing at the intersection. Vehicle number one is five times heavier than the other three vehicles. Thanks to the chosen navigation function, the velocities of the vehicles do not change significantly. The change in the velocity of the heavier vehicles is almost negligible. It is important to underline that, with the chosen navigation function parameters, none of the vehicles have to stop. Accordingly, the crossing is handled in a very smooth way. The navigation function gives the opportunity to the vehicles to accelerate at the intersection if they are not driving at their maximum speed. However, this feature is not mandatory to guarantee collision avoidance.

In the absence of other vehicles, the first term in the navigation function is still present. So, the vehicles will adjust their speed to reach the desired speed for that part of their paths. The navigation system of the vehicle can update the desired speed in an outer loop.
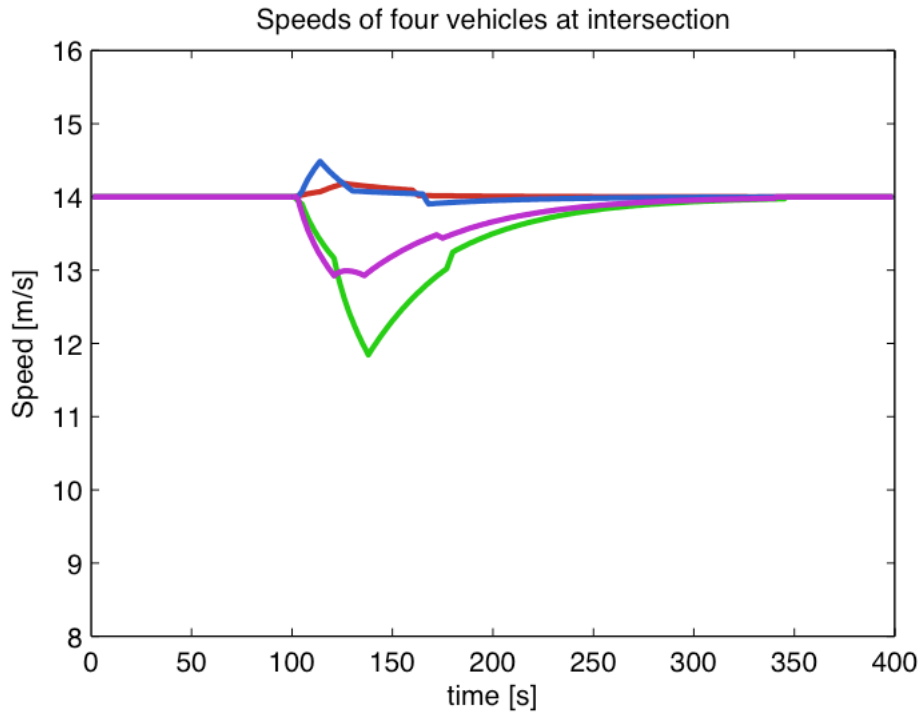
Figure 8.4: Change of velocities for four vehicles passing an intersection. Heavier vehicle shown in red has lesser change in velocity than others. Vehicle can accelerate to pass the intersection to give place to other vehicles to enter the intersection.

8.3.2 Energy efficiency

In this subsection, the coordination of autonomous vehicles at intersections using the proposed navigation function is compared to three other control methods. First, the less effective one with drivers obeying to traffic lights. Second, the most effective one with an optimal centralized control that relies on a full knowledge of all the vehicles and their environments. Third, the DNF introduced in the previous chapter. The objective is to show whether this decentralized approach that relies only on local information and limited computation power can exhibit performances close to the optimal scenario. For comparing these four scenarios, the same four-way intersection with one lane of traffic in each direction as considered in the previous subsection (Fig. 8.3) is simulated.

As first control scenario we simulate traffic lights. There are two traffic lights, which have been configured such that each vehicle is given a green light for 4 seconds, a yellow one for 1 second, and a red one for 4 second. Although there are qualified works concerning the timing of the traffic lights in the literature, they cannot be considered here for two main reasons. First, most of the works have been done for the management of multiple intersections, while our focus is in solving the problem at a single intersection. Second, vehicles appear in each direction symmetrically, which very much simplifies the timing problem. As a consequence, a symmetric timing pattern is selected as mentioned before that minimizes the global energy

Table 8.1: Technical specifications of the two different types of vehicles in the system according to the UK department of transport [91].

Vehicle type	Mass [kg]	Max deceleration [m/s^2]	Max acceleration [m/s^2]
Type 1	1300	80.0	30.47
Type 2	20000	20.9	10.54

consumption at the intersection.

As the second method, the proposed navigation function is considered with two types of vehicles with different inertias. 25% of the vehicles are heavier than the others and they are uniformly distributed in the four direction of the intersection. Table 8.1 gives the specifications of the two different kinds of vehicles. The elements of the priority matrix introduced in (9) are supposed to be known. As the vehicles have been modeled using second order dynamics, their masses are representative of their inertias.

The third scenario corresponds to the method proposed in the appendix A, which is an example of the application of centralized control approach for coordination. The forth method is the DNF introduced in the previous chapter.

The four methods are compared according to two different criteria. The first criterion is the weighted average of the energy used by the vehicles crossing the intersection. The energy consumption corresponds to the control signal, i.e. the acceleration and the deceleration of the vehicles at the intersection. The weighting is in a way that the vehicles with higher inertia are consuming more energy for acceleration and deceleration. The energy consumption index is defined as follows:

$$\bar{E} = \frac{1}{T_f N} \sum_i J_i = \sum_i \int_0^{T_f} u_i^T R_i u_i \tag{8.15}$$

where in equation (8.15), T_f is the duration of the simulation sets and N is the total number of vehicles introduced in the system. The control signal is considered being zero when a vehicle exits the system.

The second criterion is the vehicle throughput or flow, which is the number of vehicles per hour that have passed through the intersection during the simulation time. It is worth mentioning that the vehicles are counted when leaving the intersection via an exit section. This means that if a blockade occurs, the flow of the vehicles would decrease significantly. The average number of vehicles that should enter the intersection is defined using the O/D matrix of the network.

Table 8.2 shows the comparison of these four different scenarios according to the two different criteria. It is clear from this table that the presently proposed navigation function reduces

Table 8.2: Comparison of four control methods for vehicles passing through an intersection by indexes as mean of energy consumption of every vehicle and maximum through put of intersection

Control method	Energy cost according to equation (8.15)	Maximum throughput
Traffic lights	45.6	1.43
DNF	14.14	2.38
Spatio-temporal DNF	12.26	2.78
Centralized optimization	9.86	2.59

energy consumption even more than the previous DNF. The proposed method is only 24% less effective than the centralized one, while being easily implementable. It also allows a higher throughput as the vehicles have the ability to accelerate to clear the intersections more rapidly.

8.4   Conclusion

In this chapter, we modified the previous DNF proposed in the previous chapter in two ways. First, the navigation function is introduced as a function of the path. The attractive force is the one that regulates the speed of the vehicle toward its desired value. Second, the avoidance force from other vehicles is computed using the expected time of arrival of the vehicle itself and other vehicles in the communication range of this vehicle. Communication is active in the bounded sensing region of each individual vehicle. In this work, the navigation function has been modified in a way to optimize energy consumption taking the inertia of the vehicles into account. This paves the way towards on-board energy optimization by indirectly giving priority to heavier vehicles at intersections. The proposed method has been compared with the two centralized control approaches and a decentralized method proposed previously. The proposed method not only shows a significant improvement in comparison with the classic traffic lights from energy point of view, it is also more energy efficient in comparison with previously introduced navigation function. This reduction in energy consumption is achieved thanks to the absence of local minima in the new navigation function, which prevents simultaneous deceleration of both vehicles near the intersection.

✏️**Summary**

We proposed a spatio-temporal decentralized navigation function for vehicles crossing an intersection based on their desired speed and arrival time to the intersection. Then, we provided a sketch of proof to guarantee collision avoidacne. The proposed spatio-temporal DNF leads to smoother velocity profiles as the order of vehicles passing the intersection will not change over time. The novel β-function proposed in this work gives smooth acceleration profiles.

9 Model Predictive Coordination of Autonomous Vehicles Crossing Intersections [*]

Overview

In this chapter, the problem of decentralized coordination of autonomous vehicles at intersections is solved using decentralized model predictive controllers (MPC). The MPC concept have found wide acceptance in industrial applications as in intelligent transportation research area. MPC approach has been used in ground traffic management applications. MPC is a form of control in which the current control action is obtained by solving, at each sampling instant, a finite horizon optimal control problem. The solution is obtained using the current state as the initial state. The optimization produces an optimal control sequence and the first control in this sequence is applied to the system. In our approach, every vehicle is solving an optimal control problem taking into account its dynamics, dynamic constraints and constraints related to collision avoidance. Every vehicle formulates the collision avoidance constraints using the local information it gathers from the nearby vehicles. These constraints are formulated using the predicted trajectory of the other vehicles. In every time step the optimal controller produces the solution for the full horizon of control. However, the actuators will only use the input of the first step. This framework results in successfully coordinating autonomous vehicles at intersections in a decentralized fashion using local information about other vehicles.

9.1 Introduction

Model predictive control (MPC), also known as receding horizon control (RHC) is a family of control methods well-known for its ability to handle constraints. The concept is straight forward and applicable. At each sampling instant, the current control action is calculated by solving an essentially standard optimization problem in a finite horizon using the current

states as the initial conditions. The optimization will give a sequence of input from which only the first control is applied to the system and the process is redone at the next sampling instant.

The concept of MPC was first introduced in 1960 and its efficiency in process industry was shown in 1980s [94]. Since then, many researchers tackled issues such as feasibility of the online optimization, stability, robustness, and performance of MPC for linear systems [95; 96] as well as nonlinear systems [97].

MPC was traditionally implemented in a centralized fashion. New concepts such as distributed and multi-agent MPC were soon introduced mostly for large-scale systems by dividing the systems into multiple sub-systems. Decentralized MPC was introduced in a way that subsystems exchange information only before and after the decision making process. However, there is not a complete unanimity in the literature for these definitions. In both decentralized and distributed MPC, subproblems are solved for sub-systems.

In this chapter we put the decentralized coordination of vehicles at the intersection in a standard MPC framework. Each vehicle solves an optimization problem minimizing its energy consumption. The collision avoidance is tackled as constraints for MPC. At each time instant, each vehicle will solve the optimization problem and apply the first input from the solution sequence.

9.2   Problem formulation

We consider a system with N vehicles arriving at an intersection. These vehicles are modeled using second order dynamics. In this work, we consider that each vehicle knows its path, which means the vehicle can accelerate or decelerate but cannot deviate from the path. So we can use a second order one-dimensional dynamic model to describe each vehicle.

$$m_i \ddot{x}_i(t) = u_i(t) \tag{9.1}$$

where m_i is the inertia of the vehicle i (in this case this is the mass because the vehicles are in a translational move), x_i is the position of the vehicle i on its path and u_i is the input of the vehicle. We present the equation of motion using the discrete-time (time step h) state space presentation.

$$\begin{pmatrix} x_{1i}(k+1) \\ x_{2i}(k+1) \end{pmatrix} = \begin{pmatrix} 1 & h \\ 0 & 1 \end{pmatrix} \begin{pmatrix} x_{1i}(k) \\ x_{2i}(k) \end{pmatrix} + \begin{pmatrix} 0.5h^2 m^{-1} \\ hm^{-1} \end{pmatrix} u(k) \tag{9.2}$$

where x_{1i} and x_{2i} are the position and velocity of vehicles i along its path respectively. Now that we have a dynamic model for every vehicle, we need to select a control strategy to ensure that

each vehicle will pass the intersection without colliding to the other vehicles by considering the limits on the acceleration (a_{max}), deceleration (a_{min}), and speed (v_{max}).

9.3   Model predictive controller

The control strategy that we outline here provides decentralized non-cooperative control for each vehicle. In order to avoid aggressive reactions and inputs, our new approach uses predictive controller for each vehicle. To this end, we use an MPC algorithm to compute the optimal input to drive each vehicle from one side of the intersection to another avoiding collisions with other vehicles.

The key idea concerning the prediction part can be summarized assuming that at each time step, each vehicle considers that the situation will not change for all vehicles but itself. This assumption results to a problem, which can be solved in a decentralized linear quadratic optimization framework. The vehicles in the neighborhood of the intersection only need to locally share information about their position, velocity and intended direction (if they are passing straight or turning left or right) at every time step. With this strategy we will not converge to the global optimum solution, but the computation time is very quick and the required communication between the vehicles are reduced.

Every vehicle follows three successive steps to build its own MPC and optimize its velocity along its path to cross the intersection:
Step 1: Find (measure) the current state of own vehicle and communicate to get states of nearby vehicles.
Step 2: Perform an optimization on a defined cost function to find the optimal input sequence for the entire planning window taking into account dynamic constraints and collision avoidance.
Step 3: Implement only the first control action out of the whole sequence of inputs of the entire planning window.

Now, the challenge is to find a proper cost function that could guarantee a near optimal trajectory for each vehicle while the dynamic constraints and collision avoidance limits are satisfied. In the next subsection we describe the cost function and constraints used in MPC of each vehicle.

9.3.1   Cost function

In this approach we selected a quadratic cost function for each vehicle to ensure optimization regarding inputs and smoothness of the trajectories. The following cost function is proposed
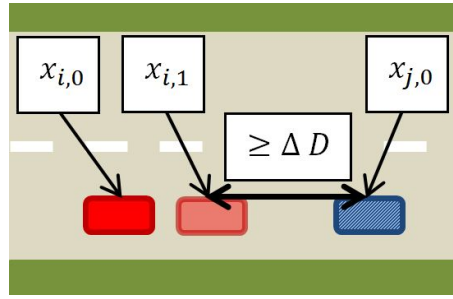
Figure 9.1: Constraints related to collision avoidance for vehicles in the same lane.

for vehicle i:

$$\sum_{j=1}^{N} q_i (v_{i,d} - x_{2i}(j))^2 + r_i u_i^2(j) \tag{9.3}$$

where $x_{2i}(j)$ is the speed of the vehicle i along its path during the jth time step. $v_{i,d}$ is the desired speed of vehicle i on the part of the path that optimization is being done and u_i is the input of the vehicle. The two constants q_i and r_i are weighting the importance of smoothness of the trajectory in comparison to the energy used by each vehicle along the optimization horizon (N). The first term penalizes the deviation of speed from desired speed. It is worth noticing that the desired speed could be different from maximum allowed speed of the road. The second term in the cost function penalizes the control input. The control input is a reference for energy consumption. Next, the collision avoidance will be integrated to the optimization problem by adding constraints.

9.3.2 Collision avoidance for crossing vehicles

To avoid collision between vehicles, we use constraints in the optimization problem. The main reason of handling collision avoidance using constraints rather than putting it in cost function is that by doing so the total MPC problem remains quadratic with linear constraints. The constraints to avoid collision is (Figure 9.1):

$$\left| d_{i,N} - d_{j,N} \right| \geq \Delta d \tag{9.4}$$

where $d_{i,N}$ is the distance of vehicle i from intersection predicted in the Nth time step. $d_{j,N}$ represents the same distance for the vehicle j. Δd is the minimum distance difference which guarantees crossing of vehicles without collision. To satisfy the constraint in equation (9.4) the vehicle i should decide whether to accelerate to pass before the vehicle j with at least a distance of Δd or to decelerate and let the other vehicle pass. In order to take a decision, we introduce a priority assignment method, which gives priority to vehicles nearer to the

intersection. It is worth mentioning that any type of priority assignment could be combined with the proposed MPC method.

The predicted arrival time for vehicle i is :

$$\tau_i = \frac{d_{i,0}}{v_i(0)} \tag{9.5}$$

$d_i(0)$ denotes the distance between the vehicle i and the intersection. The same predicted arrival time could be calculated for the vehicle j accordingly. Using the predicted arrival times as a priority index for vehicles, the constraint introduced in equation (9.4) can be rewritten as a single linear inequality:

$$\begin{cases} x_{1i}(N) - x_{1j}(N) \geq \Delta d & \tau_i \geq \tau_j \\ x_{1j}(N) - x_{1i}(N) \geq \Delta d & \tau_i < \tau_j \end{cases} \tag{9.6}$$

Of note is that every vehicle calculates the predicted arrival times for itself and nearby vehicles. These predicated arrival times are used to evaluate the priorities to pass the intersection. Given the assumption that vehicles calculate the same arrival time for all the vehicles, they will converge to the same priority list.Thus, in theory there is no need for a centralized priority assignment. However, the convergence could take time and the priorities could oscillate in the middle. To prevent the oscillation and to lower the computation time, we introduce the soft-constrained MPC in the Section 9.4.

9.3.3   Collision avoidance for vehicles in the same lane

Contrary to collision of crossing vehicles, which can only happen in one point in the intersection, the vehicles on the same lane have the potential for collision through their whole path. The constraint is valid for both vehicles in the Figure 9.2.

$$x_i(1) - x_j(0) \geq \Delta D \tag{9.7}$$

Although the constraint should be valid during the whole optimization, we only consider one-step ahead because implementation of the control input is done only for one step and simulation will run again in the next step.

9.3.4   Dynamical constraints

We take into account dynamical limits related to acceleration and braking as well as velocity limits due to the traffic regulations. All these limits could be presented as linear inequality
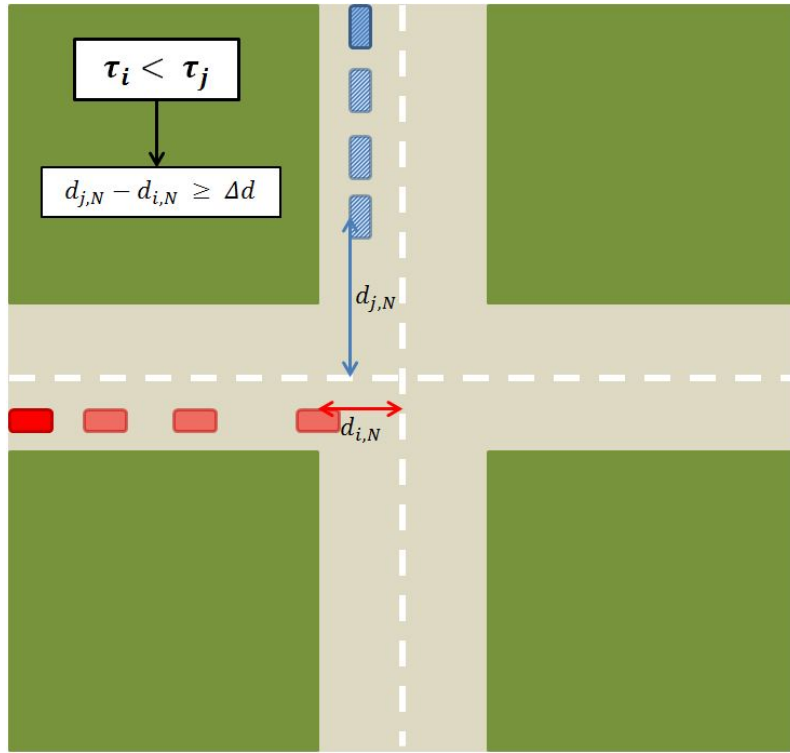
Figure 9.2: Initial and predicted positions of two vehicles. The initial positions are used to determine the priority of vehicles for passing the intersection. The predicted positions are used as constraints for MPC problem to guarantee collision avoidance.

constraints on input and state variables of each vehicle.

$$m_i a_{i,min} \leq u_i k \leq m_i a_{i,max} \quad \forall i \tag{9.8}$$

$$0 \leq x_{2i}(k) \leq v_{max} \quad \forall i \tag{9.9}$$

The constraint in equation (9.9) makes sure that vehicles neither go beyond speed limit nor drive backward.

9.4   Soft-constrained MPC

The constraints associated with collision avoidance of crossing vehicles are redundant and overly conservative for two reasons. First, the constraints need to be satisfied while vehicle are very near to the intersection, however vehicles could start optimization in a long distance to the intersection. Second, the constraints are redundant considering the cases with more than two vehicles involved. To clarify the problem, consider the case with three vehicles
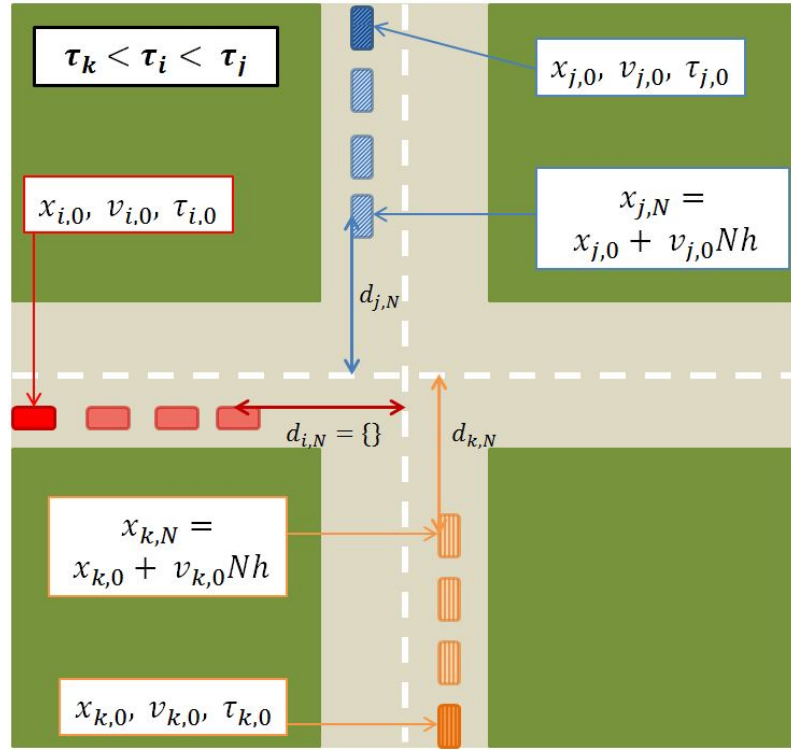
Figure 9.3: A scenario with three vehicles. This scenario clearly shows the importance of soft constraints in the MPC problem.

illustrated in Figure 9.3. If the constraint of not having collision is satisfied between the vehicle i and j and also j and k, there is no need for the constraint between vehicles i and k. We introduce soft-constrained MPC in order to solve this problem and guarantee the feasible and fast solution for optimization problem in every time step.

The main idea of soft-constrained MPC is that we allow violation of constraints related to collision avoidance of crossing vehicle in early stages of simulation for vehicles that are supposed to pass in the middle of two other vehicles. To ensure that the middle vehicle will follow a path between the two vehicles, we add a less inflexible term to the cost function. Hence, in the case of three vehicles (Figure 9.3) vehicles j and k are responsible to satisfy the collision constraints while the vehicle i can relax the collision constraints related to these two vehicles. This situation will continue until the constraints for vehicle i would be satisfied automatically. In scenarios with more vehicles, this rational is still valid which let us modify the cost function accordingly.

$$\sum_{j=1}^{N} q_i (v_{i,d} - x_{2i}(j))^2 + r_i u_i^2(j) + p_i (x_{1i}(N) - d_{average}) \tag{9.10}$$

where p_i represents the weight coefficient for the soft constraint and $d_{avearge}$ is the average

distance between the distance of two other vehicles with the intersection. The concept of soft constraint in this problem will simply allow the two other vehicles to expand their constraints and make place for the vehicle in the middle. After few steps, when the constraint of collision is satisfied for vehicle i, it switches to normal MPC. This transition is smooth because vehicle i already passed the intersection after the first vehicle and before the third one.

9.5   Crossing in a platoon

With the rapid growth of traffic volume, the problem of crossing intersections for autonomous vehicles is not only important in urban areas but also, in rural highway intersections. The idea of driving in platoons in highways is a well-studied domain in intelligent transportation area [98]. Platooning in highways not only increases the traffic flow by reducing the space between cars but also decreases the energy consumption by reducing dynamic drag force on vehicles. In general, the intersection signal timing does not take into account the presence of platoons in highways. Some studies have been made to integrate the idea of platooning of vehicles in intersection management by splitting the platoons [65]. Splitting the platoons at intersections is inevitable while controlling the intersection using traffic lights. As for autonomous vehicles, solutions could be investigated to keep the platoons while passing intersections. Moreover, closely passing vehicles can form a platoon before entering the intersection in order to decrease the computation time for optimization. In this case, the optimization could be done only for the leader and the followers will stay in the platoon. The vehicles entering from other directions rather than the platoon, would only deal with a train of vehicle as a single constraint. There is no need to consider many constraints related to every vehicle in the platoon. To integrate the concept of platooning for autonomous vehicles crossing an intersection, we modify the cost function for the vehicles in the platoon assuming that vehicle i is following vehicle k:

$$\sum_{j=1}^{N} q_i(v_{i,d} - x_{2i}(j))^2 + r_i u_i^2(j) + l_i(x_{1i}(j) - \hat{x}_{1k}(j+1) + d_{follow})^2 \tag{9.11}$$

where p_i is the weight coefficient, $\hat{x}_{1k}(j+1)$ is the predicted position of the follower in the next step. This new cost function imposes the follower vehicle to have the same speed as the leader. The only change in controller of other crossing vehicles is Δd, which should be increased in order to give enough space to the platoon to pass. Keeping the same MPC for vehicles in the platoon facilitates the smooth transition when the platoon splits or one vehicle leaves the platoon caused by unexpected communication problems.

Table 9.1: Types, constraints, and parameters of vehicles

Parameters	Values
Desired velocity (v_d)	$6m/s = 22km/h$
Maximum velocity (v_{max})	$15m/s = 54km/h$
Minimum velocity (v_{min})	$0m/s$
Mass of cars (m_{car})	$1.3e^3Kg$
Mass of lorries (m_{lorry})	$8.5e^3Kg$
Maximum acceleration of cars ($a_{max,car}$)	$3.47m/s^2$
Maximum braking of cars ($a_{min,car}$)	$-10m/s^2$
Maximum acceleration of lorries ($a_{max,car}$)	$1.15m/s^2$
Maximum braking of lorries ($a_{max,car}$)	$-5m/s^2$

Table 9.2: Control and simulation parameters

Parameters	Values
Weight of deviation of the velocity from the desired velocity (q)	1
Weight of acceleration or braking in the cost function (r)	2
Soft constraint weighting (p)	4
Platooning constraint in the cost function (l)	1
Optimization time step (h)	$500\ ms$
Optimization steps (N)	10
Collision avoidance constraint (Δd in equation (9.4))	$25m$
Following distance in a platoon (d_{follow})	10m

9.6   Simulation and results

In this section, the performance of the proposed method is evaluated by simulation. First, a scenario with two vehicles is shown in order to explain the simple model predictive controller. Then, we show a scenario with three vehicles in a symmetric situation, which could end in a deadlock using other methods. This scenario is important as it illustrates an example of switching from normal MPC to a soft-constrained MPC. A scenario with closely traveling vehicles will show the performance of MPC combined with platooning concept. Finally, A scenario with more vehicles will present the performance of MPC in normal traffic situation. The convergence, which is obtained when vehicles leave the intersection without collision will be shown in all scenarios.

Two different types of vehicles are considered in all the simulation scenarios, normal cars and lorries. The difference between normal cars and lorries are inertia, the limitations on acceleration and decelerations. Table 9.1 shows vehicle parameters as well as simulation parameters. Some parameters such as maximum velocity are road dependent and should be considered the same for both types of vehicles. Table 9.2 shows simulation parameters such as cost function weights and collision avoidance distances.
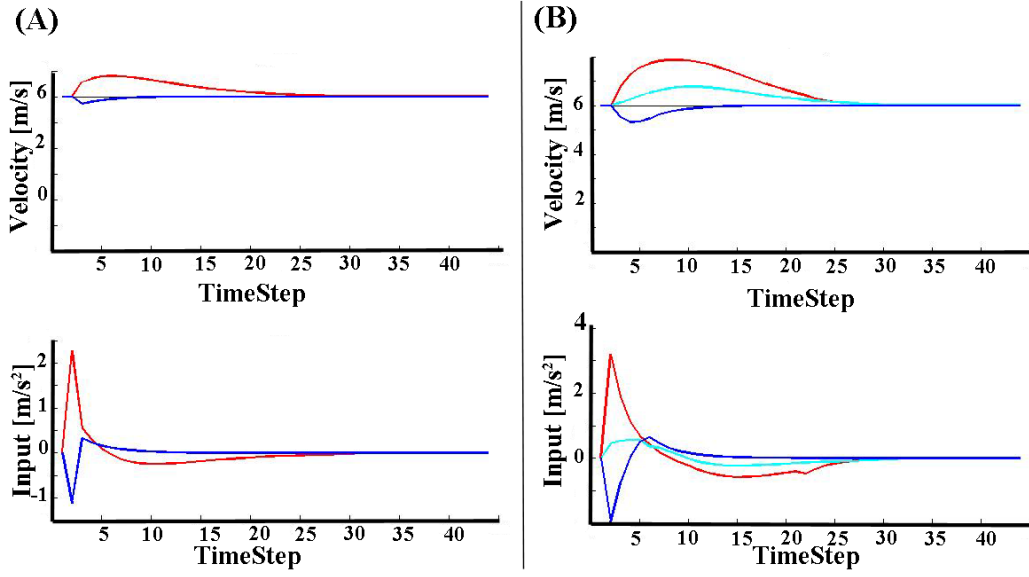
Figure 9.4: (A) A scenario with two different vehicles (one normal car, one lorry) arriving at the intersection at the same time. In order to smoothly pass the intersection one vehicle accelerates while the other decelerates.
(B) A scenario with three vehicles. First plot shows the speed and the second shows the inputs of vehicles. The vehicle shows in cyan passes in the middle of two other vehicles. In the sixth step it switches from soft constraints to normal MPC.

9.6.1 A scenario with two vehicles

Figure 9.4 shows the inputs and the speed profiles of two vehicles arriving at intersection at the same time. Without imposing control on vehicles collisions are inevitable. In order to smoothly pass the intersection one of the vehicles need to accelerate to pass before the second one. The second one decelerates so the change in the velocity will guarantee their safe passing. The red vehicle is a normal car and blue one is a lorry. The speed profiles show a smoother trajectory for the heavy lorry that results from its slower dynamics.

9.6.2 Soft-constrained MPC

A scenario with three vehicles entering the intersection from three different directions is the simplest scenario where soft constrained MPC is used. We show this simple scenario to clearly illustrate the effect of considering soft constrained MPC in controlling the vehicles. Figure 9.4 (B) shows the input and speed profiles of three vehicles. In the plot related to acceleration the switch from soft constrained MPC to a normal MPC could be seen in the sixth time step. However, this switching is smooth in speed profile.

9.6.3   Platooning vehicles

In this subsection we will show the performance of our method when vehicles arrive at the intersection in a platoon. As discussed in the previous section the vehicles in a platoon will change the cost function. We extend MPC with platooning concept not only to allow vehicles to pass in platoons but also let the vehicles to form platoons right before intersection in order to pass smoother.

Figure 9.5 shows six vehicles approaching the intersection, three of which are close at the same lane and could form a platoon. The green vehicle in the figure acts as a leader of the platoon. The two following vehicles, orange and blue, take higher speed to form a platoon. After platooning, the two vehicles follow the leader with the constant relative distance.
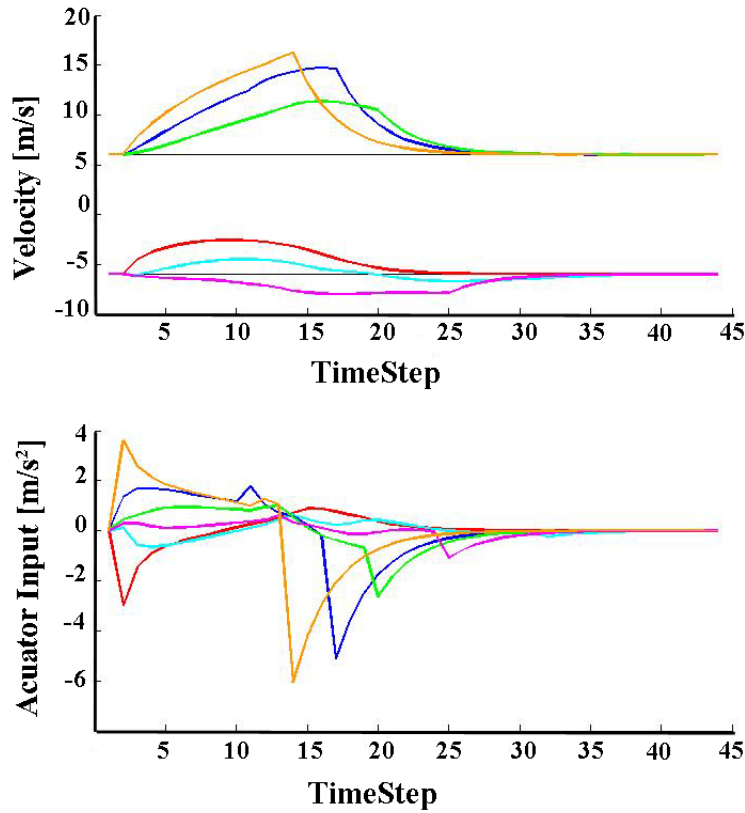
Figure 9.5: A scenario with six vehicles entering the intersection. Three vehicles (orange, blue, green) whose speeds are shown in positive, are traveling closely on the same lane. Therefore, they form a platoon. The two followers, orange and blue, accelerate to catch the leader (green) and after they follow the same speed profile.

9.6.4   A scenario with more vehicles

In order to show the convergence of the method with more vehicles crossing the intersection, we simulate a scenario with ten vehicles passing the intersection. Finding optimized solution takes more time compared to the scenarios with fewer vehicles. However, it is still possible to run the optimization in real time because the optimization problem is solved distributed for each vehicle. The flow of vehicles in this scenario is 2400 veh/hour, which is a normal traffic flow for an urban intersection. This suggests the practicality of the method since it can be used at intersections with normal traffic flow. Figure 9.6 shows the velocity and acceleration profiles of the vehicles.
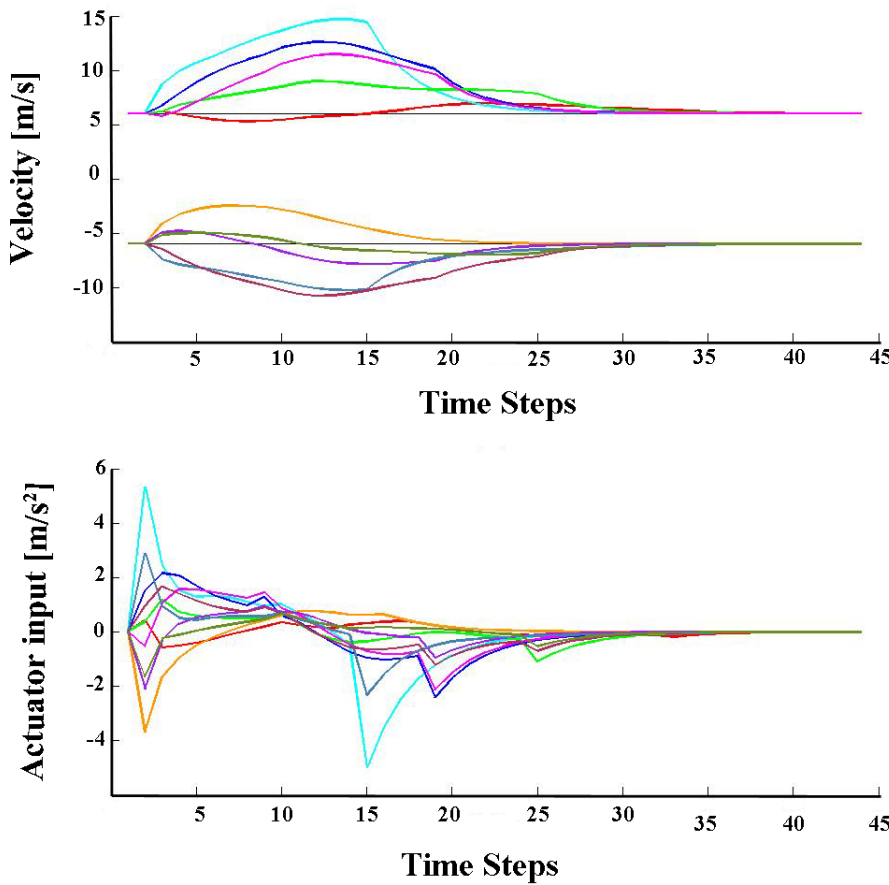
Figure 9.6: A scenario with more vehicles crossing the intersection. This simulation shows the convergence of the method and optimization problem in normal traffic flow. In order to clearly show the speed profile of all vehicles in a single plot, we multiply the speed profiles of some vehicles in a negative sign.

9.7   Conclusion

In this chapter, we introduced a decentralized model predictive controller framework to solve the problem of coordination of autonomous vehicles at intersections. This model predictive controller consists of a quadratic cost function and linear constraints. The quadratic cost function, assures minimum energy and smoothest trajectories for vehicles. The collision avoidance is guaranteed using linear constraints and predicted time of arrival at the intersections. In order to run the optimization in real time the approach is elaborated using soft constraints. In the framework of this problem, every vehicle is modeled using a second order dynamic. Dynamic constraints such as acceleration, deceleration and speed limits are taken into account. The convergence of the proposed method is shown using simulations for different scenarios. The proposed method not only assures near optimal solution in a decentralized approach but also has the capacity to be run in real time for normal urban traffic flow.

Summary

We presented an MPC framework for coordination of autonomous vehicles at intersection modeling vehicles with linear second order dynamics. The introduction of the quadratic cost function and setting collision avoidance as a set of linear constraints ensures the existence of solution in a linear-quadratic MPC framework. The approach takes velocity and acceleration constraint into account as well as realistic vehicle communication models. We showed the practicality of the proposed method for platoon of the vehicles crossing an intersection.

Coordination of Fiber-fed Robotic Spectrographs

10 Introduction to Fiber Positioners

Overview

Massive spectroscopic surveys allow astronomers to measure the redshifts of distant objects, and in particular to unveil the large-scale structure of the Universe. In order to improve the surveys compared to what is currently possible, a paradigm shift in the observation techniques is required. The currently developing massive parallel measurement systems aim at using mechanical fiber positioners that will automatically place a fiber in front of a source to be targeted. These positioners need to be fast (repositioning in ideally less than 30 seconds corresponding to the readout time of the detectors), should not collide with a nearby one (or we will not be able to conduct the redshift measurement), and be very accurate (positioning accuracy of less than 5 micron: in order to align most of the distant galaxy light in a $107\mu m$ fiber).

10.1   Introduction

In 1998, three astrophysicists - Perlmutter, Schmidt, and Riess- and their teams announced that not only our universe is expanding but also this expansion is accelerating ([3; 4]). Later, in 2011 they won the Nobel Laureates in Physics for their discovery. The reintroduction of Einstein's cosmological constant to explain this acceleration, although matching all the cosmological data so far, cannot be understood within the standard theory based on Quantum Field Theory. So, theoreticians have proposed many alternatives to the cosmological constant. In particular, the concept of Dark Energy as an invisible fluid that pervades the cosmos is the widely accepted proposal. Since then, for a large group of scientists, one of the main challenges in cosmology is to discern the nature of the dark energy. In order to achieve this goal, different observational techniques have been proposed to tackle the question of the

geometry and the evolution of the universe. One of the key techniques is the measurement of the Baryonic Acoustic Oscillations (BAO) in massive spectroscopic surveys.

The very first large-scale spectroscopic survey ([99]) revealed a cosmic web structure with filaments and voids, and soon after, further investigations questioned the existence of a cosmological constant ([100]). More recently, following the discovery of the imprint of the BAO in the sloan digital sky survey (SDSS; [101]), massive spectroscopic surveys have been developed to measure accurately the evolution of the distance-redshift relation using the BAO technique. In particular, 1) the WiggleZ redshift survey ([102]) has completed a ~250,000 redshift survey of star-forming galaxies (at $z < 0.8$) at the 4m Anglo Australian Telescope (AAT), 2) the Baryonic Oscillation Spectroscopic Survey (BOSS; [103]) will complete a major redshift survey of 1.4 million galaxy redshift (at $z < 0.7$) and 160,000 high-redshift Lyman-α quasars using the SDSS telescope in 2014, and 3) the extended-BOSS survey (2014-2020) will complete the first BAO survey over the redshift range $0.7 < z < 2.2$ on galaxies and quasars using the SDSS facility.

To go beyond the throughput limits of current surveys, new technologies are being developed to hasten the future spectroscopic facilities. The way forward is not only to use larger aperture telescopes, but also to benefit from larger multiplexing. Over the past few years two major projects have been approved for construction. First, the Primary Focus Spectrograph (PFS), is a Japanese lead project that aims to develop a 2400-fiber spectrograph on the 8.2 m Subaru telescope. Second, the Dark Energy Spectroscopic Instrument (DESI)[*], a DOE lead project, that aims to develop a 5000-fiber spectrograph on the Mayall 4m telescope. Other less advanced projects are also being prepared such as 4MOST and WEAVE.

Spectrographs fed by massive fiber bundles are one of the most advanced and proven methods compared with multi-slit approach. Various technologies have been proposed for fiber positioning. For example, in the case of the SDSS spectrograph, fibers are placed manually into the holes drilled in an aluminum plate. This operation is done during the day time prior to observations. In the case of the AAT spectrograph, a robot places fibers one at a time at the target points. This operation is done while another set of fibers are observing. In the case of the Chinese Large Sky Area Multi-Object Fibre Spectroscopic Telescope (LAMOST; [104]), and the Japanese Fibre Multi-Object Spectrograph (FMOS; [105]) robotic fiber positioners are placing in parallel the fibers at the target points just before the observations are conducted. The key advantage of using robotic positioners is that the fibers could be positioned simultaneously. So if the robotic system is fast, reconfiguration time could be executed during the observation overheads (readout time of the detectors and slewing of the telescope).

In the next-generation fibre-fed spectrographs such as DESI, MOONS[†], and PFS[‡], projects, small robots are responsible to position the fiber-ends. Figure 10.1 shows a 8mm in diameter fiber positioner designed and built in collaboration between EPFL and Instituto de Física

---

[*]   http://desi.lbl.gov
[†]   http://www.roe.ac.uk/ ciras/MOONS/VLT-MOONS.html
[‡]   http://sumire.ipmu.jp/en/2652
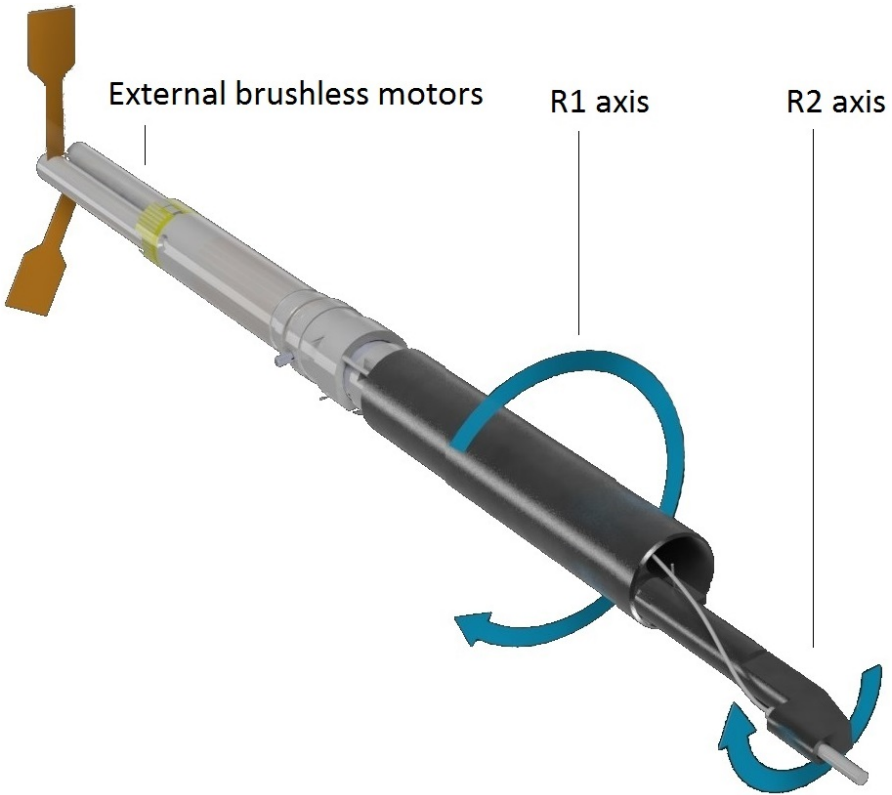
Figure 10.1: CHESbot, a fiber positioner prototype designed and built by EPFL in Switzerland and Instituto de Física Teórica, Universidad Autónoma de Madrid in Spain. CHESbot has two rotational degrees of freedom R_1 and R_2. Each degree of freedom is actuated by a DC brushless motor.

Teórica, Universidad Autónoma de Madrid in Spain. In order to improve the versatility of the system and ensure the maximum number of observed galaxies, the robots share working spaces. All the three mentioned projects will use a robot with two degrees of freedom and eccentric rotary joints (so called $\theta - \phi$ design shown in Figure 10.2). Our initial motivation for taking $\theta - \phi$ design as an example in this thesis, undertaken as part of DESI project, is to solve the collision challenge in motion planning of these robots. The proposed method could directly overcome the collision problem for any robot with two rotary joints that move a single fiber-end such as for the aforementioned DESI and PFS projects. This work presents a new motion planning method for the positioner based on Decentralized Navigation Functions (DNF). The proposed trajectories guarantee collision-free paths for all the fiber-ends. The motion planning is decentralized in order to be able to extend the solution for large-scale positioner. In addition, the DNF method could be adopted for other fiber positioning systems with different geometry patterns in case they have potential risk of collision. At the time of writing this thesis, three main ongoing projects were directly dealing with the coordination and collision avoidance problem for fiber positioners [106]. In the following sections, we describe the aims and specifications of these projects. In the next chapter, we propose a framework based on the DNF that can coordinate the fiber positioners for all these projects
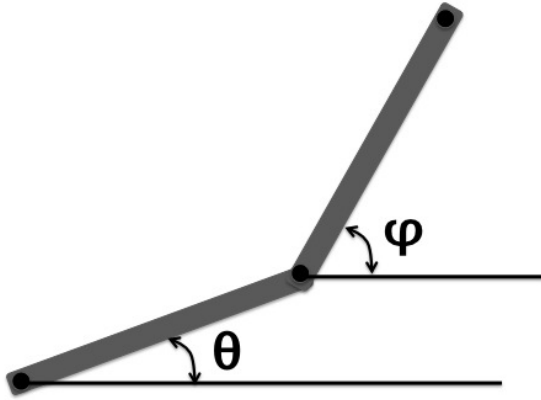
Figure 10.2: Schematics of a robot with two degrees of freedom and eccentric rotary joints called $\theta - \phi$ design.

and guarantee collision and deadlock avoidance.

10.2   Dark energy spectroscopic instrument

The dark energy spectroscopic instrument (DESI) project is a next-generation ground-based dark energy experiment to study BAO and RSD with a wide-area ($14,000$ square degree) [8]. DESI is an international project guided by the Lawrence Berkeley National Laboratory. With its wide area, DESI will survey tens of millions of galaxies and quasars. The survey is planned to operate from 2018 through 2022.

DESI will observe a part of the universe with a density larger than 1500 galaxies/deg^2. Performing such a deep and wide spectroscopic survey in a five-year period requires a high-tech spectrograph capable of observing thousands of spectra simultaneously. To achieve this goal, DESI includes the following components in a currently existing 4-meter optical telescope (Fig. 10.3):

- Prime focus corrector optics to attain a wide field of view,

- A focal plane with robotic fiber positioners,

- Fiber optics cables,

- Spectrographs,

- A realtime controller and data acquisition systems,

- Data processing pipeline that ingests raw data from the detectors and produces calibrated spectra useful for cosmological investigation.
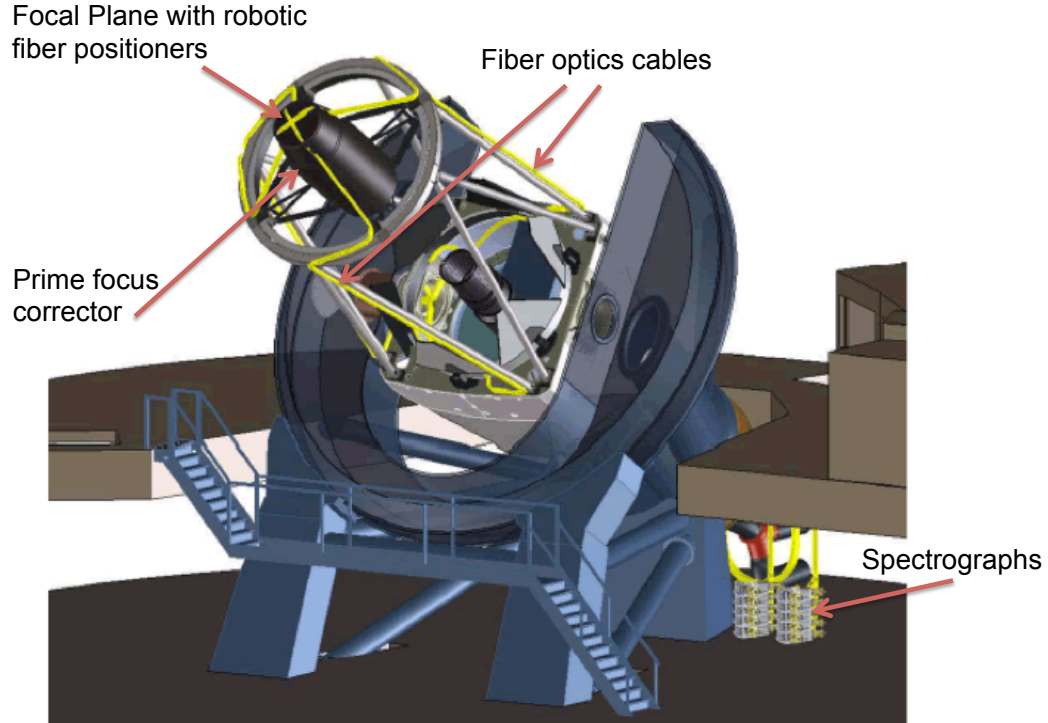
Figure 10.3: The dark energy spectroscopic instrument mounted on a 4-m telescope. A corrector lens and the fiber positioner will be installed at the prime focus. The yellow trace is a fiber routing path from the focal plane to the spectrograph room. Image taken from (http://desi.lbl.gov/cdr)

The host telescope is capable of supporting the prime focus instruments. According to the lenses' field of view, the survey duration, and the spectrography quality (signal to noise), the focal plane needs to accommodate 5000 optical fibers, each with 12 mm workspace. For each exposure, all the fibers should be reconfigured in less than a minute with the fiber tips placed with an accuracy of $5\mu m$ from a target point. This target point is the projection of a galaxy on the focal plane. In other word, by putting the fiber in that point, all optical information from the galaxy could be read with that fiber.

During the exposure time, fibers transport the light from the focal plane to the spectrographs in the control room approximately $40m$ away. In order to maximize the survey throughput, the fibers should be positioned for the next observation while the data is analyzed and stored. The telescope also slews to a new field at the same time.

The focus of this part of the thesis is motion planning and collision avoidance for the fiber positioner. Therefore, we view the focal plane with robotic fiber positioners in details in the next subsection.
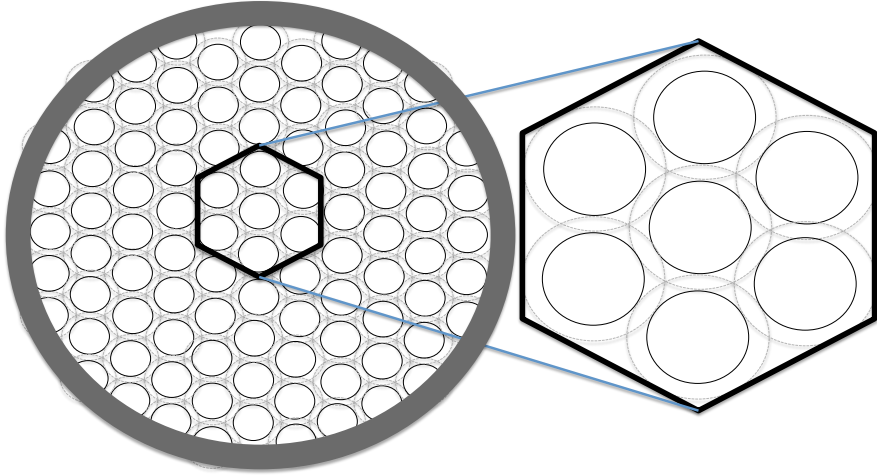
Figure 10.4: Configuration of fiber positioners on a focal plane. Positioners shown as black circles, form a hexagonal array in order to cover a patrol disc (shown in a dashed gray circle), as versatile as possible.

10.2.1 Focal plane with robotic fiber positioners

The main concept in the design of the focal plane in DESI is a collection of identical positioners distributed over a hexagonal array (See Fig. 10.4).

Each positioner is therefore assigned to a single target. If no target is accessible, the positioner will observe the sky. The positioner could cover the entire focal plane and each moves a fibre head toward a desired location within the patrol disc of positioner. Because we require that any point of the focal plane to be accessible by a fiber, there will be regions of the focal plane where the workspaces of adjacent positioners will overlap. In these overlap zones, there is a risk of actuator collision. Target assignment and collision avoidance strategies will therefore be among the challenges in the design of such a massively parallel fibre-fed spectrograph.

10.3 Prime focus spectrograph

The Prime Focus Spectrograph (PFS) [107] is an optical near-infrared multi-fiber spectrograph with 2400 fibers, each of which is set onto a target position quickly by a fiber positioner using two-staged rotational motors. It is planned to be mounted on a 8.2-meter telescope called Subaru at Mauna Kea, Hawaii. The project has been endorsed by the Japanese community as one of the main future instruments of Subaru . The spectrograph system targets galaxy surveys, Galactic archaeology, and studies of galaxy/AGN evolution.
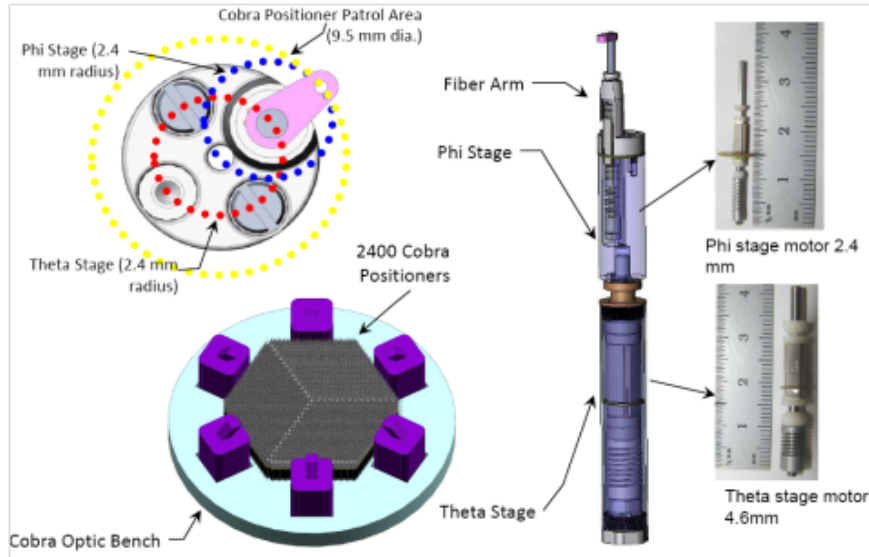
Figure 10.5: Focal plate configuration and a single fiber positioner designed and built for PFS. The image is taken from (http://sumire.ipmu.jp/pfs/instrumentation.html)

Very similar to DESI, the fiber positioners are distributed in a hexaonal shape with 8-mm separations from their six adjacent poisitioners each [108] (Figure 10.5). The fiber positioner is called Cobra. Cobra consists of two-stage piezo-electric rotary motors. This two-motor rotation provides a total of 9.5 mm-diameter patrol region. The main difference between DESI and PFS is the use of different electrical motors. PFS uses piezo motors, while DESI benefits from the state-of-the-art very small (4 mm) DC brushless motors. This difference affects the electronics that control the positioners. However, the concept of coordination, motion planning and collision avoidance is very similar for both projects. The final trajectories in the two project could be different due to different constraints on the velocity and acceleration of the motors.

10.4   Multi-Object Optical and Near-infrared Spectrograph

The Multi-Object Optical and Near-infrared Spectrograph (MOONS), is a european project supported by the European Southern Observatory (ESO). The goal of the project is to build and operate an array of 1000 fiber positioners, to study the galactic structures and galaxy evolutions [109]. The main difference between MOONS and the two previously mentioned projects is the range of spectrography. The spectrography range in MOONS is near infrared and consequently more noisy than the other two projects. Due to the different requirements on the sky subtraction for bright and faint targets (the noise on the spectrography), the positioners should be able to act in pairs to perform the cross-beam switching. This means each fiber that is looking at a galaxy has a partner, which is dedicated to observe the sky with a distance of few arcsecs. Therefore, the positioners should be coordinated in a way that two positioners could cover a small area near a galaxy. In MOONS, each positioner needs to cover a patrol
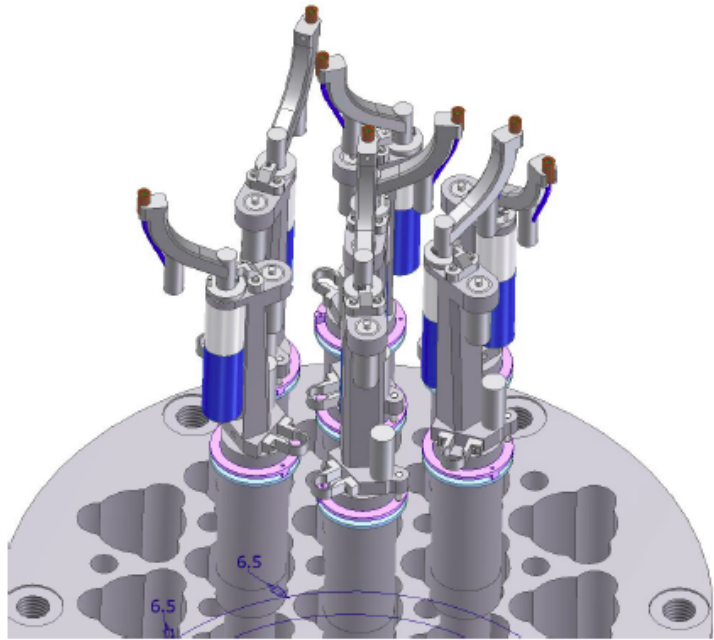
Figure 10.6: Current design of fiber positioner in MOONS. The robot can reach a distance almost twice as its radius.

area much larger than its own size, so that it can guarantee the feasibility of operating the positioners in pairs. Figure 10.6 shows the most updated design of the positioners that fulfils these requirements. Due to the larger overlap between the working spaces of the positioners, the coordination and collision avoidance are more challenging compared with that of DESI and PFS.

10.5   Target assignment

Several strategies can be developed in order to assign targets -galaxies, quasars or stars- to the end effectors -fiber-ends- of the positioner. The simplest approach is to select randomly for each positioner any of the targets lying within the corresponding working space (patrol disc). To achieve an optimal solution, which means that the maximum number of targets is observed during a certain period of time, the drain algorithm was introduced [110]. The method ensures the observation of the maximum number of targets in the first few sets of observations. Using both randomly distributed targets and mock galaxy catalogues, the authors showed that the number of observed galaxies could be increased by 2 percents in the first set of observations.

In this thesis we assume that target assignment has been effectively done by one of the mentioned algorithms under three main assumptions. First, each target is assigned to one positioner only, and each positioner is assigned to one target maximum. Second, the target assigned to each positioner is always within its patrol disc and hence reachable by the positioner. The minimum distance between two assigned targets is d. Thus, the focus of the work
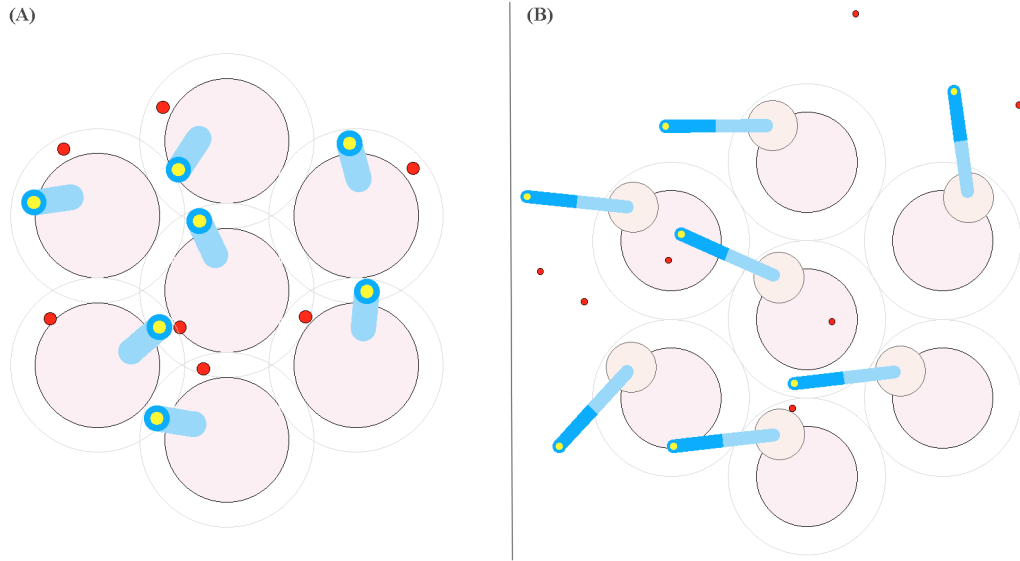
Figure 10.7: Seven fiber positioners of (A) DESI and (B) MOONS. The red dots show the target points of the positioners. Each fiber positioner is assigned to one of the targets.The longer second arm in the MOONS fiber positioner increases the risk of collision.

presented here is on the coordination of positioners in motion to avoid collision. We assume that the target of each positioner is fixed and known to the positioner.

10.6 Collision avoidance

In all the three mentioned ongoing projects, the fiber positioners share patrol discs. Figure 10.7 shows the seven positioners of DESI and MOONS. In MOONS, the risk of collision is even higher due to the longer length of the second arm. In this subsection, we show why a simple fold-turn-extend algorithm fails in motion planning of fiber positioners. A simple fold-turn-extend algorithm could be summarized as follows:

1. Retract R2 to a safe area by the folding the arms

2. Rotate R1 to a position in which the arms can be retracted without collision

3. Retract R2 to a safe area

4. Rotate R1 of all the actuators to their starting positions, at which we can deploy all the arms without collisions

5. Deploy R2 of the arms

6. Rotate R1 of all positioners to the final positions

7. Deploy R2 to the final position

The problem with this simple step-by-step algorithm is that in both step 1 and 7, the risk of collision is present. In the next chapter, Figure 11.6 shows a configuration of the positioners that can not be solved using this algorithm and needs precise trajectory planning to guarantee collision avoidance.

✏ Summary

Many international projects in the field of astrophysics are designing very large telescopes that include thousands of fiber positioners. The fiber positioners are tightly packed in a focal plate of the telescope and share the working space. The direct path from the initial point of the positioners to their goal points are prone to collision. In the next chapter, we propose a decentralized framework for coordination of the fiber positioners based on navigation functions. Although the coordination (calculating the collision-free trajectories) could be done offline, decentralization, in this framework, allows us to decrease the complexity of the algorithm ($O(N)$), which guarantees the scalability of the approach.

11 Decentralized Coordination of Fiber Positioners Using DNF [*]

Overview

Some of the next generation massive spectroscopic survey projects, such as DESI and PFS, plan to use thousands of fiber positioner robots packed at a focal plane to quickly move in parallel the fiber-ends from the previous to the next target points. The most direct trajectories are prone to collision that could damage the robots and impact the survey operation. We thus present here a motion planning method based on a novel decentralized navigation function for collision-free coordination of fiber positioners. The navigation function takes into account the configuration of positioners as well as the actuator constraints. We provide details for the proof of convergence and collision avoidance. Decentralization results in linear complexity for the motion planning as well as dependency of motion duration with respect to the number of positioners. Therefore the coordination method is scalable for large-scale spectrograph robots. The short in-motion duration of positioner robots, will thus allow the time dedicated for observation to be maximized.

11.1 Problem formulation

We consider a system composed of N positioner robots. The goal of each robot is to put its end effector (fiber-end) on an assigned target point. Each positioner is a planar robot with two degrees of freedom, each moving by a rotational motor (Figure 11.1).

Each positioner robot covers the patrol area (workspace) through two correlated rotations: θ rotates around the actuator's main axis, while ϕ moves the fiber arm tip from the peripheral circle to the central axis (Figure 11.1). The optical fiber is attached to a ferrule at the arm tip,

---
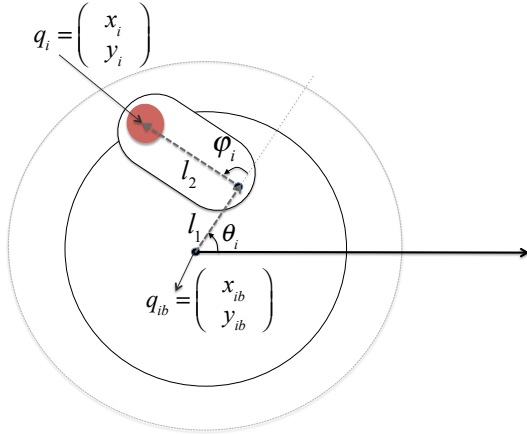
Figure 11.1: A positioner robot with two degrees of freedom. The main disk (black circle) rotates along its central axis. Its angular position is shown as θ_i. The arm with the length of l_2 rotates around an eccentric axis (with the distance of l_1 from the center) fixed on the main disk and its angular position is shown as ϕ_i. q_{ib} is the position of the robot base fixed to the telescope structure in a global frame attached to the focal plane. q_i is the position of the fiber attached to the robot i in that global frame.

and passes through the center of the actuator and exits by the rear side of the robot.

The forward kinematics of each positioner robot can be described as:

$$\begin{pmatrix} x_i \\ y_i \end{pmatrix} = \begin{pmatrix} x_{ib} \\ y_{ib} \end{pmatrix} + \begin{pmatrix} cos\theta_i & cos(\theta_i + \phi_i) \\ sin\theta_i & sin(\theta_i + \phi_i) \end{pmatrix} \begin{pmatrix} l_1 \\ l_2 \end{pmatrix} \tag{11.1}$$

Where the end-effector position of positioner i is $q_i = (x_i, y_i)$ in a global frame attached to the focal plane. l_1 and l_2 are first and second rotation links respectively (Figure 11.1). θ and ϕ are angular positions of the two joints of the positioner i. Each positioner is controllable by its angular velocity, meaning the speed of each of the two motors.

The main challenge is to coordinate the robots in motion to reach a predefined target point while avoiding collisions. The proposed approach should be expandable to a more large-scale problems. A centralized solution for such a problem would be practically infeasible and costly due to the presence of numerous positioners and constraints ([111]). Therefore, among all the methods found in the literature for coordinating agents, decentralized and reactive control approaches seem promising.
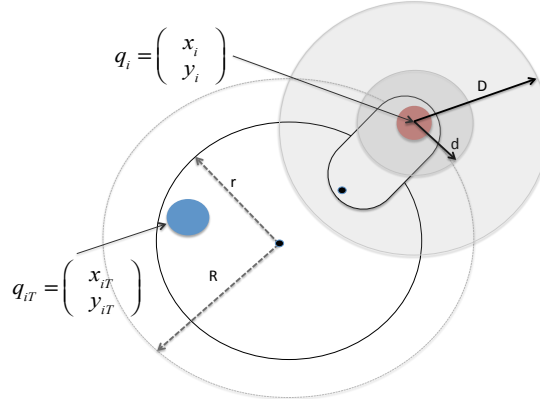
Figure 11.2: The target point q_{iT} is the destination of the robot end-effector. The collision detection envelope with radius of D, is the area where collision avoidance term in the navigation function is activated. The collision avoidance term in the navigation function ensures that the two positioner end-effectors will keep a distance larger than d.

11.2 Decentralized Navigation Function

We propose a navigation function ψ_i for the positioner i in (11.2) which is composed of two components. The first term, the attractive component, is the squared distance of the end-effector of positioner robot i from its target point. This term of navigation function attains small values as the positioner brings the fiber closer to its target point (Figure 11.2). The second term, the repulsive component, aims at avoiding collisions between positioner i and the six other positioners located in its vicinity. This term is activated when the two positioner robots are closer than a distance D, otherwise this term is zero. D defines the radius of a collision avoidance envelope and $d < D$ defines the radius of the safety region. The closer the two robots get, the higher values this repulsive term attains. Moving toward the minimum point of this navigation function will guarantee the minimum distance of d between the positioners (Figure 11.3). λ_1 and λ_2 are the two weighting parameters related to the two terms in the navigation function.

$$\psi_i = \lambda_1 \left\| q_i - q_{iT} \right\|^2 + \lambda_2 \sum_{j \neq i} min(0, \frac{\left\| q_i - q_j \right\|^2 - D^2}{\left\| q_i - q_j \right\|^2 - d^2}) \tag{11.2}$$

According to the navigation function presented in (11.2) and the forward kinematics defined in (11.1), the following control law is proposed:

$$u_i = -\nabla_{\theta_i \phi_i} \psi_i(q_i) \tag{11.3}$$
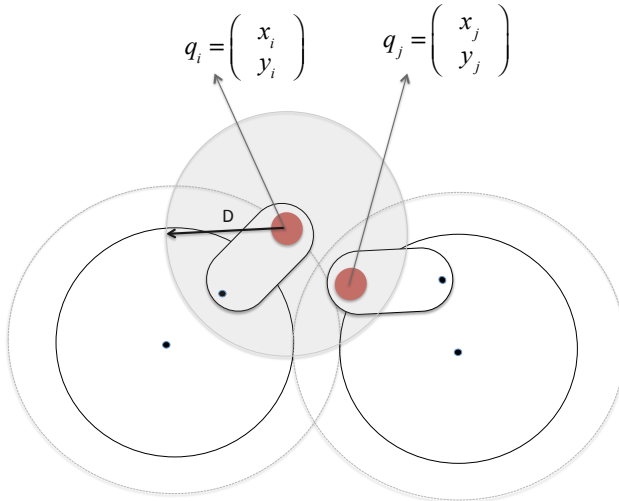
Figure 11.3: A configuration in which there is a risk of collision between the end-effectors of two robots. In this configuration the collision avoidance term in the navigation functions of the two robots are active which means they take values more than zero.

At each step, the robot will move the fiber according to a gradient descent method. It is worth mentioning that the navigation function is directly a function of the end-effector positions. In order to obtain the angular velocities of each of two motors, we calculate the gradient of the navigation function with respect to the angular positions of the links using the chain derivatives and the forward kinematics in (11.1).

$$\left(\begin{array}{c} \omega_{i1} \\ \omega_{i2} \end{array} \right) = u_i = -\left(\begin{array}{c} \frac{\partial \psi_i}{\partial x_i}\frac{\partial x_i}{\partial \theta_i} + \frac{\partial \psi_i}{\partial y_i}\frac{\partial y_i}{\partial \theta_i} \\ \frac{\partial \psi_i}{\partial x_i}\frac{\partial x_i}{\partial \phi_i} + \frac{\partial \psi_i}{\partial y_i}\frac{\partial y_i}{\partial \phi_i} \end{array} \right) \tag{11.4}$$

ω_{i1} and ω_{i2} are the angular velocity of the first and second motor of positioner robot i respectively. There could be two final configurations that result in the same target point. However, when traveling from a known configuration, reaching to one of those configurations is faster considering no collision. In this work we assumed that the faster configuration is the goal configuration.

11.2.1 Algorithm complexity

Table 11.1 describes the motion planning algorithm. In each time step dt, each positioner robot computes the speed of its two motors knowing its current position and the target point as well as the position of adjacent robots. In each time step, each positioner calls the module that computes the gradient of decentralized navigation function (Table 11.2). So, the algorithm runs in a for loop as many times as the number of positioner robots. On the other hand, the

Table 11.1: Motion planning algorithm for all positioner robots. T_0 and T_f are the beginning and end times of the algorithm respectively. dt is the time step and M is the number of time steps i.e. $M = \frac{T_f - T_0}{dt}$

Trajectory planning algorithm	
Inputs:	Initial end-effector position of all the positioners:
	$Q_{init} = [q_1, q_2, \ldots, q_N]$
	and target position of all fibers assigned to each positioner:
	$Q_{goal} = [q_{1T}, q_{2T}, \ldots, q_{NT}]$
outputs:	A sequence of motor peed values for each positioner
	$\Omega_1 = [\omega_1(1), \ldots, \omega_1(M)]$
	$\Omega_2 = [\omega_2(1), \ldots, \omega_2(M)]$
	$\vdots$
	$\Omega_N = [\omega_N(1), \ldots, \omega_N(M)]$

m = 0
repeat until $\nabla \psi = 0$
    for each positioner(i=1:N)
        $\omega_i(m) = -\nabla \psi(q_i(m), q_{iT}, Q(m))$ See: Table 11.2
        $q_i(m+1) = q_i(m+1) + dt.\omega_i(m)$
        m = m + 1
        $\nabla \psi = \max_i(\nabla \psi(q_i(m), q_{iT}, Q(m)))$
    end for
end repeat

inner loop that calculates the gradient of the DNF runs constant times (number of adjacent positioners = 6). Therefore the complexity of the algorithm will remain O(N), where N is the number of positioner robots.

Considering the fact that all the robots' bases are fixed to the focal plane, collisions can occur locally and chances of collision is only with the certain adjacent robots. Decentralizing motion planning and trajectory generation takes advantage of limited number of adjacent robots and the locality of collisions and significantly reduces the complexity of the algorithm to a linear order. Low complexity of the algorithm guarantees its ease of use in mid-scale and large-scale robotic telescopes where there are thousands, or tens of thousands of positioners respectively.

11.3 Collision-Free Motion Toward the Equilibrium

The following part provides conditions under which the DNF (11.2) in combination with the control law (11.3) ensures convergence of robots to their target points. Convergence of robots means that using this method, practically no blocking will occur even if some complex manoeuvres are needed in case of intricate initial configurations of the robots (See simulation example in Figure 11.6).

Table 11.2: Motion planning algorithm calls this module that calculates gradient of the DNF. This function gets the current and target position of the robot as well as current position of its adjacent positioners. The output of the function is the gradient of the DNF.

Gradient of the DNF for the positioner i	
Inputs:	Current position of the positioner q_i,
	target position of the positioner q_{iT},
	and current position of the neighbor positioners $Q_{neighbor} \in Q$
outputs:	The gradient of the navigation function for positioner i
	which is a vector of a two elements $G = \begin{pmatrix} G_1 \\ G_2 \end{pmatrix}$

$G = 0$
$G = G + 2\lambda_1 (q_i - q_{iT})$
for each neighbor positioner(j=1:6)
$\quad G = G + 2\lambda_2 \frac{(R^2 - r^2)(q_i - q_j)}{(\|q_i - q_j\|^2 - r^2)^2}$
end for

Collision avoidance for fiber positioner robots

If the following inequality is satisfied:

$$\frac{\lambda_1}{\lambda_2} < \frac{1}{R} \frac{D}{D^2 - d^2} \tag{11.5}$$

then the function (11.2) will drive fiber positioners to their desired goals avoiding any deadlock situation.

When $\nabla_{\theta_i} \psi(q_i) = 0$ It is either in the presence of no other positioner in the vicinity of positioner i, where $\|q_i - q_j\| \geq D$ or there is a risk of collision $\|q_i - q_j\| < D$ with at least one other positioner. The gradient of the navigation function for both cases is:

$$\nabla \psi(q_i) = \begin{cases} 2\lambda_1(q_i - q_{iT}) = 0 & \|q_i - q_j\| \geq D \\ \lambda_1(q_i - q_{iT}) + 2\lambda_2 \sum\limits_{j=1}^{6} \frac{(D^2 - d^2)(q_i - q_j)}{(\|q_i - q_j\|^2 - d^2)^2} & \|q_i - q_j\| < D \end{cases} \tag{11.6}$$

In case when there is no other positioner near the positioner i, $\nabla_{\theta_i} \psi(q_i) = 0$ means $2\lambda_1(q_i - q_{iT}) = 0$, which directly indicates that the positioner robot is in its target point. Otherwise, there is at least one other positioner in the collision avoidance envelope (D):

$$\nabla \psi(q_i) = \lambda_1(q_i - q_{id}) + 2\lambda_2 \sum_{j=1}^{6} \frac{(D^2 - d^2)(q_i - q_j)}{(\|q_i - q_j\|^2 - d^2)^2} \tag{11.7}$$

The first term in the gradient of the potential field always satisfies the following inequality:

$$\lambda_1 \left\| q_i - q_{id} \right\| < 2\lambda_1 R \tag{11.8}$$

In addition, the second term in the gradient of the potential field is:

$$\begin{aligned}
&\frac{(D^2-d^2)\left\|(q_i-q_j)\right\|}{(\left\|q_i-q_j\right\|^2-d^2)^2} > \frac{D}{D^2-d^2} \\
&\rightarrow \lambda_2 \sum_{j=1}^{6} \frac{(D^2-d^2)\left\|(q_i-q_j)\right\|}{(\left\|q_i-q_j\right\|^2-d^2)^2} > \lambda_2 \frac{2D}{D^2-d^2}
\end{aligned} \tag{11.9}$$

So, if $\lambda_2 \frac{2D}{D^2-d^2} > 2\lambda_1 R$ then there is no point where the gradient of the potential field could be zero except at the target point. It is worth noticing that, there are two possibilities two have velocities equal to zero in angular coordination. One possibility is that the velocities are zero in the (x, y) coordination that is covered in the proof. The other possibility is that the positioner is in one of its singular configurations such as fully stretched or fully bent second arm. Technically, in any robotic manipulation, we try to avoid singularities, as the smoothness of motion and load on the motors are largely affected near singular points. So, we can assure that, in practice, the algorithm can guarantee deadlock-free motion. This guarantees that there will be no blocking (also called deadlock) in the method in practice.

11.3.1   Parameter tuning

There are two weighting parameters that can be tuned in the DNF (11.2); λ_1 and λ_2. Section 11.3 gives a condition for tuning this parameters which facilitates convergence of positioners to their target point. In order to ensure the success of the motion planning algorithm, the maximum velocity generated should not exceed the maximum velocity feasible for motors. Lower values of λ_1 and λ_2 will result in lower values for velocity of motors and increase the convergence time. For an application in which fast convergence is desirable, the two parameters will be tuned to the highest values that still keep maximum generated velocity in the feasible range. We soft-tuned these two parameters through simulations.

11.4   Simulation Results

In order to study the performance of the motion planning algorithm, we conducted various sets of simulations for different number of positioners all in hexagonal configuration patterns. The size of positioners and the share volume between positioners are selected in a way to be compatible with next-generation spectrograph robots such as the one in DESI (Table 11.3). Therefore, the overlapping area of the robots are the fiber-ends. In a scenario with different specifications, the robots may have collision risks with other parts. In these scenarios, the collision avoidance envelope, D, should be modified in order to cover all collision risks. For each set of simulations, We selected different numbers of positioners to verify our expectation

Table 11.3: Specifications of positioner robots (see Figure 11.2 and Figure 11.3)

Parameter	Value
R	7 mm
r	5 mm
ferule size	1 mm
arm diameter	2 mm
arm length	3mm
D	4 mm
d	2 mm

Table 11.4: Simulation parameters used for all sets of simulations

Parameter	Value
Maximum speed of the first acuator	30 rpm
Maximum speed of the second acuator	20 rpm
λ_1	1
λ_2	0.05
dt (time steps)	10 ms
Convergence distance	100 μm

on complexity of the algorithm. In addition, we can extrapolate the simulation time and motion duration for other number of positioners for larger scales of robotic spectrographs. For each set we repeated the simulations 100 times. In all sets, initial angular position of the two motors of each positioner robot and their target point are randomly generated. Table. 11.4 shows simulation parameters. The two weighting parameters in DNF (11.2) should satisfy the condition presented in Section 11.3. According to positioners' specifications in Table 11.3, λ_1 and λ_2 should fit the inequality of $\frac{\lambda_1}{\lambda_2} < \frac{1}{R} \frac{D}{D^2 - d^2}$. This means $\lambda_1 < 72\lambda_2$.

As expected, we observe no collision during all sets of simulations (4100 sets). Figure 11.4 and Figure 11.5 show the simulation time and in-motion duration of robots respectively. In-motion duration is the convergence time needed for all the positioner robots to arrive in their target points considering constraints on actuator velocities in Table. 11.4. Regarding values for simulation time, the processor for all simulations is a 3.33 GHz 6-Core Intel Xeon.

As expected , simulation time increases in a near linear manner with the number of positioners. This enables us to use this method for immediate motion planning for thousands of positioners. From the results, the amount of time needed to generate collision-free trajectories for 5000 positioners is less than 3 minutes (140 seconds) on today's typical computers. This amount of time is very reasonable as it is smaller than the typical exposure time foreseen for the DESI and PFS experiment, thus allowing to have an interactive planning of the observation. This would
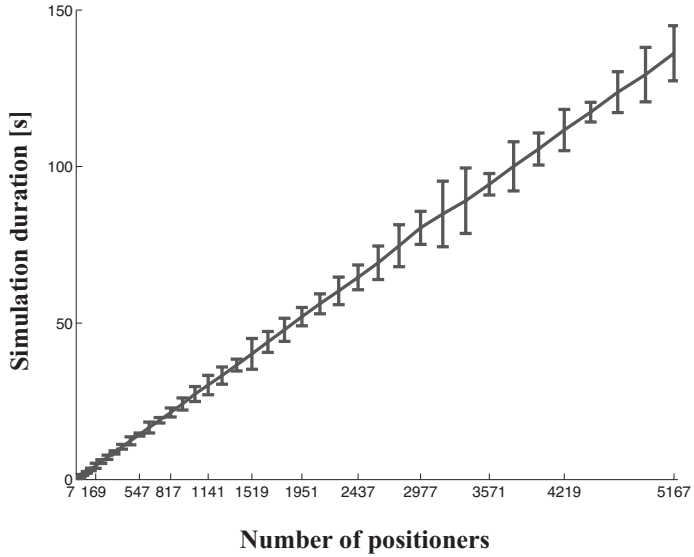
Figure 11.4: Mean value simulation duration for sets with different number of positioners. Repeating sets of simulation, the simulation durations do not significantly vary. The lengths of the error bars are therefore chose 10 times of the standard deviation at each point.

allow to modify in real time the target list due to many reasons, for example meteorological disturbances or even the last minute discovered transient targets such as SuperNovae or Gamma Ray Burst.

The main advantage of the method that derives from the idea of decentralization is that the motion duration does not change with the number of positioner robots. Decentralization benefits from the configuration of positioner robots and the fact that collisions could happen locally and they do not affect the motion of non-neighbor positioners. With realistic actuator constraints (Table 11.4), as used in simulation sets, we can expect to accomplished the first run of motion for positioners of a mid-scale robot positioners in less than 2.5 seconds. Such small duration of time for coordination of all positioners will allow to maximize the duration of observation and survey efficiency.

So far, in all sets of simulations, we study the performance of our motion planning algorithm for randomly distributed initial positions and randomly distributed target points. However, galaxies are not randomly distributed, but clustered. Therefore, in a realistic situation, positioners will move toward very close targets and consequently start the next set of observation from a very close position toward other set of target points. Therefore, It is expected that adjacent positioner robots will need sets of complex maneuvers in order to find a collision-free path toward their target points. Figure 11.6 shows snap-shots of a simulation set where three positioners are engaged in a very close space. The motion planning algorithm succeeds in
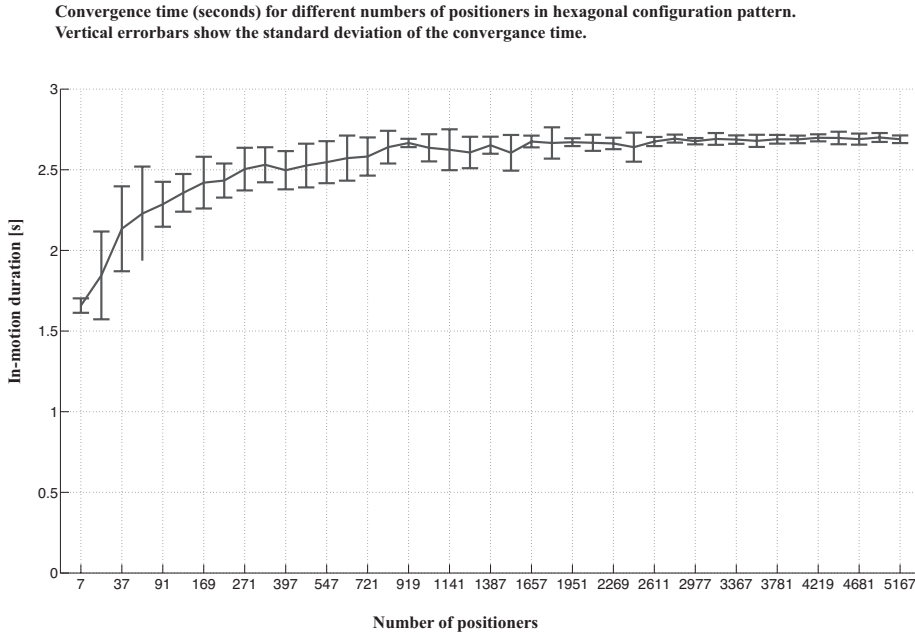
Figure 11.5: Mean value and standard deviation of convergence time (seconds) for simulation sets with different numbers of positioners. Note that the scaling of the x-axis is not linear.

solving the conflict by directly executing the complex maneuvers from DNF and taking positioner robots to their target points. The main advantage of this method is that these type of conflicts could be solved in a decentralized manner which significantly decreases simulation time and motion duration. Therefore, the algorithm is reliable for large number of positioners.

11.5 Profile discretization

Consider $v(t)$ and $p(t)$ general velocity and its corresponding position profile for a motor respectively (Figure 11.8). $p(t)$ is a continuous nonlinear function, of a single variable t in an interval $[t_0, t_f]$. To send the minimum data to the motors the goal is to find minimum number of intervals of constant velocity and send the velocity and its duration to the motors. To this end, we approximate the position profiles by piecewise linear functions. Consequently, the velocity profiles will be piecewise constant functions. When approximating the position profiles, the collision avoidance constraints should be considered.

Piecewise linear functions are used in many applications and therefor various methods have been introduced in the literature. The main focus of piecewise linearization appears on optimization problem with a nonlinear cost function [112; 113; 114]. The main goal in many different applications is to find the number and location of the break points along the function. In our application, due to collision risk the breaking points play an important role. On the other hand, lower number of breaking points means less communication cost in the electronics side.
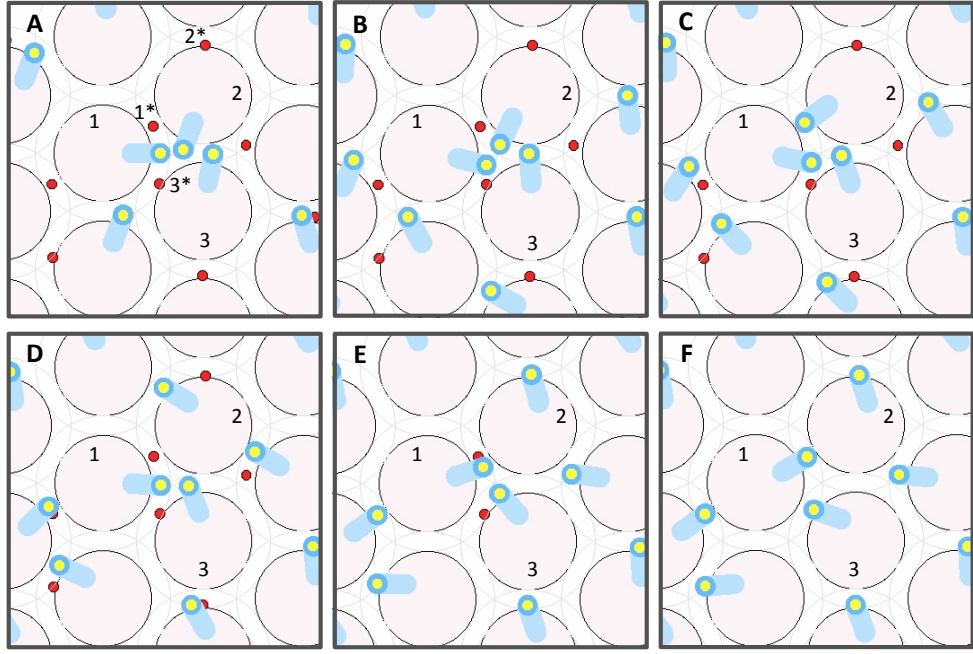
Figure 11.6: The six boxes (A to F) show six snap shots of the simulation. 1*, 2* and 3* are respectively the target positions for positioner 1,2 and 3. This three positioners are engaged in a local conflict in which positioner 1 needs to make space for positioner 2 to pass. positioner 2 can not make room for positioner 1 because positioner 3 is blocking the way. Positioner 3 needs to pass both positioners to reach its target point. The small maneuver from positioner 1 that comes directly from DNF moves this positioner farther from its target point but it makes room for the positioner 2 to pass safely. When positioner 2 clears the way, positioner 1 starts moving toward its target point and this gives a safe way to the positioner 3. The simulation videos for DESI and MOONS could be found: https://www.youtube.com/watch?v=pxtkRt8j5Ks and https://www.youtube.com/watch?v=rwjR-fOjlZc

Keeping these two constraints in mind, the position profiles are linearized by the following algorithm:

Step one: the position profile of the first motor is filled with a safety margin. The safety margin is the projection of the half the distance from the positioner's fiber end to that of its nearest adjacent positioner on the angular position of the motors. (Figure 11.9).

Step two: draw a line from t_0 to t_f on the position profile.

Step three: If the whole line is inside the safety margin, the profile has been linearized with only one line segment (Figure 11.9 (A)). If the line passes over the safety margin put $t_n = t_0$ (Figure 11.9 (B))

Step four: find the mean of the start point (t_n) and the final point (t_f), call it t_m.

Step five: draw a line from t_n to t_m on the position profile (Figure 11.9 (C)).

Step six: If the whole line is inside the safety margin, one part of the profile has been linearized with one line segment. put $t_n = t_m$ and repeat from step five, else find the mean value of the points t_n and t_m and put is as t_m and repeat from step five (Figure 11.9 (D)).
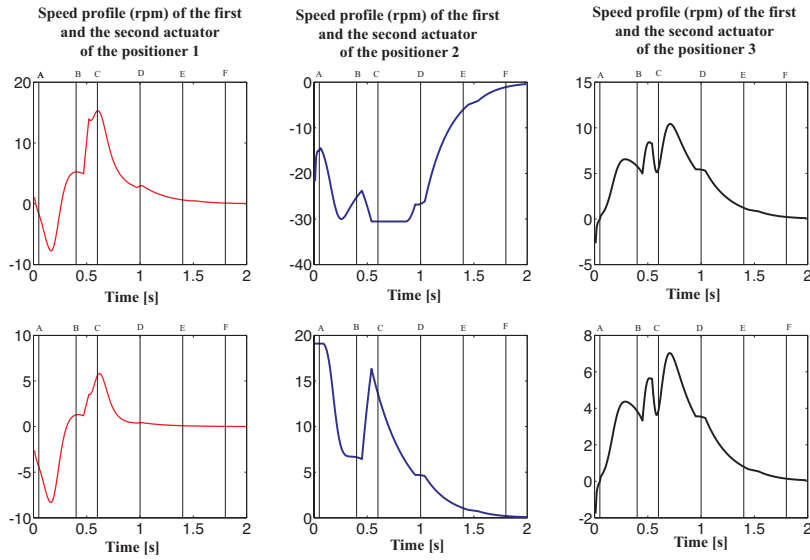
Figure 11.7: Velocity profiles that correspond to the pairs of actuators for positioners 1,2 and 3 in Figure 11.6. Columns show the velocity profiles for each positioner. The first and second profiles of each column correspond to the first and second actuator of each positioner respectively. Vertical lines indicate the moment at which the snapshots of Figure 11.6 were taken.

Step seven: compute the gradient of the line segments, these correspond to the velocity profiles.

For the second motor, we should take into account the new profile of the first motor. The safety margin needs to be recalculated. It is worth mentioning that calculating the safety margin does not add a big computational load, since in each time step during the motion planning algorithm the distance of each two adjacent positioner is computed. We only need to store that data to use further for piecewise linearization of position profiles.

Figure 11.10 shows the corresponding position profiles to the velocity profiles shown in Figure 11.7. By continuing the steps of the proposed discretization algorithm, we will get piecewise linearized profiles for the motor positions. In such a challenging scenarios with respect to the collision avoidance and discretization, profiles could be linearized with maximum three segments. Representing each velocity profile with a maximum three segments with constant value and yet ensuring collision avoidance is a promising step toward realization of the positioners.

11.6 Conclusion

In the near future fibre-fed spectrograph robots such as the ones envisioned in DESI (5000 fiber positioners) or PFS (2400 fiber positioner) will provide a 3D map of a large portion of our universe. The main concept which is common between the designs is the use of small mechanical robot positioners. These robot positioners are responsible for moving the
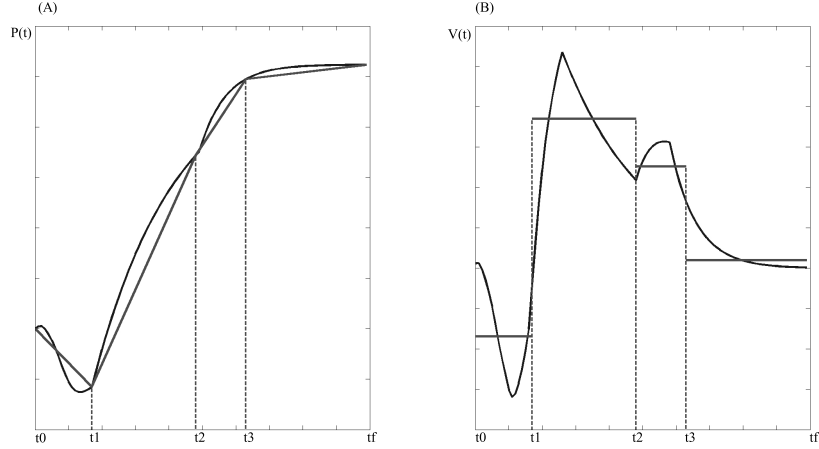
Figure 11.8: (A) An example of position profile calculated using DNF for motion planning. (B) A velocity profile of a motor, corresponding to the position profile in the left. By piecewise linearizing the position profile, the velocity profile is piecewise constant.
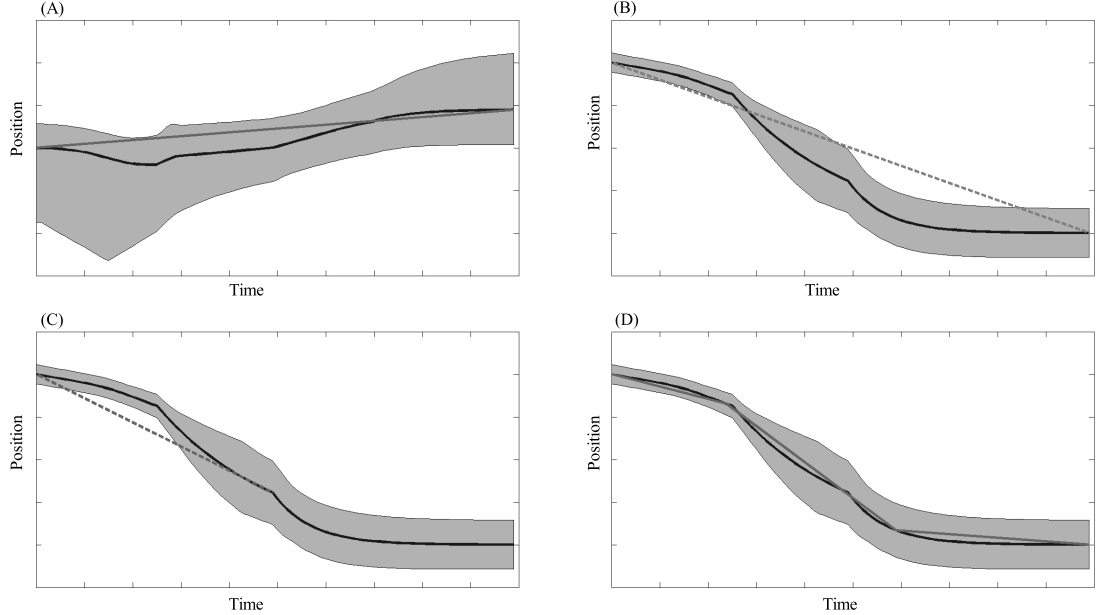
Figure 11.9: (A) A position profile with the safety margin shown in grey. In the first step, we draw a line from t_0 to t_f on the profile. This line is entirely in the safety zone. By changing the position profile from the continuous curve to the single line, still collision avoidance is guaranteed. (B,C,D) A single line can not provide a collision free trajectory for the positioner. (C)Therefore, we find a middle point between t_0 and t_f as a breaking point. But the line is not still entirely in the safety margin, so we need to repeat the last step, till we get line segments entirely in the safety margin (D).
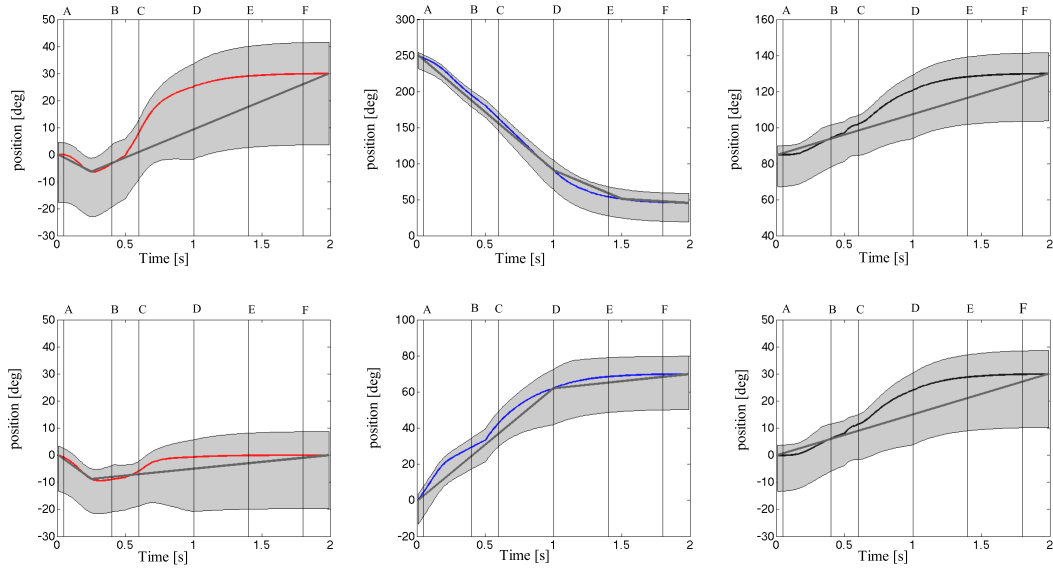
Figure 11.10: Position profiles that correspond to the pairs of actuators for positioners 1,2, and 3 in Figure 11.6. Columns show the position profiles for each positioner and the piecewise linearized estimation of the profiles. The first and second profiles of each column correspond to the first and second actuator of each positioner, respectively. Vertical lines indicate the moment at which the snapshots in Figure 11.6 were taken. Each profile of the six motor can be piecewise linearized using maximum two breaking points.

fiber-ends toward their target points where they can observe different sets of objects such as galaxies, quasars or stars. As the robot positioners share workspace, the key challenge is designing a motion planning algorithm which guarantees collision avoidance. Our proposed decentralized method for coordination of positioners is a potential field that ensures collision avoidance as well as convergence of fiber positioners (no blocking) to their target points. Simulation results show feasibility of using this method for mid-scale and large scale fiber-fed spectrograph robots. In-motion duration only lasts 2.5 seconds for any number of positioners. In addition, the massive spectroscopic projects could take advantage of short simulation time to compute trajectories and the ability of interactive motion planning of the robots to target recently discovered transient sources at the last minute. Granting the fact that the initial motivation of this work came from the collision challenges in DESI project, the proposed method can be directly applied to PFS project where number of robots is half of DESI. From simulation results we can predict that the 4800 trajectories of 2400 robots could be generated with a typical computer in less than one minute and the motion duration would be less than 3 minutes. Moreover, this DNF could be adopted for other fiber positioning systems with different geometry patterns to avoid collisions.

Our future research directions include the discretization of velocity profiles in order to ensure the feasibility of a real-time coordination for large number of fiber positioners. In a framework where a centralized computer communicates with positioners, in order to minimize the communication time, the motor velocities should be discretized to fit in few bits. Moreover, we are exploring the connection between motion planning and target assignment in order to further minimize the in-motion duration of positioners.

📝 Summary

We have provid a decentralized coordination framework for fiber positioenrs. The goal is to move in parallel and in minimum time all positioners that are initially packed at a focal plane.We propose a new decentralized navigation function that ensures the collision avoidance. We provide a sketch of proof for that the framework avoides dead-locks, using the proposed navigation function. In order to guarantee feasible control electronics and communication between control center and the fiber positioners, we proposed a recursive algorithm that gives piecewise linearized profiles for trajectories. Finally, we present a visual simulation environment for the whole 5000 positioners for test and validation of target assignment, motion planning and collision avoidance algorithms.

Conclusion Part V

12 Conclusion and Outlook

Overview

I N its fullest form, this dissertation investigated the collision-free coordination of autonomous robots in crowded workspaces. The motivation for this thesis was born from the fact that many robotic applications are growing fast and involving a large number of robots. Realizing that the coordination of autonomous robotic systems needs to be fast, reliable, and dependent of local communication, we studied decentralized solutions. As frameworks, we investigated two real-world yet challenging and open to be solved coordination problems. The two problems are from two very different families of robotics applications. In this chapter we summerize the contributions of this thesis and extend our view over the outlooks.

12.1 Summary

Our work provided three main contributions. The first contribution concerns the formulation of coordination, based on decentralized navigation functions (DNF), in the framework of a normal game. The second contribution is proposing a novel decentralized navigation function for coordination of autonomous vehicles at intersections. Finally, our third main contribution is providing collision-free coordination framework for the next-generation spectrogragh surveys that use fiber positioners. These fiber positioners are packed tightly in a focal plate and share workspaces.

- In the framework of a normal form game, our first major contribution is proving that coordination of robots using decentralized potential functions (as utility functions), and gradient descent directions (as the control law) leads the robots to a Nash equilibrium.

With this proof, the Morse constraints on navigation functions can be relaxed. So, the resulted trajectories for the robots are more reactive and rapid.

- Our second major contribution addresses coordination of autonomous vehicles at intersections. We model each autonomous vehicle as a first order dynamic system and propose a decentralized navigation function that guarantees safe passing for vehicles. By introducing the inertia of the vehicles into the navigation functions and studying the vector fields (derivatives of the navigation functions), we derive the conditions on parameters (wighting parameters of navigation functions), which ensure deadlock-free coordination. The simulation results show that autonomous vehicles can perform three times better in terms of throughput at intersections, compared to traffic lights.

- To get an even shorter travel time for vehicles passing an intersection, we propose a new navigation function that allows the vehicles not only to decelerate but also to accelerate to avoid collisions. The navigation functions use the desired velocities of the vehicles and computes the arrival time of the vehicles using their position and current velocity. As the navigation functions are based on both the predicted arrival times and the positions of the vehicles, we call them spatio-temporal navigation functions. Without a large affect on the throughput of the intersection, the spatio-temporal navigation functions allow some vehicles to accelerate, which subsequently results in lower energy consumption.

- To extend our decentralized approach to a deterministic optimization problem, we address the coordination problem of autonomous vehicles at intersections by introducing a linear- quadratic model predictive control framework. We introduce a second order dynamic model and propose a quadratic cost function for each vehicle. We formulate the collision avoidance, as well as velocity and acceleration limits, as a set of linear constraints. Moreover, we adapt the framework in such a way that vehicles crossing in a platoon are handled as such and do not need to be considered separately.

- As our final major contribution, we investigate a coordination framework based on decentralized navigation functions for large number of fiber positioners. The fiber positioners are tightly packed focal plate. Their direct movement from the initial point to their goals are prone to collisions, which can damage the fiber positioners. The proposed framework ensures the functionality of fiber positioners of massive spectroscopic surveys with respect to collision avoidance. Using the proposed navigation function, fiber positioners move simultaneously and their mechanical constraints such as speed of the motors and mechanical hard stops have been taken into account. As a secondary contribution, we developed an animated 2-D environment of the 5000 positioners for test and validation.

12.2 Outlooks

This work constitutes a first step towards understanding and building a groundwork for coordination of large number of autonomous robots that act in crowded workspaces. For both

frameworks tackled in this thesis, several aspects remain to be taken into consideration.

This thesis considers a first-order and second-order models to describe the dynamics of the robots in the both frameworks. At the core of our groundwork, other dynamic models need to be integrated in order to present the robots in finer details. We recognize that communication constraints are more than the range of communication that has been considered in this thesis. Thus, a very important future step will be the integration of communication models in our coordination framework. The information shared among the robots, has been considered with a white noise, however an additional information sharing model can meet many more realistic constrains. Therefore, the effect of communication and observation topologies on performance of the decentralized coordination framework could be studied.

In our first coordination framework, the autonomous vehicles at intersections, lack of energy for electrical vehicles and optimization of acceleration profiles for hybrid vehicles should be studied. Different profiles of acceleration will result in various driving experience. The comfort of the passengers related to these profiles could be studied given the acceleration profiles provided by the decentralized navigation functions. Finally, an adaptation of the framework for semi-autonomous vehicles would be a fundamentally crucial step in integrating the autonomous vehicles in the urban roads while the human drivers are still behind the wheels of vehicles.

In our proposed model predictive controller approach, we guarantee collision avoidance by adding linear constraints to the optimization problem. We apply the so-called soft constraints for computing the priorities of the vehicles that enter the intersection. An efficient algorithm that computes the priorities [81] of the vehicles can be combined with the model predictive controller approach, in order to reduce the computation time and guarantee the convergence of model predictive controller in a short period of time.

In the framework of coordination of fiber positioners, the relation between motion planning and target assignment should be explored in order to further minimize the in-motion duration of fiber positioners. To accomodate the communication constraints, we have introduced a recursive piecewise linear approach for discretization of velocity profiles. At the time of preparation of this thesis, we are adapting the proposed navigation functions, in order to take into account the larger collision area of the fiber positioners in MOONS. Future research directions could include optimizing the discretization process to reduce computational efforts.

Bibliography

[1] J. Ferber, *Multi-agent systems: an introduction to distributed artificial intelligence*, vol. 1. Addison-Wesley Reading, 1999.

[2] NASA, "Mars exploration rover mission." http://mars.jpl.nasa.gov/mer/home/.

[3] A. G. Riess, A. V. Filippenko, P. Challis, A. Clocchiatti, A. Diercks, P. M. Garnavich, R. L. Gilliland, C. J. Hogan, S. Jha, R. P. Kirshner, *et al.*, "Observational evidence from supernovae for an accelerating universe and a cosmological constant," *The Astronomical Journal*, vol. 116, no. 3, p. 1009, 1998.

[4] S. Perlmutter, G. Aldering, G. Goldhaber, R. Knop, P. Nugent, P. Castro, S. Deustua, S. Fabbro, A. Goobar, D. Groom, *et al.*, "Measurements of ω and λ from 42 high-redshift supernovae," *The Astrophysical Journal*, vol. 517, no. 2, p. 565, 1999.

[5] P. J. E. Peebles and B. Ratra, "The cosmological constant and dark energy," *Reviews of Modern Physics*, vol. 75, no. 2, p. 559, 2003.

[6] H. Aihara, C. A. Prieto, D. An, S. F. Anderson, É. Aubourg, E. Balbinot, T. C. Beers, A. A. Berlind, S. J. Bickerton, D. Bizyaev, *et al.*, "The eighth data release of the sloan digital sky survey: first data from sdss-iii," *The Astrophysical Journal Supplement Series*, vol. 193, no. 2, p. 29, 2011.

[7] A. D. Myers, E. Armengaud, J. Bovy, W. N. Brandt, E. Burtin, J. Comparat, K. S. Dawson, T. Delubac, S. Ho, J.-P. Kneib, *et al.*, "Using quasars from sdss-iii/sequels to characterize sdss-iv/eboss selection," in *American Astronomical Society Meeting Abstracts*, vol. 224, 2014.

[8] M. Levi, C. Bebek, T. Beers, R. Blum, R. Cahn, D. Eisenstein, B. Flaugher, K. Honscheid, R. Kron, O. Lahav, *et al.*, "The desi experiment, a whitepaper for snowmass 2013," *arXiv preprint arXiv:1308.0847*, 2013.

[9] E. Hubble, "Effects of red shifts on the distribution of nebulae," *Proceedings of the National Academy of Sciences of the United States of America*, vol. 22, no. 11, p. 621, 1936.

[10] F. Simpson and J. A. Peacock, "Difficulties distinguishing dark energy from modified gravity via redshift distortions," *Physical Review D*, vol. 81, no. 4, p. 043512, 2010.

[11] N. Fahim, F. Prada, and J. P. Kneib, "An 8-mm diameter fiber robot positioner for massive spectroscopy surveys," *arXiv preprint arXiv:1410.4722*, 2014.

[12] L. Makarem, J.-P. Kneib, D. Gillet, H. Bleuler, M. Bouri, L. Jenni, F. Prada, and J. Sanchez, "Collision avoidance in next-generation fiber positioner robotic system for large survey spectrograph," *Astronomy and Astrophysics*, vol. 566, 2014.

[13] F. Ge, Z. Wei, Y. Lu, Y. Tian, and L. Li, "Decentralized coordination of autonomous swarms inspired by chaotic behavior of ants," *Nonlinear Dynamics*, vol. 70, no. 1, pp. 571–584, 2012.

[14] D. V. Dimarogonas and K. J. Kyriakopoulos, "Decentralized motion control of multiple agents with double integrator dynamics," in *16th IFAC World Congress*, 2005.

[15] M. C. De Gennaro and A. Jadbabaie, "Formation control for a cooperative multi-agent system using decentralized navigation functions," in *American Control Conference*, pp. 6–12, 2006.

[16] Scopus, "The bibliography database." www.scopus.com.

[17] A. Farinelli, L. Iocchi, and D. Nardi, "Multirobot systems: a classification focused on coordination," *IEEE Transactions on Systems, Man, and Cybernetics, Part B: Cybernetics*, vol. 34, no. 5, pp. 2015–2028, 2004.

[18] L. E. Parker, "Current research in multirobot systems," *Artificial Life and Robotics*, vol. 7, no. 1-2, pp. 1–5, 2003.

[19] Y. U. Cao, A. S. Fukunaga, and A. Kahng, "Cooperative mobile robotics: Antecedents and directions," *Autonomous robots*, vol. 4, no. 1, pp. 7–27, 1997.

[20] L. Iocchi, D. Nardi, and M. Salerno, "Reactivity and deliberation: a survey on multi-robot systems," in *Balancing reactivity and social deliberation in multi-agent systems*, pp. 9–32, Springer, 2001.

[21] C. M. Clark, S. M. Rock, and J.-C. Latombe, "Motion planning for multiple mobile robots using dynamic networks," in *Proceedings of IEEE International Conference on Robotics and Automation*, vol. 3, pp. 4222–4227, 2003.

[22] A. Yamashita, T. Arai, J. Ota, and H. Asama, "Motion planning of multiple mobile robots for cooperative manipulation and transportation," *IEEE Transactions on Robotics and Automation*, vol. 19, no. 2, pp. 223–237, 2003.

[23] K. M. Wurm, C. Stachniss, and W. Burgard, "Coordinated multi-robot exploration using a segmentation of the environment," in *International Conference on Intelligent Robots and Systems*, pp. 1160–1165, 2008.

[24] R. Gayle, W. Moss, M. C. Lin, and D. Manocha, "Multi-robot coordination using generalized social potential fields," in *IEEE International Conference on Robotics and Automation*, pp. 106–113, 2009.

[25] A. K. Das, R. Fierro, V. Kumar, J. P. Ostrowski, J. Spletzer, and C. J. Taylor, "A vision-based formation control framework," *IEEE Transactions on Robotics and Automation*, vol. 18, no. 5, pp. 813–825, 2002.

[26] W. Ren, R. W. Beard, and E. M. Atkins, "A survey of consensus problems in multi-agent coordination," in *American Control Conference*, pp. 1859–1864, 2005.

[27] W. Sheng, Q. Yang, J. Tan, and N. Xi, "Distributed multi-robot coordination in area exploration," *Robotics and Autonomous Systems*, vol. 54, no. 12, pp. 945–955, 2006.

[28] Z. Yan, N. Jouandeau, and A. A. Cherif, "A survey and analysis of multi-robot coordination," *International Journal of Advanced Robotic Systems*, vol. 10, 2013.

[29] J. T. Feddema, C. Lewis, and D. A. Schoenwald, "Decentralized control of cooperative robotic vehicles: theory and application," *IEEE Transactions on Robotics and Automation*, vol. 18, no. 5, pp. 852–864, 2002.

[30] Z. Yan, N. Jouandeau, and A. A. Cherif, "Multi-robot decentralized exploration using a trade-based approach.," in *ICINCO (2)*, pp. 99–105, 2011.

[31] B. P. Gerkey and M. J. Mataric, "Sold!: Auction methods for multirobot coordination," *IEEE Transactions on Robotics and Automation*, vol. 18, no. 5, pp. 758–768, 2002.

[32] P. Song and V. Kumar, "A potential field based approach to multi-robot manipulation," in *IEEE International Conference on Robotics and Automation*, vol. 2, pp. 1217–1222, 2002.

[33] M. Jager and B. Nebel, "Decentralized collision avoidance, deadlock detection, and deadlock resolution for multiple mobile robots," in *International Conference on Intelligent Robots and Systems*, vol. 3, pp. 1213–1219, 2001.

[34] L. E. Parker, "Alliance: An architecture for fault tolerant, cooperative control of heterogeneous mobile robots," in *Proceedings of the IEEE/RSJ/GI International Conference on Intelligent Robots and Systems*, vol. 2, pp. 776–783, 1994.

[35] O. Khatib, "Real-time obstacle avoidance for manipulators and mobile robots," *The international journal of robotics research*, vol. 5, no. 1, pp. 90–98, 1986.

[36] S. I. Choi and B. K. Kim, "Obstacle avoidance control for redundant manipulators using collidability measure," in *IEEE/RSJ International Conference on Intelligent Robots and Systems*, vol. 3, pp. 1816–1821, 1999.

[37] D. Murray and J. J. Little, "Using real-time stereo vision for mobile robot navigation," *Autonomous Robots*, vol. 8, no. 2, pp. 161–171, 2000.

[38] R. Olfati-Saber, "Flocking for multi-agent dynamic systems: Algorithms and theory," *IEEE Transactions on Automatic Control*, vol. 51, no. 3, pp. 401–420, 2006.

[39] N. E. Leonard and E. Fiorelli, "Virtual leaders, artificial potentials and coordinated control of groups," in *Proceedings of the 40th IEEE Conference on Decision and Control*, vol. 3, pp. 2968–2973, 2001.

[40] H. M. Choset, *Principles of robot motion: theory, algorithms, and implementation.* MIT press, 2005.

[41] J. Barraquand, L. Kavraki, R. Motwani, J.-C. Latombe, T.-Y. Li, and P. Raghavan, "A random sampling scheme for path planning," in *Robotics Research*, pp. 249–264, Springer, 1996.

[42] E. Rimon and D. E. Koditschek, "Exact robot navigation using cost functions: the case of distinct spherical boundaries in e n," in *IEEE International Conference on Robotics and Automation*, pp. 1791–1796, 1988.

[43] J. Milnor, "Morse theory, volume 51 of annals of mathematics studies," *Princeton, NJ, USA*, 1963.

[44] D. Dimarogonas, M. Zavlanos, S. Loizou, and K. Kyriakopoulos, "Decentralized motion control of multiple holonomic agents under input constraints," in *Decision and Control, 2003. Proceedings. 42nd IEEE Conference on*, vol. 4, pp. 3390–3395, 2003.

[45] D. V. Dimarogonas and K. J. Kyriakopoulos, "A feedback control scheme for multiple independent dynamic non-point agents," *International Journal of Control*, vol. 79, no. 12, pp. 1613–1623, 2006.

[46] S. Loizu, D. V. Dimarogonas, and K. J. Kyriakopoulos, "Decentralized feedback stabilization of multiple nonholonomic agents," in *IEEE International Conference on Robotics and Automation*, vol. 3, pp. 3012–3017, 2004.

[47] I. D. Couzin, J. Krause, R. James, G. D. Ruxton, and N. R. Franks, "Collective memory and spatial sorting in animal groups," *Journal of theoretical biology*, vol. 218, no. 1, pp. 1–11, 2002.

[48] J. K. Parrish, S. V. Viscido, and D. Grünbaum, "Self-organized fish schools: an examination of emergent properties," *The biological bulletin*, vol. 202, no. 3, pp. 296–305, 2002.

[49] D. Helbing and P. Molnar, "Social force model for pedestrian dynamics," *Physical review E*, vol. 51, no. 5, p. 4282, 1995.

[50] A. Farinelli and L. Iocchi, "Planning trajectories in dynamic environments using a gradient method," in *Robot Soccer World Cup VII*, pp. 320–331, Springer, 2004.

[51] R. Branzei, D. Dimitrov, S. Tijs, D. Dimitrov, and S. Tijs, *Models in cooperative game theory*, vol. 556. Springer, 2008.

[52] C. A. C. Coello, "A comprehensive survey of evolutionary-based multiobjective optimization techniques," *Knowledge and Information systems*, vol. 1, no. 3, pp. 269–308, 1999.

[53] T. Basar, G. J. Olsder, G. Clsder, T. Basar, T. Baser, and G. J. Olsder, *Dynamic noncooperative game theory*, vol. 200. SIAM, 1995.

[54] S. M. LaValle, "Robot motion planning: A game-theoretic foundation," *Algorithmica*, vol. 26, no. 3-4, pp. 430–465, 2000.

[55] B. P. Gerkey and M. J. Matarić, "A formal analysis and taxonomy of task allocation in multi-robot systems," *The International Journal of Robotics Research*, vol. 23, no. 9, pp. 939–954, 2004.

[56] K. Y. Goldberg, "Stochastic plans for robotic manipulation," 1990.

[57] Y. Shoham and K. Leyton-Brown, *Multiagent systems: Algorithmic, game-theoretic, and logical foundations*. Cambridge University Press, 2008.

[58] H. Roozbehani, S. Rudaz, and D. Gillet, "A hamilton-jacobi formulation for cooperative control of multi-agent systems," in *IEEE International Conference on Systems, Man and Cybernetics (SMC)*, pp. 4813–4818, 2009.

[59] D. E. Kirk, *Optimal control theory: an introduction*. Courier Dover Publications, 2012.

[60] R. Horowitz and P. Varaiya, "Control design of an automated highway system," *Proceedings of the IEEE*, vol. 88, no. 7, pp. 913–925, 2000.

[61] C. Thorpe, M. Herbert, T. Kanade, and S. Shafer, "Toward autonomous driving: the cmu navlab. i. perception," *IEEE expert*, vol. 6, no. 4, pp. 31–42, 1991.

[62] C. Thorpe, M. H. Hebert, T. Kanade, and S. A. Shafer, "Vision and navigation for the carnegie-mellon navlab," *IEEE Transactions on Pattern Analysis and Machine Intelligence*, vol. 10, no. 3, pp. 362–373, 1988.

[63] C. Thorpe, M. Hebert, T. Kanade, and S. Shafer, "Vision and navigation for the carnegie-mellon navlab," *Annual Review of Computer Science*, vol. 2, no. 1, pp. 521–556, 1987.

[64] M. Buehler, K. Iagnemma, and S. Singh, *The DARPA urban challenge: Autonomous vehicles in city traffic*, vol. 56. springer, 2009.

[65] M. Parent and A. De La Fortelle, "Cybercars: Past, present and future of the technology," *arXiv preprint cs/0510059*, 2005.

[66] Cybercars2, "Final report, close communications for co-operation between cybercars," tech. rep., European commity, 2009.

[67] V. Milanés, J. Alonso, L. Bouraoui, and J. Ploeg, "Cooperative maneuvering in close environments among cybercars and dual-mode cars," *IEEE Transactions on Intelligent Transportation Systems*, vol. 12, no. 1, pp. 15–24, 2011.

[68] J. Markoff, "Google cars drive themselves, in traffic," *The New York Times*, vol. 10, p. A1, 2010.

[69] R. Fierro, A. Das, J. Spletzer, J. Esposito, V. Kumar, J. P. Ostrowski, G. Pappas, C. J. Taylor, Y. Hur, R. Alur, *et al.*, "A framework and architecture for multi-robot coordination," *The International Journal of Robotics Research*, vol. 21, no. 10-11, pp. 977–995, 2002.

[70] H. Hartenstein and K. P. Laberteaux, "A tutorial survey on vehicular ad hoc networks," *IEEE Communications Magazine*, vol. 46, no. 6, pp. 164–171, 2008.

[71] S. Grafling, P. Mahonen, and J. Riihijarvi, "Performance evaluation of ieee 1609 wave and ieee 802.11 p for vehicular communications," in *Second International Conference on Ubiquitous and Future Networks (ICUFN)*, pp. 344–348, 2010.

[72] C. Bergenhem, S. Shladover, E. Coelingh, C. Englund, and S. Tsugawa, "Overview of platooning systems," in *Proceedings of the 19th ITS World Congress, Vienna, Austria*, 2012.

[73] SARTRE, "The sartre project," 2009. http://www.sartre-project.eu.

[74] C. Bergenhem, Q. Huang, A. Benmimoun, and T. Robinson, "Challenges of platooning on public motorways," in *17th World Congress on Intelligent Transport Systems*, pp. 1–12, 2010.

[75] iQFleet, "The i.q.fleet wiki." http://www.iqfleet.org/.

[76] S. Tsugawa, S. Kato, and K. Aoki, "An automated truck platoon for energy saving," in *IEEE/RSJ International Conference on Intelligent Robots and Systems (IROS)*, pp. 4109–4114, 2011.

[77] K. Dresner and P. Stone, "Multiagent traffic management: A reservation-based intersection control mechanism," in *Proceedings of the Third International Joint Conference on Autonomous Agents and Multiagent Systems*, pp. 530–537, IEEE Computer Society, 2004.

[78] K. Dresner and P. Stone, "Turning the corner: improved intersection control for autonomous vehicles," in *Proceeding of IEEE Intelligent Vehicles Symposium*, pp. 423–428, 2005.

[79] K. M. Dresner and P. Stone, "A multiagent approach to autonomous intersection management." *J. Artif. Intell. Res.(JAIR)*, vol. 31, pp. 591–656, 2008.

[80] O. Mehani and A. de La Fortelle, "Trajectory planning in a crossroads for a fleet of driverless vehicles," in *Computer Aided Systems Theory–EUROCAST*, pp. 1159–1166, Springer, 2007.

[81] J. Grégoire, S. Bonnabel, and A. de La Fortelle, "Priority-based intersection management with kinodynamic constraints," *arXiv preprint arXiv:1310.5828*, 2013.

[82] A. de La Fortelle, "Analysis of reservation algorithms for cooperative planning at intersections," in *International IEEE Conference on Intelligent Transportation Systems (ITSC)*, pp. 445–449, 2010.

[83] J. Grégoire, S. Bonnabel, and A. de La Fortelle, "Optimal cooperative motion planning for vehicles at intersections," *arXiv preprint arXiv:1310.7729*, 2013.

[84] F. Perronnet, A. Abbas-Turki, and A. El Moudni, "A sequenced-based protocol to manage autonomous vehicles at isolated intersections," in *International IEEE Conference on Intelligent Transportation Systems*, pp. 1811–1816, 2013.

[85] R. Naumann, R. Rasche, J. Tacken, and C. Tahedi, "Validation and simulation of a decentralized intersection collision avoidance algorithm," in *IEEE Conference on Intelligent Transportation Systems*, pp. 818–823, 1997.

[86] R. Naumann and R. Rasche, *Intersection collision avoidance by means of decentralized security and communication management of autonomous vehicles.* Univ.-GH, SFB 376, 1997.

[87] L. Makarem, M.-H. Pham, A.-G. Dumont, and D. Gillet, "Microsimulation modeling of coordination of automated guided vehicles at intersections," *Transportation Research Record: Journal of the Transportation Research Board*, vol. 2324, no. 1, pp. 119–124, 2012.

[88] L. Makarem and D. Gillet, "Decentralized coordination of autonomous vehicles at intersections," in *IFAC World Congress*, vol. 18, pp. 13046–13051, 2011.

[89] A. Jadbabaie, J. Lin, and A. S. Morse, "Coordination of groups of mobile autonomous agents using nearest neighbor rules," *IEEE Transactions on Automatic Control*, vol. 48, no. 6, pp. 988–1001, 2003.

[90] P. F. Hokayem, M. W. Spong, and D. D. Siljak, "Cooperative avoidance control for multiagent systems," *Urbana*, vol. 51, p. 61801, 2007.

[91] Research and U. d. f. T. analysis section, "Road vehicle emission factors 2009," June 2009.

[92] L. Makarem and D. Gillet, "Fluent coordination of autonomous vehicles at intersections," in *IEEE International Conference on Systems, Man, and Cybernetics (SMC)*, pp. 2557–2562, 2012.

[93] L. Makarem and D. Gillet, "Model predictive coordination of autonomous vehicles crossing intersections," in *Proceeding of the 16th International IEEE Conference on Intelligent Transportation Systems (ITSC)*, pp. 1799–1804, 2013.

[94] C. E. Garcia, D. M. Prett, and M. Morari, "Model predictive control: theory and practice a survey," *Automatica*, vol. 25, no. 3, pp. 335–348, 1989.

[95] R. Soeterboek, *Predictive control a unified approach.* Prentice-Hall, Inc., 1992.

[96] E. F. Camacho and C. A. Bordons, *Model predictive control in the process industry.* Springer-Verlag New York, Inc., 1997.

[97] F. Allgöwer and A. Zheng, *Nonlinear model predictive control*, vol. 26. Birkhäuser Basel, 2000.

[98] D. Swaroop and J. Hedrick, "Constant spacing strategies for platooning in automated highway systems," *Journal of dynamic systems, measurement, and control*, vol. 121, no. 3, pp. 462–470, 1999.

[99] J. Huchra, M. Davis, D. Latham, and J. Tonry, "A survey of galaxy redshifts. iv-the data," *The Astrophysical Journal Supplement Series*, vol. 52, pp. 89–119, 1983.

[100] G. Efstathiou, W. Sutherland, and S. Maddox, "The cosmological constant and cold dark matter," *Nature*, vol. 348, no. 6303, pp. 705–707, 1990.

[101] D. J. Eisenstein, I. Zehavi, D. W. Hogg, R. Scoccimarro, M. R. Blanton, R. C. Nichol, R. Scranton, H.-J. Seo, M. Tegmark, Z. Zheng, *et al.*, "Detection of the baryon acoustic peak in the large-scale correlation function of sdss luminous red galaxies," *The Astrophysical Journal*, vol. 633, no. 2, p. 560, 2005.

[102] C. Blake, E. A. Kazin, F. Beutler, T. M. Davis, D. Parkinson, S. Brough, M. Colless, C. Contreras, W. Couch, S. Croom, *et al.*, "The wigglez dark energy survey: mapping the distance–redshift relation with baryon acoustic oscillations," *Monthly Notices of the Royal Astronomical Society*, vol. 418, no. 3, pp. 1707–1724, 2011.

[103] L. Anderson, E. Aubourg, S. Bailey, D. Bizyaev, M. Blanton, A. S. Bolton, J. Brinkmann, J. R. Brownstein, A. Burden, A. J. Cuesta, *et al.*, "The clustering of galaxies in the sdss-iii baryon oscillation spectroscopic survey: baryon acoustic oscillations in the data release 9 spectroscopic galaxy sample," *Monthly Notices of the Royal Astronomical Society*, vol. 427, no. 4, pp. 3435–3467, 2012.

[104] X. Cui, S.-g. Wang, D.-q. Su, Y. Zhao, Y.-n. Wang, Y. Chu, and G. Li, "Southern lamost for all sky spectroscopic survey," in *SPIE Astronomical Telescopes and Instrumentation: Observational Frontiers of Astronomy for the New Decade*, pp. 77330B–77330B, International Society for Optics and Photonics, 2010.

[105] M. Kimura, T. Maihara, K. Ohta, F. Iwamuro, S. Eto, M. Lino, D. Mochida, T. Shima, H. Karoji, J. Noumaru, *et al.*, "Fibre-multi-object spectrograph (fmos) for subaru telescope," in *Astronomical Telescopes and Instrumentation*, pp. 974–984, International Society for Optics and Photonics, 2003.

[106] D. Weinberg, D. Bard, K. Dawson, O. Dore, J. Frieman, K. Gebhardt, M. Levi, and J. Rhodes, "Facilities for dark energy investigations," *arXiv preprint arXiv:1309.5380*, 2013.

[107] P. F. Spectograph, "Official website." http://sumire.ipmu.jp/en/2652.

[108] H. Sugai, H. Karoji, N. Takato, N. Tamura, A. Shimono, Y. Ohyama, A. Ueda, H.-H. Ling, M. V. de Arruda, R. H. Barkhouser, *et al.*, "Prime focus spectrograph: Subaru's future," in *SPIE Astronomical Telescopes+ Instrumentation*, pp. 84460Y–84460Y, International Society for Optics and Photonics, 2012.

[109] M. Cirasuolo, J. Afonso, R. Bender, P. Bonifacio, C. Evans, L. Kaper, E. Oliva, and L. Vanzi, "Moons: The multi-object optical and near-infrared spectrograph," *The Messenger*, vol. 145, pp. 11–13, 2011.

[110] I. Morales, A. D. Montero-Dorta, M. Azzaro, F. Prada, J. Sánchez, and S. Becerril, "Fibre assignment in next-generation wide-field spectrographs," *Monthly Notices of the Royal Astronomical Society*, vol. 419, no. 2, pp. 1187–1196, 2012.

[111] H. G. Tanner and A. Kumar, "Towards decentralization of multi-robot navigation functions," in *Proceedings of the IEEE International Conference on Robotics and Automation*, pp. 4132–4137, 2005.

[112] E. Sontag, "Nonlinear regulation: The piecewise linear approach," *IEEE Transactions on Automatic Control*, vol. 26, no. 2, pp. 346–358, 1981.

[113] A. Rantzer and M. Johansson, "Piecewise linear quadratic optimal control," *IEEE Transactions on Automatic Control*, vol. 45, no. 4, pp. 629–637, 2000.

[114] M. Rewienski and J. White, "A trajectory piecewise-linear approach to model order reduction and fast simulation of nonlinear circuits and micromachined devices," *IEEE Transactions on Computer-Aided Design of Integrated Circuits and Systems*, vol. 22, no. 2, pp. 155–170, 2003.

[115] D. M. Stipanović, P. F. Hokayem, M. W. Spong, and D. D. Šiljak, "Cooperative avoidance control for multiagent systems," *Journal of Dynamic Systems, Measurement, and Control*, vol. 129, no. 5, pp. 699–707, 2007.

Appendix Part VI

A | Cooperative coordination of a multi robot system

Overview

THIS appendix presents a cooperative solution for coordinating individual robots in multi-robot systems. This methodology guarantees collision free manoeuvres using a barrier function as an avoidance control law. The avoidance control laws are computed using a new parameter called collision risk indicator that predicts the risk of collision between two agents in their bounded sensing regions. The proposed method solves an existing problems of coordination of agents with second order dynamics while being generally applicable to all other dynamical models.

A.1   Problem formulation

We consider a multi-agent system with a group of N independent agents moving in $I \subset R^2$. The state of an agent i is characterized by a position vector $q(t) \in R^2$ and a velocity vector $\dot{q}(t) \in R^2$, for $i = 1, 2, ..., N$. Each agent occupies a dis of radius r with $q_i \in I$ as its center .Every agent has access to its global position q_i, its velocity $\dot{q}_i$ and to the position of the other agents q_j in its sensing region. The other agent's velocities $\dot{q}_j$ can be derived by the variation of their position over time. Furthermore, each agent has access to its own target point but does not have access to the target point of the other agents. The motion of each agent can be described by a second order system.

$$\dot{q}_i = g_i(q_i, u_i, t) \tag{A.1}$$

$$\ddot{q}_i = h_i(q_i, u_i, t) \tag{A.2}$$

Defining the state vector $x_i^T = [q_i^T \quad \dot{q}_i^T]$ the dynamic model in (A.1) and (A.2) can be written as

$$\dot{x}_i = f_i(x_i, u_i, t) \tag{A.3}$$

Second-order dynamics are of key interest in systems obeying Newtonian mechanics. As the state vector contains not only position but also velocity of the agents. Definition (Distance between two agents). Consider a full state vector containing positions and velocities as state variables. The distance separating two agents with state vectors x_i and x_j is defined as

$$p_{ij}(x_i, x_j)^2 = \|q_i - q_j\|^2 = (q_i - q_j)^T(q_i - q_j) = (x_i - x_j)^T W(x_i - x_j) \tag{A.4}$$

Where

$$W = \begin{bmatrix} 1 & 0 & 0 & 0 \\ 0 & 1 & 0 & 0 \\ 0 & 0 & 0 & 0 \\ 0 & 0 & 0 & 0 \end{bmatrix} \tag{A.5}$$

is the position selector matrix. The sensing region as well as the avoidance region are respectively defined for each pair of agents as [115]

$$\begin{aligned} \Omega_{ij} &= \{x_i, x_j \in R^2 : \rho_{ij}(x_i, x_j) \leq r\} \\ S_{ij} &= \{x_i, x_j \in R^2 : \rho_{ij}(x_i, x_j) \leq R\} \end{aligned} \tag{A.6}$$

Therefore, the overall sensing and avoidance region can be respectively written as

$$\begin{aligned} \Omega &= \bigcup_{i,j \in N, j \neq i} \Omega_{ij} \\ S &= \bigcup_{i,j \in N, j \neq i} S_{ij} \end{aligned} \tag{A.7}$$

Furthermore a region

$$\Gamma_{ij} = \{x_i, x_j \in R^2, x_i, x_j \notin \Omega : r < \rho_{ij}(x_i, x_j) \leq \bar{r}\} \tag{A.8}$$

is defined as a safety region where two agents i and j, $j \neq i$ are able to detect each other but do not collide and where $r < \bar{r} \leq R$. The main challenge in this step is finding the control inputs for each agent so that the agent can reach its destination without entering avoidance region.

A.2   Optimal control

The main objective is to find a control law that minimizes a cost function for each agent of the following form

$$J_i = \int_0^\infty l_i(x_i, u_i) dt \qquad \forall i \in N \tag{A.9}$$

These cost functions defines the strategy adopted by every agent to arrive to its destination point $x_i^e \in R^2$, and the applied control is split into two intervals $[0; \tau]$ and $[\tau; \infty[$ so that:

$$J_i = \int_0^\tau l_i(x_i, u_i) dt + v_i[x_i(\tau)] \qquad \forall i \in N \tag{A.10}$$

Where:

$$v_i[x_i(\tau)] = \int_\tau^\infty l_i(x_i, u_i]) dt \qquad \forall i \in N \tag{A.11}$$

According to the maximum principle law the system must behave optimally from τ onwards. An optimal control law $u_i = u_i^o(x_i(\tau))$ is deployed, ensuring that the value function in equation (A.11) behave optimally.

$$v_i^o[x_i] = \int_\tau^\infty l_i(x_i(\tau), u_i^o[x_i(\tau)]) d\tau \qquad \forall i \in N \tag{A.12}$$

In order to obtain the optimal control input $u_i = u_i^o(x_i(\tau))$ the following expression has to be minimized:

$$u_i^o(x_i) = \min_{u_i(t)}\{l_i(x_i, u_i) + \frac{\partial v_i^o}{\partial x_i} f_i(x_i, u_i)\} \qquad \forall i \in N \tag{A.13}$$

The Hamiltonian function of the agents can be formulated as follows:

$$H_{f_i}(x_i, \frac{\partial v_i}{\partial x_i}, u_i) = l_i(x_i, u_i) + \frac{\partial v_i}{\partial x_i} f_i(x_i, u_i) \qquad \forall i \in N \tag{A.14}$$

The optimal value function and the optimal control laws satisfy the hamilton-Jacobi-Bellman equations:

$$\min_{u_i(t)}\{l_i(x_i, u_i) + \frac{\partial v_i}{\partial x_i} f_i(x_i, u_i)\} = 0 \qquad \forall i \in N \tag{A.15}$$

Which leads to:

$$l_i(x_i, u_i^o(x_i)) + \frac{\partial v_i^o}{\partial x_i} f_i(x_i, u_i^o(x_i)) = 0 \qquad \forall i \in N \tag{A.16}$$

The time derivative of the value function is given by:

$$\frac{dv_i^o}{dt} = \frac{\partial v_i^o}{\partial x_i} f_i(x_i, u_i^o(x_i)) = l_i(x_i, u_i^o(x_i)) \qquad \forall i \in N \tag{A.17}$$

The cost functions $l_i(x_i, u_i^o(x_i))$ are positive functions for all $x_i \neq x_i^e$ and the time derivative from equation(A.17) is smaller than zero. So, we can prove the convergence to the destination points using the Lyapunov theory. The destination points satisfy the equilibrium equations:

$$f_i(x_i^e, u_i^o(x_i^e)) = 0 \qquad \forall i \in N \tag{A.18}$$

The main goal of this methodology is not only the convergence to equilibrium points but also collision avoidance between agents. Therefore we define new barrier functions that allow us to prove collision-free motion towards the destination point for each agent.

A.3   Literature review

In this subsection we present the relevant results from [115]. In their work, authors have successfully obtained an optimization scheme for coordination of agents without collision using a barrier-type functions in equation (A.19). This scheme works properly for agents that are modeled with first order dynamics.

$$v'_{ij}(x_i, x_j) = (\min(0, \frac{\left\| x_i - x_j \right\|^2 - R^2}{\left\| x_i - x_j \right\|^2 - r^2}))^2 \qquad i, j \in N, i \neq j \tag{A.19}$$

In order to avoid collisions while the agents converge to their target points, they used the following function :

$$v'_i = \sum_{j=1}^{N} v'_{ij}(x_i, x_j) \qquad \forall i \in N \tag{A.20}$$

Where $v'_i i(x_i, x_i) = v^o_i(x_i)$, and a Lyapunov function has been chosen as:

$$v'(x) = \sum_{i=1}^{N} \sum_{j=1}^{N} v'_{ij}(x_i, x_j) \qquad \forall i \in N \tag{A.21}$$

In this formulation it is assumed that state vectors represent only the positions of agents. By minimizing the Hamiltonians the avoidance control laws of the agents are:

$$u^a_i(x_i) = \min_{u_i(t)} \{l_i(x_i, u_i) + \frac{\partial v'_i}{\partial x_i} f_i(x_i, u_i)\} \qquad \forall i \in N \tag{A.22}$$

In the following theorem, authors of [115], gave the sufficient conditions to guarantee collision avoidance for the general nonlinear system.

Theorem 5. *If the inequality (A.23) is satisfied, then the set Ω is avoidable for the system (A.3) with the subsystem control strategies defined in equation (A.22).*

proof

$$\sum_{i=1}^{N} H_{f_i}[x_i, \frac{\partial v'_i}{\partial x_i}, u^a_i(x)] - \sum_{i=1}^{N} q_i[x_i, u^a_i(x)] \leq 0 \qquad \forall x \in \Gamma \tag{A.23}$$

A.4   Barrier function

In this section, we introduce a new factor called Collision Risk Indicator (CRI). This indicator takes the velocities of the agents into account in the control criteria. We describe the interpretation of this factor as well as its properties. Finally, we formulate a new barrier function the new collision risk indicator.

Collision Risk Indicator

Definition 1 *(collision risk indicator ξ). Consider two agents with their state vectors x_i and $x_j, i \neq j$. Using notation defined in previous section, the collision risk indicator is defined as follows*:

$$\xi(x_i, x_j) = \frac{(x_i - x_j)^T V(x_i - x_j)}{\rho_{ij}(x_i, x_j)} \tag{A.24}$$
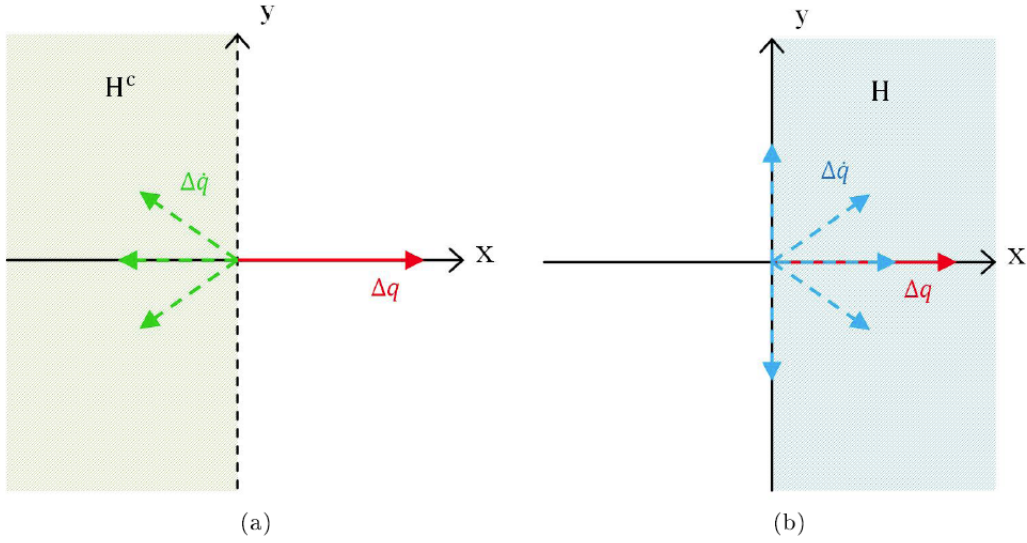
Figure A.1: Geometrical Interpretation of the Collision Risk Indicator: on the open left half plane collisions have to be avoided (a), and on the closed right half plane there is not a risk of collision (b).

Where V is

$$
V = \begin{bmatrix} 0 & 0 & \frac{1}{2} & 0 \\ 0 & 0 & 0 & \frac{1}{2} \\ \frac{1}{2} & 0 & 0 & 0 \\ 0 & \frac{1}{2} & 0 & 0 \end{bmatrix}
\tag{A.25}
$$

The idea of the CRI is that there is no risk of collision for agents that are moving apart from each other. Two relevant scenarios are represented in Figure(**??**). Case (a) represents the situation where two agents are moving toward each other and in case (b) two agents are moving apart from each other. Collision is possible and should be avoided when the product between the difference of positions and the difference of velocities is negative (case (a)). Otherwise, the risk of collision is negligible unless one of the agents changes its direction. In quantitative terms, this is as follows:

$$
(q_i - q_j)^T (\dot{q}_i - \dot{q}_j) \begin{cases} \geq 0 & \text{no collision risk} \\ < 0 & \text{collision risk} \end{cases}
\tag{A.26}
$$

Note that two different configurations can indicate the same collision risk, but their behavior can be totally different. We can consider that the product of the two vectors (relative velocity and relative distance) gives the same value in both cases. However in the one case the collision risk could be much lower because the agents are more separated(larger relative distance) and

the relative velocity has a smaller value. The second scenario can represent two agents that are quit close and they are approaching quit fast. To distinguish between these two cases, the CRI is normalized by the difference of the distance between the two agent. Based on these ideas, the CRI is constructed using the normalized inner product of relative distance and relative velocity.

The new barrier function

A new barrier function is defined taking into account the collision risk indicator. the function defined in equation (A.19) is reformulated as:

$$v_{ij}(x_i, x_j) = (\min(0, \frac{\rho_{ij}(x_i, x_j)^2 - R^2}{\rho_{ij}(x_i, x_j)^2 - r^2}))^2 (\min(0, \alpha\xi(x_i, x_j)))^2 \qquad i, j \in N, \qquad i \neq j \text{ (A.27)}$$

Where $\xi(x_i, x_j)$ is the collision risk indicator and $\alpha > 0$ is a scalar tuning parameter. It is worth noting that the term $\min(0, \alpha\xi(x_i, x_j))$ makes the barrier function identically zero when $\xi(x_i, x_j) > 0$, reflecting a case where there is no risk of collision. On the other hand, the barrier function is nonzero when $\xi(x_i, x_j) < 0$, which is consistent with the assessment of higher risk. The parameter α is introduced to add an additional degree of freedom. The default value is $\alpha = 1$, but it can be modified as needed to magnify or reduce the impact of the collision risk indicator as long as $\alpha > 0$ it guarantees collision free movements.

The partial derivative of $v_{ij}(x_i, x_j)$ with respect to x_i when $r < \rho_i j(x_i, x_j) < R$ and $\xi(x_i, x_j) < 0$ is given by:

$$\begin{aligned} \frac{\partial v_{ij}(x_i, x_j)}{\partial x_i} &= \frac{4\alpha^2 \xi^2(x_i, x_j)(R^2 - r^2)(\rho_{ij}^2(x_i, x_j) - R^2)}{(\rho_{ij}^2(x_i, x_j) - r^2)^3}(x_i - x_j)^T W \\ &+ \frac{4\alpha^2 \xi(x_i, x_j)}{\rho_{ij}(x_i, x_j)}(\frac{\rho_{ij}^2(x_i, x_j) - R^2}{\rho_{ij}^2(x_i, x_j) - r^2})^2 (x_i - x_j)^T V \\ &- \frac{4\alpha^2 \xi^2(x_i, x_j)}{\rho_{ij}(x_i, x_j)}(\frac{\rho_{ij}^2(x_i, x_j) - R^2}{\rho_{ij}^2(x_i, x_j) - r^2})^2 (x_i - x_j)^T W \\ &:= \beta_{ij}(x_i, x_j) \end{aligned} \qquad \text{(A.28)}$$

It is worth mentioning that, unlike the [115] the derivative of new barrier function over velocity of agents is not equal to zero. This is the reason that this barrier function is suitable to be used with system described by second order dynamics. The derivatives of the new barrier function with respect to position and velocity is as follows:

$$\begin{aligned} \frac{\partial v_{ij}(x_i, x_j)}{\partial q_i} &= \frac{4\alpha^2 \xi^2(x_i, x_j)(R^2 - r^2)(\rho_{ij}^2(x_i, x_j) - R^2)}{(\rho_{ij}^2(x_i, x_j) - r^2)^3}(q_i - q_j)^T \\ &+ \frac{4\alpha^2 \xi(x_i, x_j)}{\rho_{ij}(x_i, x_j)}(\frac{\rho_{ij}^2(x_i, x_j) - R^2}{\rho_{ij}^2(x_i, x_j) - r^2})^2 (\dot{q}_i - \dot{q}_j)^T \\ &- \frac{4\alpha^2 \xi^2(x_i, x_j)}{\rho_{ij}(x_i, x_j)}(\frac{\rho_{ij}^2(x_i, x_j) - R^2}{\rho_{ij}^2(x_i, x_j) - r^2})^2 (q_i - q_j)^T \end{aligned} \qquad \text{(A.29)}$$

$$\frac{\partial v_{ij}(x_i, x_j)}{\partial \dot{q}_i} = \frac{2\alpha^2 \xi(x_i, x_j)}{\rho_{ij}(x_i, x_j)} (\frac{\rho_{ij}^2(x_i, x_j) - R^2}{\rho_{ij}^2(x_i, x_j) - r^2})^2 (q_i - q_j)^T \qquad (A.30)$$

Theorem 6. *The following property is satisfied by x_i and x_j. Let $\Omega_i j^c$ be the complement of the avoidance region $\Omega_i j$ and let the pair of full state vectors x_i and x_j be in region $\Omega_i j^c$. If the relative distance between two agents goes to the boundary limit, then the CRI has to be negative:*

$$\lim_{\rho_{ij}(x_i, x_j) \to r^+} \xi(x_i, x_j) < 0 \qquad (A.31)$$

Proof. Consider the case where $\rho_{ij}(x_i, x_j) > 0$. So if $\rho_{ij}(x_i, x_j) \to r^+$, the time derivative of the relative distance has to be negative.

If $\rho_{ij}(x_i, x_j) > 0$ and $\rho_{ij}(x_i, x_j) \to r^+$
$\Leftrightarrow \xi(x_i, x_j) = (q_i - q_j)^T (\dot{q}_i - \dot{q}_j) < 0$

In the other words, two agents can get closer if and only if collisions have to be avoided. Otherwise the distance does not decrease and the norm $\rho_i j(x_i, x_j)$ does not go to r^+.

$\frac{d\rho_{ij}(x_i, x_j)}{dt} < 0 \Leftrightarrow \xi(x_i, x_j) < 0$

and therefore:

$$\lim_{\rho_{ij}(x_i, x_j) \to r^+} \xi(x_i, x_j) < 0$$

A.5   Analysis of collision avoidance

In this section, we give a proof for collision-free motion for a general nonlinear model as well as for a linear system with quadratic cost.

Collision-free motion toward the equilibrium

The following theorem provides conditions under which the optimal control law including the proposed barrier function (A.27) ensures collision-free cooperative control motion.

Lemma 1. *Let $v(x) = \sum \sum v_i j(x_i, x_j)$ where $v_i j$ is given in equation (A.27). Then the following properties hold:*
(i) The values of the function $v(x)$ are finite for finite values of its arguments x that are outside of region Ω.

(ii) $\displaystyle\lim_{\|x_i - x_j\| \to r^+} v_{ij}(x_i, x_j) \to +\infty$ $\qquad i, j \in N, \qquad i \neq j$

Proof. (i) The function $v(x)$ has finite values for all possible positions outside Ω if the velocities are finite. Only finite values for the states x is considered, so the velocities and the CRI is finite and therefore the function $v(x)$ is finite outside of the region Ω.

(ii) Consider the case where the collision risk indicator is negative and finite so that collision has to be avoided. In that case we have:

$$\lim_{\rho_{ij}(x_i, x_j) \to r^+} (\min(0, \frac{\rho_{ij}^2(x_i, x_j) - R^2}{\rho_{ij}^2(x_i, x_j) - r^2}))^2 . \max(0, -\xi(x_i, x_j)) \to \infty \tag{A.32}$$

The CRI is supposed to be non-zero in this case, so the value of the function $v(x)$ reaches infinity when the distance approaches the security region. As the initial positions are supposed to be outside the security regions the agents will never enter the avoidance discs of other agents.

Theorem 7. *If the following inequality is satisfied:*

$$\sum_{i=1}^{N} H_{f_i}[x_i, \frac{\partial v_i}{\partial x_i}, u_i^a(x)] - \sum_{i=1}^{N} q_i[x_i, u_i^a(x)] \leq 0 \qquad \forall x \in \Gamma \tag{A.33}$$

Then the value function $v(x)$ is non-increasing and the set Ω is avoidable for the system $\dot{x} = f(x, u)$ with the subsystem control strategies $u_i^a(x)$.

Proof.

$$\begin{aligned}
\frac{dv}{dt} &= \sum_{i=1}^{N} \sum_{j=1}^{N} \frac{dv_{ij}}{dt} = \sum_{i=1}^{N} \frac{dv_{ii}}{dt} + \sum_{i=1}^{N} \sum_{j>i} \frac{dv_{ij}}{dt} \\
&= \sum_{i=1}^{N} \frac{dv_{ii}}{dt} + \sum_{i=1}^{N} \sum_{j>i} \{\frac{\partial v_{ij}}{\partial x_i} f_i[x_i, u_i^a(x)] + \frac{\partial v_{ij}}{\partial x_j} f_i[x_j, u_j^a(x)]\} \\
&= \sum_{i=1}^{N} \frac{dv_{ii}}{dt} + \sum_{i=1}^{N} \sum_{j>i} \frac{\partial v_{ij}}{\partial x_i} f_i[x_i, u_i^a(x)] + \sum_{i=1}^{N} \sum_{j>1} \frac{\partial v_{ij}}{\partial x_j} f_i[x_j, u_j^a(x)]
\end{aligned} \tag{A.34}$$

The new value function satisfies this condition:

$$\sum_{i=1}^{N} \sum_{j>i} \frac{\partial v_{ij}}{\partial x_j} f_i[x_j, u_j^a(x)] = \sum_{i=1}^{N} \sum_{j<i} \frac{\partial v_{ij}}{\partial x_i} f_i[x_j, u_j^a(x)] \tag{A.35}$$

Therefore the expression in (A.34) can be simplified using the property $v_{ij}(x_i, x_j) = v_{ji}(x_j, x_i)$.

$$
\begin{aligned}
\frac{dv}{dt} &= \sum_{i=1}^{N} \frac{dv_{ii}}{dt} + \sum_{i=1}^{N} \sum_{j>i} \frac{\partial v_{ij}}{\partial x_i} f_i[x_i, u_i^a(x)] + \sum_{i=1}^{N} \sum_{j>1} \frac{\partial v_{ij}}{\partial x_j} f_i[x_j, u_j^a(x)] \\
&= \sum_{i=1}^{N} \sum_{j=1}^{N} \frac{\partial v_{ij}}{\partial x_i} f_i[x_i, u_i^a(x)] \\
&= \sum_{i=1}^{N} \frac{\partial v_i}{\partial x_i} f_i[x_i, u_i^a(x)] \\
&= \sum_{i=1}^{N} H_{f_i}[x_i, \frac{\partial v_i}{\partial x_i}, u_i^a(x)] - \sum_{i=1}^{N} q_i[x_i, u_i^a(x)] \le 0 \qquad \forall x \in \Gamma
\end{aligned}
\tag{A.36}
$$

The time derivative of the function $v(x)$ is non-increasing in the region Γ if and only if $\sum_{i=1}^{N} H_{f_i}[x_i, \frac{\partial v_i}{\partial x_i}, u_i^a(x)] - \sum_{i=1}^{N} q_i[x_i, u_i^a(x)] \le 0$.
In order to proof collision-free motion to their equilibrium point x_i^e theorem 3 in [115] is used.

The following expression $\sum_{i=1}^{N} H_{f_i}[x_i, \frac{\partial v_i}{\partial x_i}, u_i^a(x)] - \sum_{i=1}^{N} q_i[x_i, u_i^a(x)] \le 0$ has to be verified for all $x \ne x^e$ which guarantees that the agents are able to reach their target points without collision. The Lyapunov function $v(x)$ is equal to zero only at the equilibrium. The optimal control laws minimize the cost function along this curve and the condition ($\frac{dv}{dt} < 0$) guarantees convergence to the equilibrium using the Lyapunov theory. Collision-free coordination has been proved previously.

A.6 Linear system with quadratic cost

As the new barrier function satisfies all the properties in Theorem 2., the avoidance control law could be computed explicitly for the linear time-invariant system that is presented as:

$$
\dot{x} = A_i x_i + B_i u_i
\tag{A.37}
$$

The quadratic cost for the linear system is:

$$
l_i(x_i, u_i) = \frac{1}{2}[(x_i - x_i^e)^T Q_i(x_i - x_i^e) + (u_i - u_i^e)^T R(u_i - u_i^e)]
\tag{A.38}
$$

The control law defined in (A.22) could be rewritten for a linear system:

$$
u_i^a(x_i) = R_i^{-1} B_i^T P_i(x_i - x_i^e) + u_i^e - R_i^- 1 B_i^T \left(\sum_{i \ne j} \frac{\partial v'_{ij}}{\partial x_i}^T \right)
\tag{A.39}
$$

Theorem 8. *Let k_1 and k_2 be positive finite scalars such that $k_2 \neq 0$ and let n and m be integers such that $n < m$. Then there always exist a scalar tuning parameter $\alpha > 0$ and a weighting parameter r such that the inequality:*

$$k_1 \alpha^n < k_2 \alpha^m \frac{1}{r} \tag{A.40}$$

Proof. We can prove this inequality by dividing the both sides of the inequality by α^n.

Theorem 9. *Let $\dot{x}_i = A_i x_i + B_i u_i$ be a linear kinematic model of the agent $i \in N$ and let $v_{ij}(x_i, x_j)$ be the value function defined in (A.27), then the avoidance control laws in equation (A.39) guarantees collision-free motion.*

Proof. We can rewrite the time derivative of the value function in equation (A.36) using the avoidance control law as follows:

$$
\begin{aligned}
\frac{dv}{dt} &= \sum_{i=1}^{N} \left(\sum_{j=1}^{N} \frac{\partial v_{ij}}{\partial x_i} \right) A_i x_i + \sum_{i=1}^{N} \left(\sum_{j=1}^{N} \frac{\partial v_{ij}}{\partial x_i} \right) B \left(u_i^e - R_i^{-1} B_i^T \sum_{j=1}^{N} \frac{\partial v_{ij}}{\partial x_i}^T \right) \\
&= \sum_{i=1}^{N} \left(\sum_{j=1}^{N} \frac{\partial v_{ij}}{\partial x_i} \right) A_i x_i - \sum_{i=1}^{N} \left(\sum_{j=1}^{N} \frac{\partial v_{ij}}{\partial x_i} \right) B R_i^{-1} B_i^T \left(\sum_{j=1}^{N} \frac{\partial v_{ij}}{\partial x_i}^T \right)
\end{aligned}
\tag{A.41}
$$

The control input at the equilibrium u_i^e is equal to zero as described earlier in this work. After choosing the weighting matrix as $R_i = \begin{bmatrix} r_{i,1} & 0 \\ 0 & r_{i,2} \end{bmatrix}$, we rewrite the time derivative of value function once more:

$$\frac{dv}{dt} = \sum_{i=1}^{N} \sum_{j=1}^{N} \frac{\partial v_{ij}}{\partial q_i} \dot{q}_i - \sum_{i=1}^{N} \left[\frac{1}{r_{i,1}} \left(\sum_{j=1}^{N} \frac{\partial v_{ij}}{\partial \dot{q}_{i,1}} \right)^2 + \frac{1}{r_{i,2}} \left(\sum_{j=1}^{N} \frac{\partial v_{ij}}{\partial \dot{q}_{i,2}} \right)^2 \right] \tag{A.42}$$

In order to guarantee collision free motion, the time-derivative has to be smaller than zero. This condition can be written as:

$$\sum_{j=1}^{N} \frac{\partial v_{ij}}{\partial q_i} \dot{q}_i < \left[\frac{1}{r_{i,1}} \left(\sum_{j=1}^{N} \frac{\partial v_{ij}}{\partial \dot{q}_{i,1}} \right)^2 + \frac{1}{r_{i,2}} \left(\sum_{j=1}^{N} \frac{\partial v_{ij}}{\partial \dot{q}_{i,2}} \right)^2 \right] \tag{A.43}$$

If the equation holds for one agent, then it can be summed up for all the agents and the condition will still hold. Using Lemma 2 it can be shown that the inequality (A.43) can always be satisfied with properly chosen parameters.

Laleh MAKAREM

PERSONAL
INFORMATION

Born: 31 March 1985, Iran

Married

☎ (+41) 78-821-4266

✉ laleh.makarem@gmail.com

EDUCATION

PhD Ecole Polytechnique Fédérale de Lausanne (EPFL), Switzerland,

Manufacturing and Robotics,   2010- Dec. 2014 (Expected)

Dissertation: "Decentralized Coordination of Multi-Robot Systems
in Crowded Workspaces"

Supervisor: Dr. Denis GILLET (MER)

M.Sc.University of Tehran, Iran,

Electrical Engineering (Control engineering),   2007-2009

Thesis: "Optimal Control of a Quadruped Robot on the Gallop Gait"

Supervisor: Prof. Majid NILI AHMADABADI

B.Sc.University of Tehran, Iran,

Electrical Engineering (Control engineering),   2003-2007

Thesis: Large Margin Classification Based on Shannon Entropy

Supervisor: Prof. Babak N. ARABI

HONORS AND
AWARDS

National Physics Olympiad, 2002

10th Bronze medal, three month intensive training on Mechanics and Optics

Ranked 2rd, 2009

Control Engineering Master Programme, University of Tehran, Iran

Ranked 3rd, 2007

Electrical Engineering Bachelor Programme, University of Tehran, Iran

RESEARCH
EXPERIENCE

Research Assistant   Feb. 2013- Present

Ecole Polytechnique Fédérale de Lausanne (EPFL), Switzerland

Path Analysis for Fiber Positioners in DESI and MOONS

Research Assistant   May 2014. -Present

Ecole Polytechnique Fédérale de Lausanne (EPFL), Switzerland

Automation of a Micro-cogeneration System

Research Assistant   Feb. 2010- March. 2013

Ecole Polytechnique Fédérale de Lausanne (EPFL), Switzerland

Hierarchical Traffic Coordination of Automated Guided Vehicles

Research Assistant   June. 2008- Aug. 2008

University of Tehran, Iran

Vision-based Localization of a Rescue Blimp Model

151

1 of 4

Teaching Assistantship	**Teaching Assistant**	Fall 2010 + Fall 2011

Teaching Assistant   Fall 2010 + Fall 2011
Ecole Polytechnique Fédérale de Lausanne (EPFL), Switzerland
Multi-variable Systems:
For student in Electrical engineering, Mechanical engineering and Microtechnics engineering

Teaching Assistant   Fall 2012 + Fall 2013 + Fall 2014
Ecole Polytechnique Fédérale de Lausanne (EPFL), Switzerland
Dynamic Coordination:
For student in Electrical engineering and Microtechnics engineering

Laboratory Assistant   Fall 2010 + Fall 2011
Ecole Polytechnique Fédérale de Lausanne (EPFL), Switzerland
Automatic Control

Teaching Assistant   Fall 2009
University of Tehran, Iran
Robotics:
a masters course in Robotics, covering the following topics: Kinematics and dynamics of rigid bodies, Inverse kinematics and dynamics problems, Design and select of robots, Trajectory and motion planning

Supervised Student Projects

- Corinne Doppmann, "Comfort Adaptation for Coordination of Autonomous vehicles", Semester project in Mechanical Engineering   Fall 2013

- Cedric Berger, "Predictive Coordination of Autonomous vehicles using DNF", Semester project in Mechanical Engineering   Spring 2012

- Yves Buntschu, "Smooth Crossing of Automated Guided Vehicles at intersection", Semester project in Mechanical Engineering   Fall 2012

- Martin Liniger, "Webots Simulation Platform of Autonomous Vehicles at Intersections", Semester project in Microtechnics Engineering   Fall 2012

- Igor Zablotchi, "Graph-based Crossing in Flocks", Bachelor project in Computer Science   Spring 2011

- Benjamin Frankhauser, "Energy Efficient Crossing of Automated Guided Vehicles", Master thesis project in Microtechnics Engineering   Fall 2011

- Daniel Nellen, "Cooperative coordination of autonomous vehicles", Master project in Electrical Engineering   Spring 2010

- Gergely Nardai, "Communication testbed preparation for e-pucks", Bachelor thesis project in Automation Engineering   Fall 2010

152

JOURNAL
PUBLICATION

- **L. Makarem**, J-P. Kneib, D. Gillet, H. Bleuler, M. Bouri, L. Jenni, F. Prada, J. Sanchez, "Collision Avoidance in Next-generation Fiber Positioner Robotic System for Large Survey Spectrograph," Astronomy and Astrophysics, Vol. 566, (2014).

- N. Fahim, F. Prada, J. P. Kneib, D. Gillet, **L. Makarem**, et al., "An 8-mm diameter Fiber Robot Positioner for Massive Spectroscopy Surveys," submitted to Astronomy and Astrophysics (2014).

- **L. Makarem**, M.-H. Pham, A.-G. Dumont and D. Gillet, "Microsimulation Modeling of Coordination of Automated Guided Vehicles at Intersections," Transportation Research Record: Journal of the Transportation Research Board 2324, No. 1 (2012): 119-124.

CONFERENCE
PAPERS

- **L. Makarem**, J-P. Kneib, D. Gillet, H. Bleuler, M. Bouri, P. Horler, L. Jenni, F. Prada, J. Sanchez, "Collision-free Motion Planning for Fiber Positioner Robots: Discretization of Velocity profiles," in SPIE Astronomical Telescopes+ Instrumentation. International Society for Optics and Photonics, Montreal, Canada, 2014.

- L.Jenni, **L. Makarem**, P. Horler, P Kneib, D Gillet, H Bleuler and M Bouri, "Developing Micro DC-brushless Motor Driver and Position Control for Fiber Positioners," in SPIE Astronomical Telescopes+ Instrumentation. International Society for Optics and Photonics, Montreal, Canada, 2014.

- **L. Makarem**, and D. Gillet "Model predictive coordination of autonomous vehicles crossing intersections," 16th International IEEE Conference on Intelligent Transport Systems (ITSC), 2013, The Hague, The Netherlands.

- **L. Makarem**, and D. Gillet, "Fluent Coordination of Autonomous Vehicles at Intersections," IEEE International Conference on Systems, Man, and Cybernetics (SMC), Seoul, Korea, 2012.

- **L. Makarem**, and D. Gillet, "Information Sharing among Autonomous Vehicles Crossing an Intersection," IEEE International Conference on Systems, Man, and Cybernetics (SMC), Seoul, Korea, 2012.

- **L. Makarem**, and D. Gillet, "Micro-simulation Modeling of Coordination of Automated Guided Vehicles at Intersection," Transportation research board 91st annual meeting, Washington D.C., USA, 2012.

- **L. Makarem**, and D. Gillet, "Autonomous Vehicles Share Information Crossing an Intersection," 1st European Symposium on Quantitative Methods in Transportation Systems, Lausanne, Switzerland, 2012.

- **L. Makarem**, and D. Gillet, "Decentralized Coordination of Autonomous Vehicles at Intersections," Proceeding of IFAC World Congress. Vol. 18. No. 1. 2011.

- B. Fankhauser, **L. Makarem** and D. Gillet, "Collision-free Intersection Crossing of Mobile Robots Using Decentralized Navigation Functions on Predefined Paths," in IEEE Cybernetics and Intelligent Systems (CIS), Qingndao, China, 2011.

- **L. Makarem**, A. Akbarimajd, and M.N. Ahmadabadi, "Dynamic Manipulation of Active Objects: Modeling and Optimization," in IEEE/ASME International Advanced Intelligent Mechatronics, Singapore, 2009.

LANGUAGES   English (fluent), French (B2), German (A2), Persian (Native), Turkish (Native)

SKILLS   **Programming Languages:** Matlab, Simulink, C, C++, Java
                 Softwares: Adobe Suite, LabView, Latex, AIMSUN,